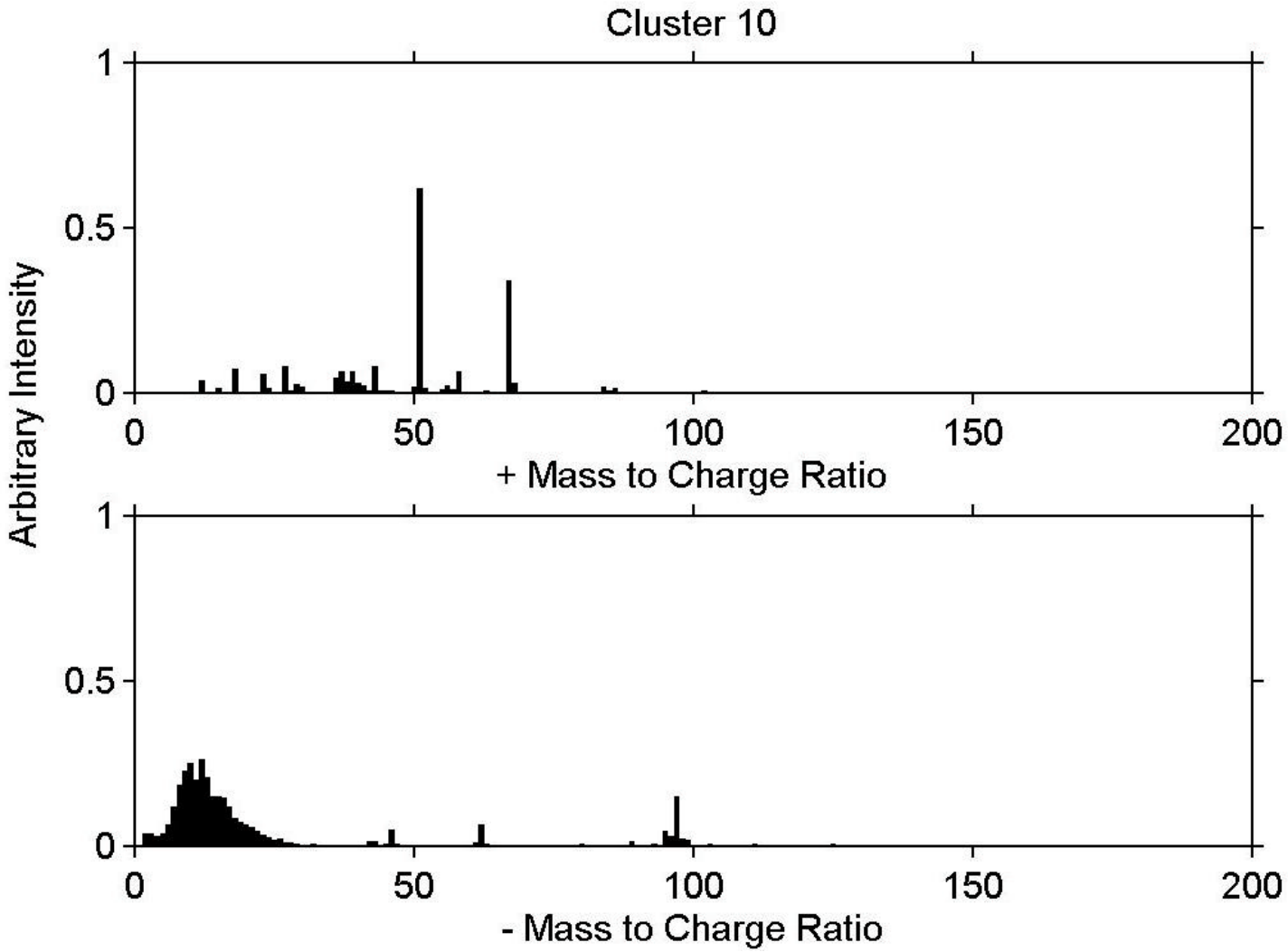
Cluster 10
Arbitrary Intensity
1
0.5
0
0
50
100
150
200
+ Mass to Charge Ratio
1
0.5
0
0
50
100
150
200
- Mass to Charge Ratio

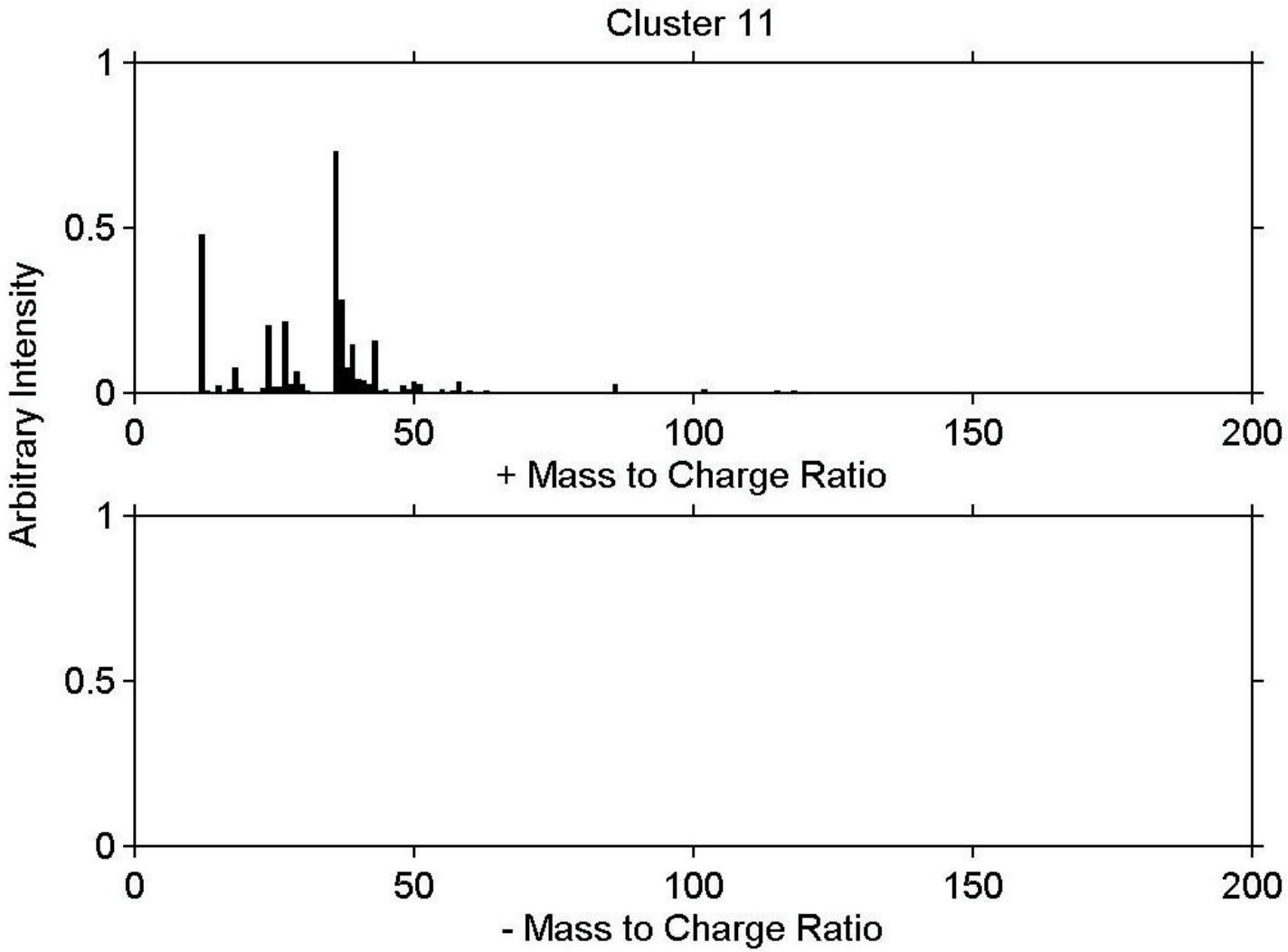
Cluster 11
Arbitrary Intensity
1
0.5
0
0
50
100
150
200
+ Mass to Charge Ratio
1
0.5
0
0
50
100
150
200
- Mass to Charge Ratio

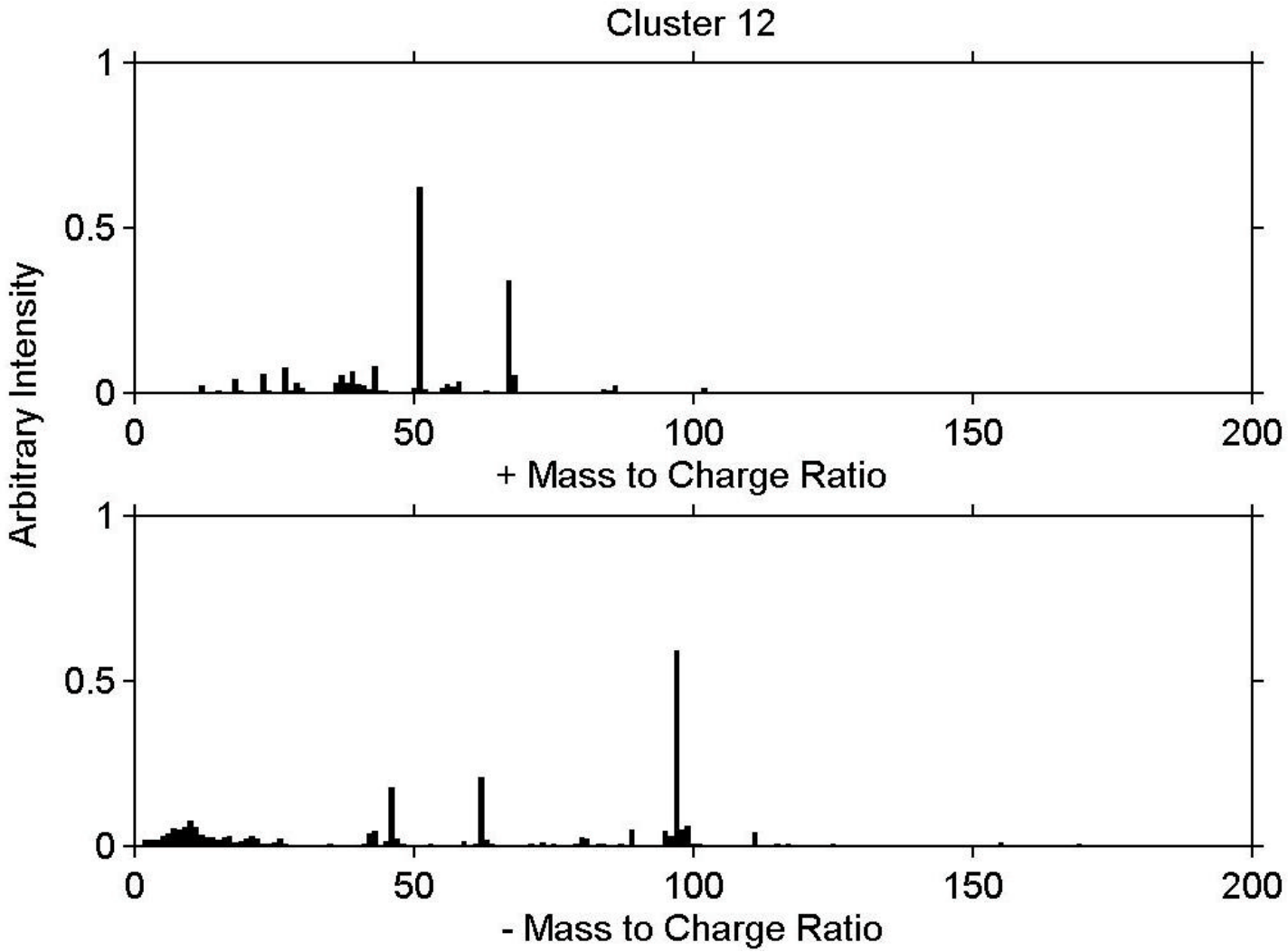
Cluster 12
Arbitrary Intensity
1
0.5
0
0
50
100
150
200
+ Mass to Charge Ratio
1
0.5
0
0
50
100
150
200
- Mass to Charge Ratio

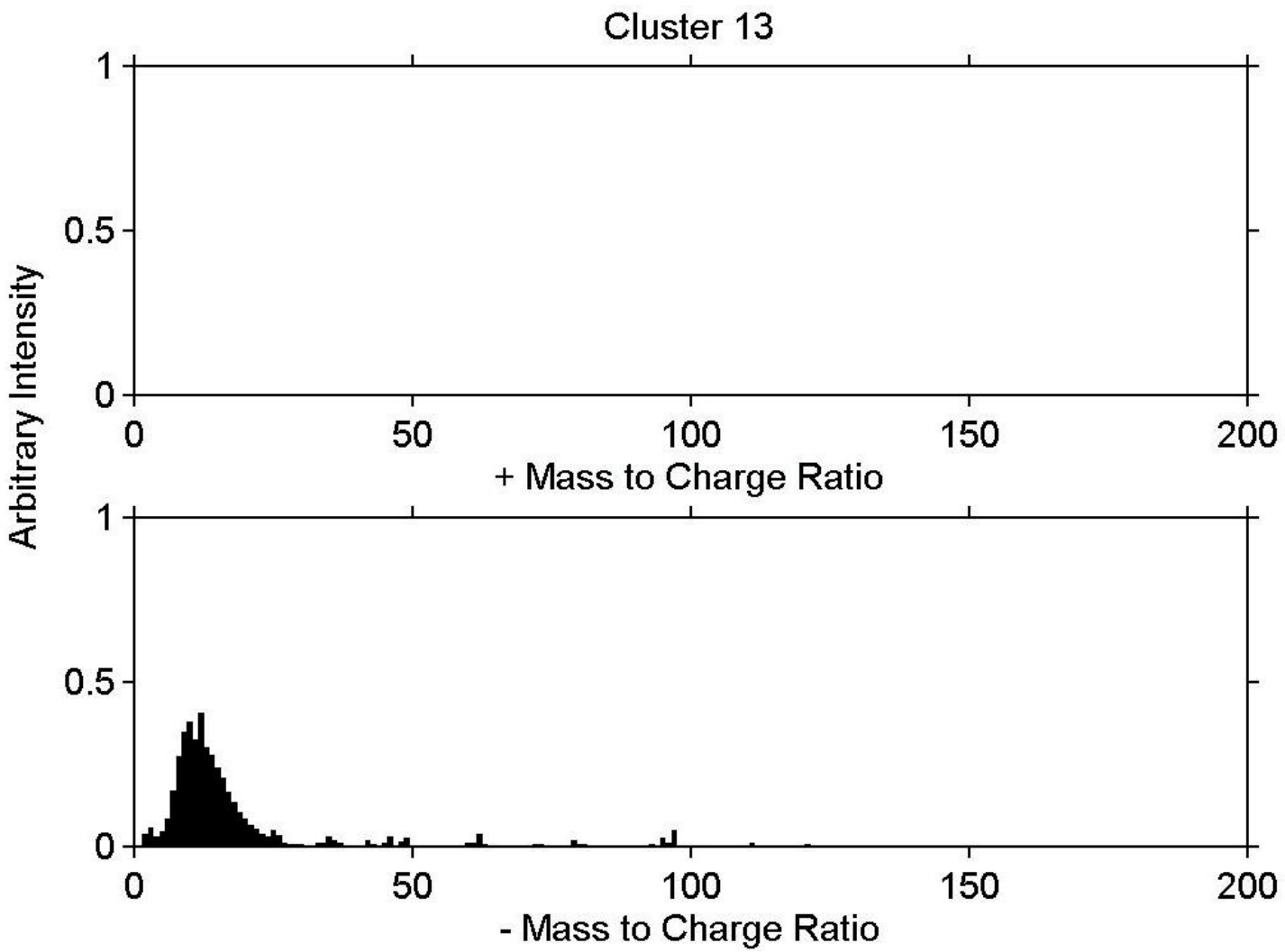
Cluster 13
Arbitrary Intensity
1
0.5
0
0
50
100
150
200
+ Mass to Charge Ratio
1
0.5
0
0
50
100
150
200
- Mass to Charge Ratio

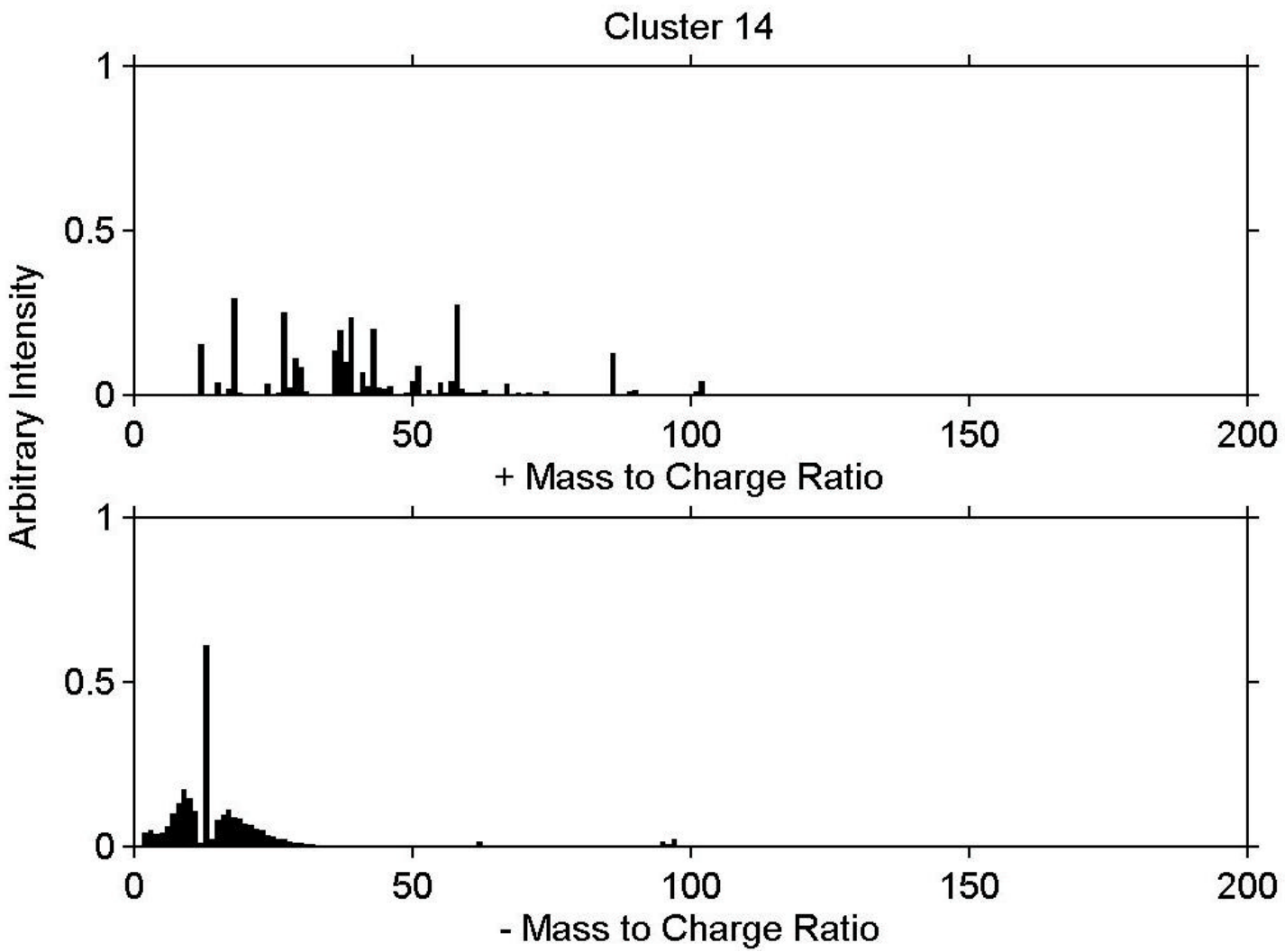
Cluster 14
Arbitrary Intensity
1
0.5
0
0
50
100
150
200
+ Mass to Charge Ratio
1
0.5
0
0
50
100
150
200
- Mass to Charge Ratio

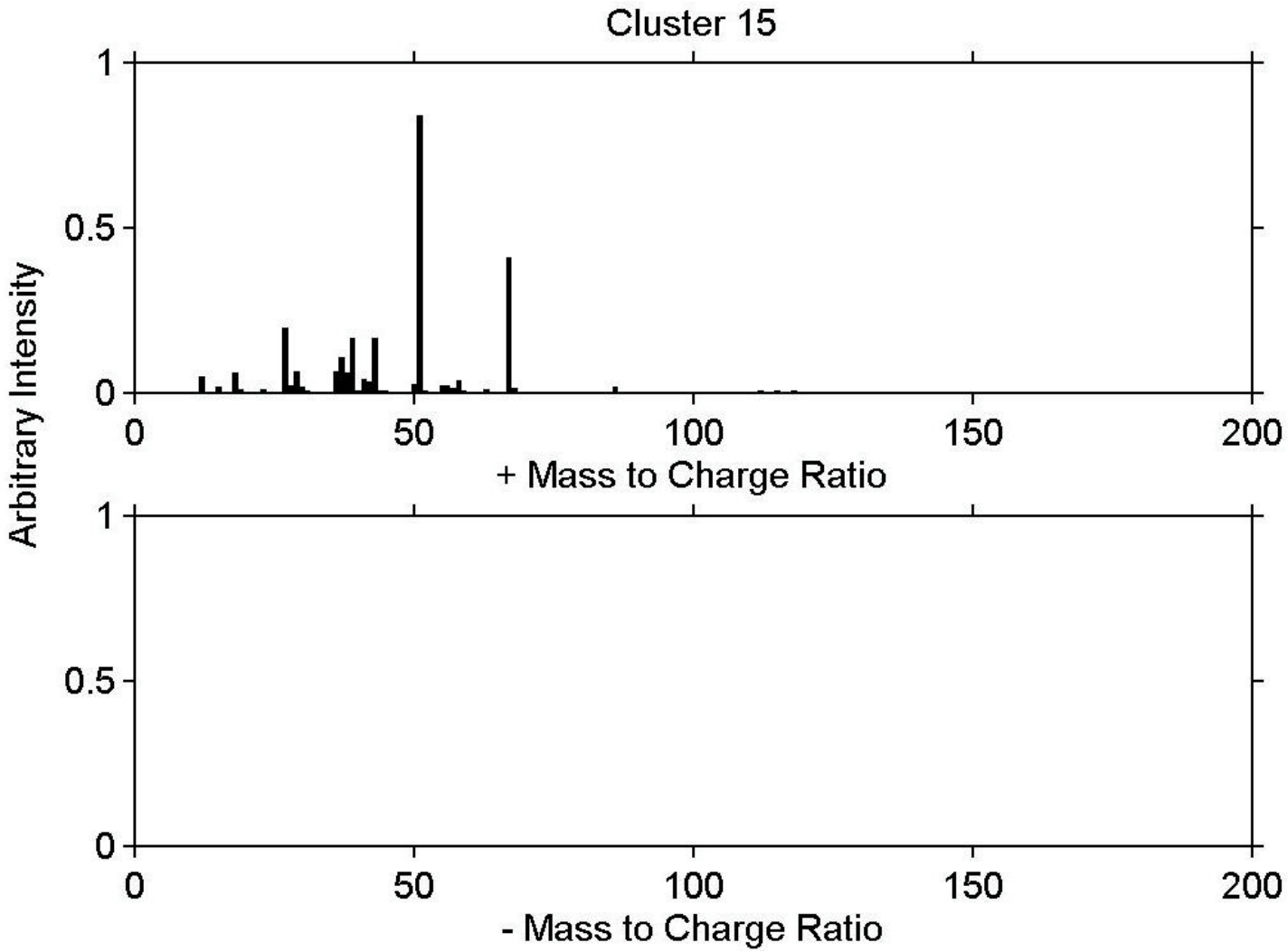
Cluster 15
Arbitrary Intensity
1
0.5
0
0
50
100
150
200
+ Mass to Charge Ratio
1
0.5
0
0
50
100
150
200
- Mass to Charge Ratio

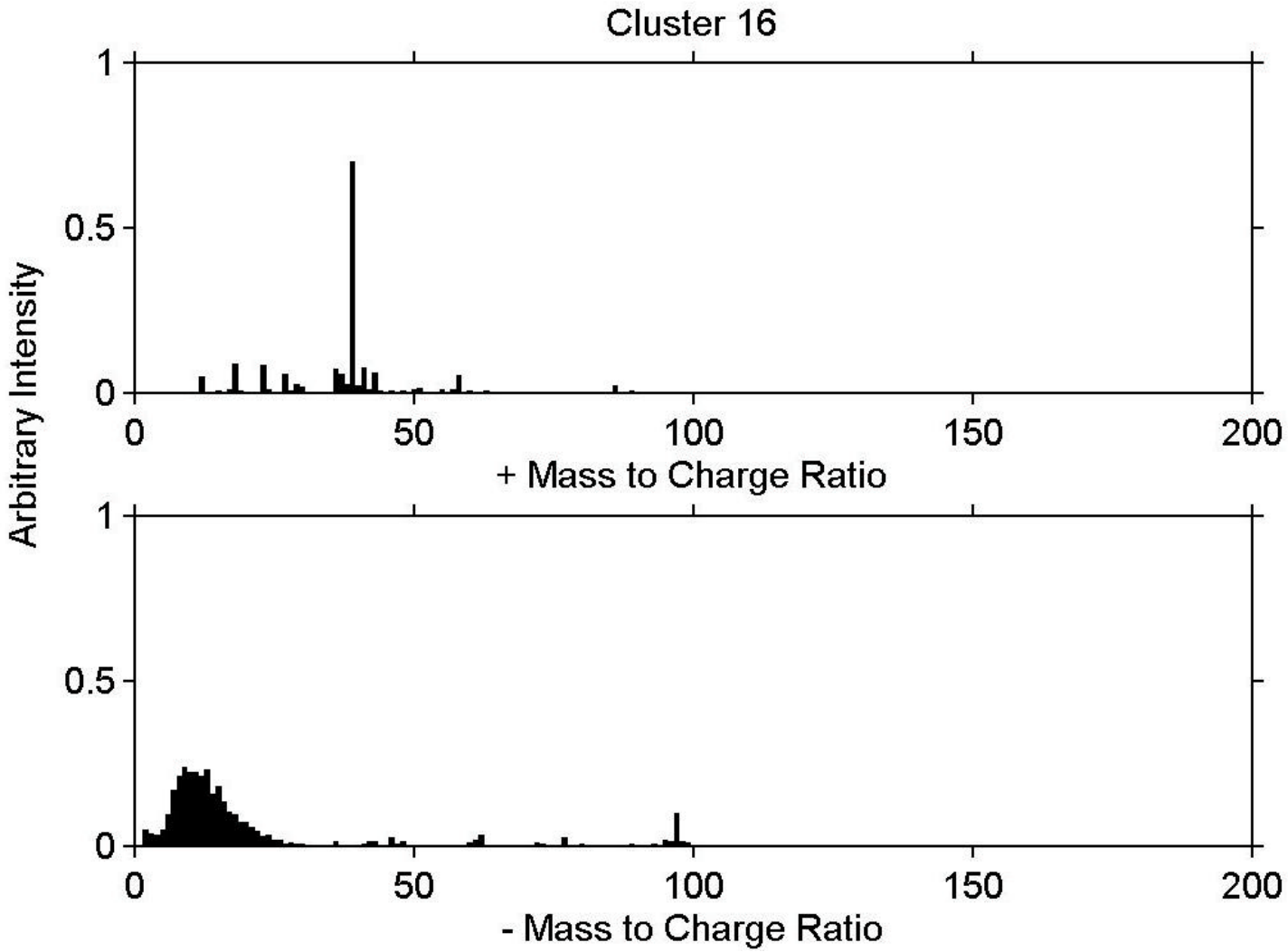
Cluster 16
Arbitrary Intensity
1
0.5
0
0
50
100
150
200
+ Mass to Charge Ratio
1
0.5
0
0
50
100
150
200
- Mass to Charge Ratio

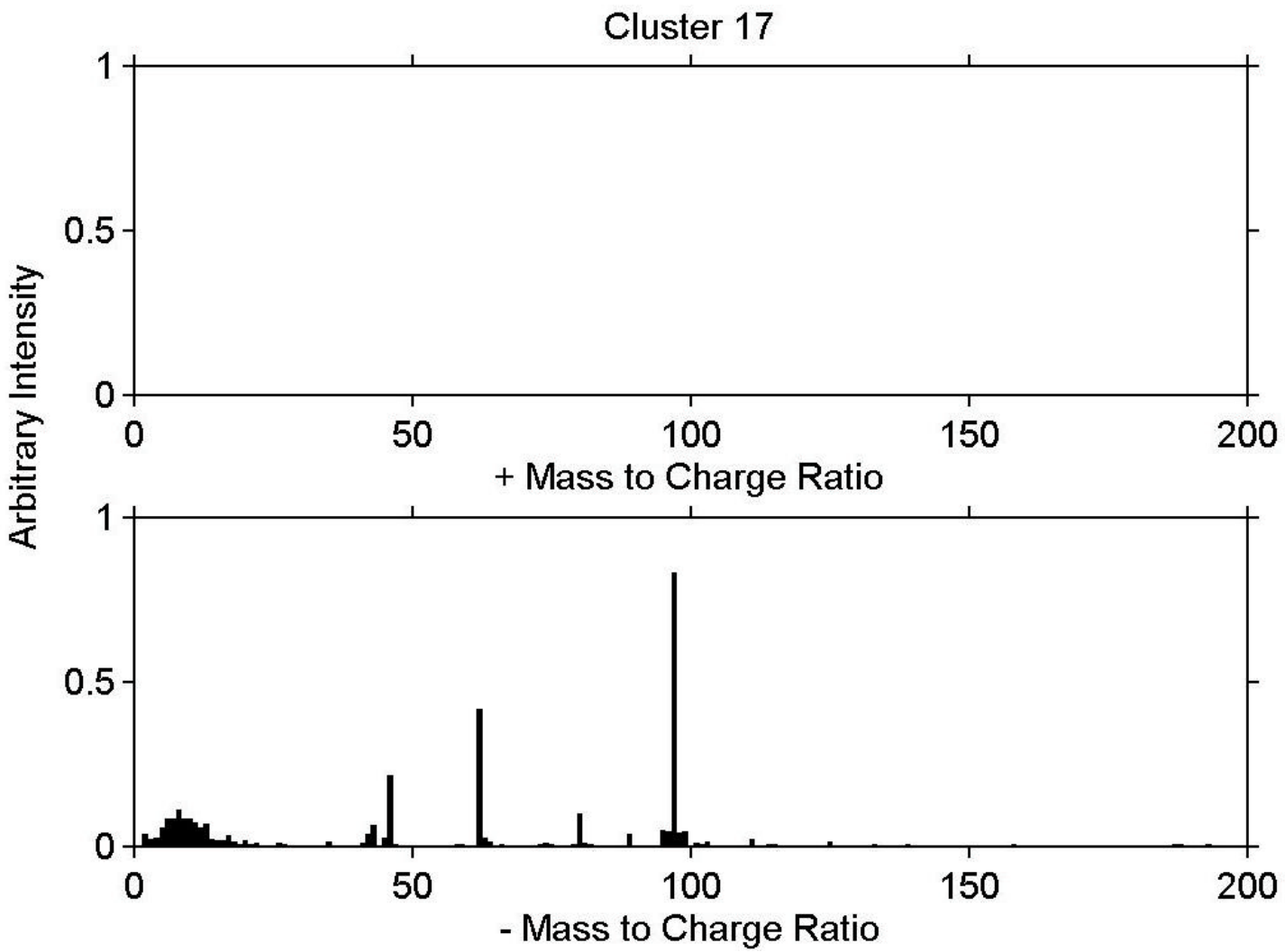
Cluster 17
Arbitrary Intensity
1
0.5
0
0
50
100
150
200
+ Mass to Charge Ratio
1
0.5
0
0
50
100
150
200
- Mass to Charge Ratio

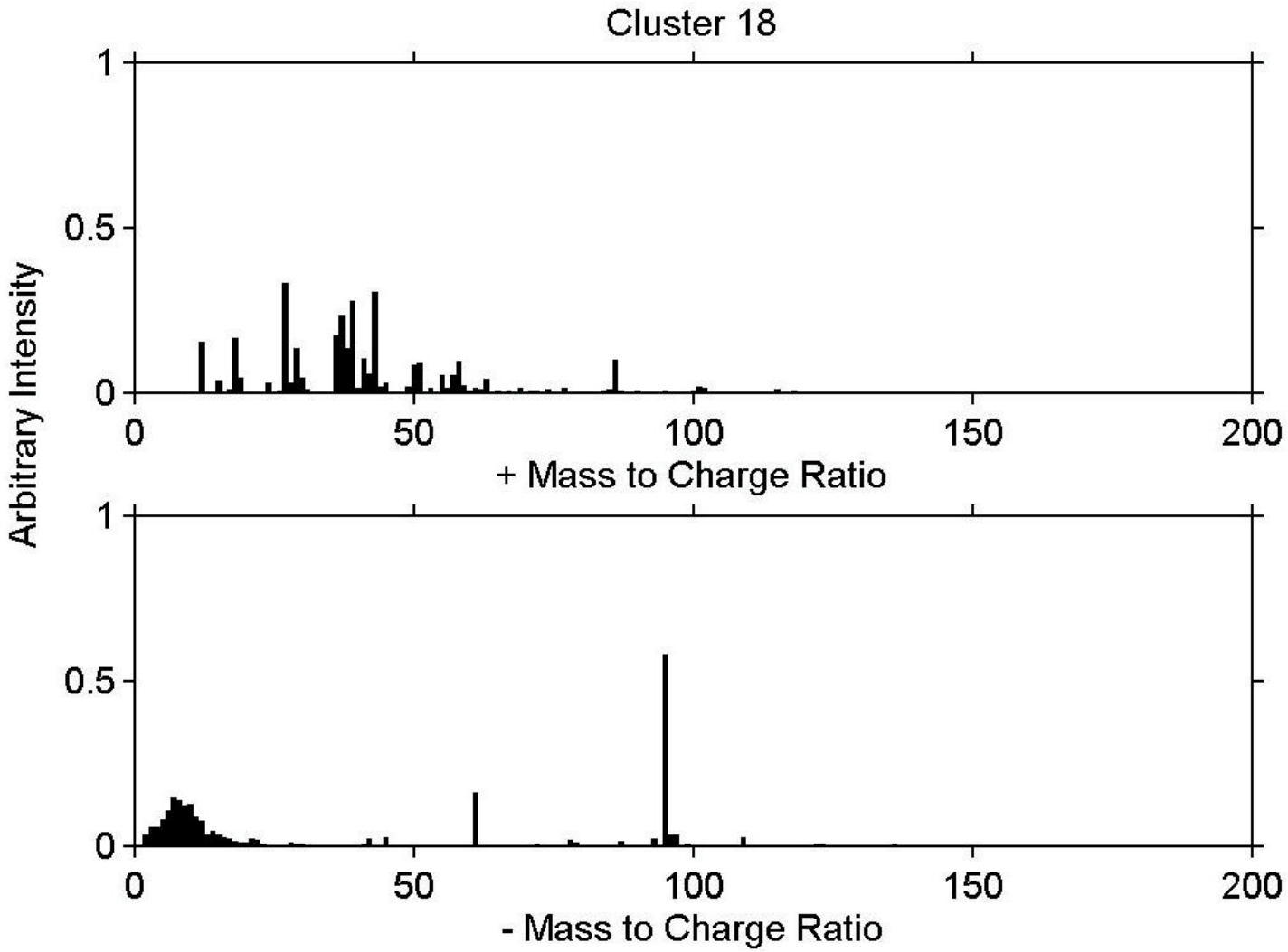
Cluster 18
Arbitrary Intensity
1
0.5
0
0
50
100
150
200
+ Mass to Charge Ratio
1
0.5
0
0
50
100
150
200
- Mass to Charge Ratio

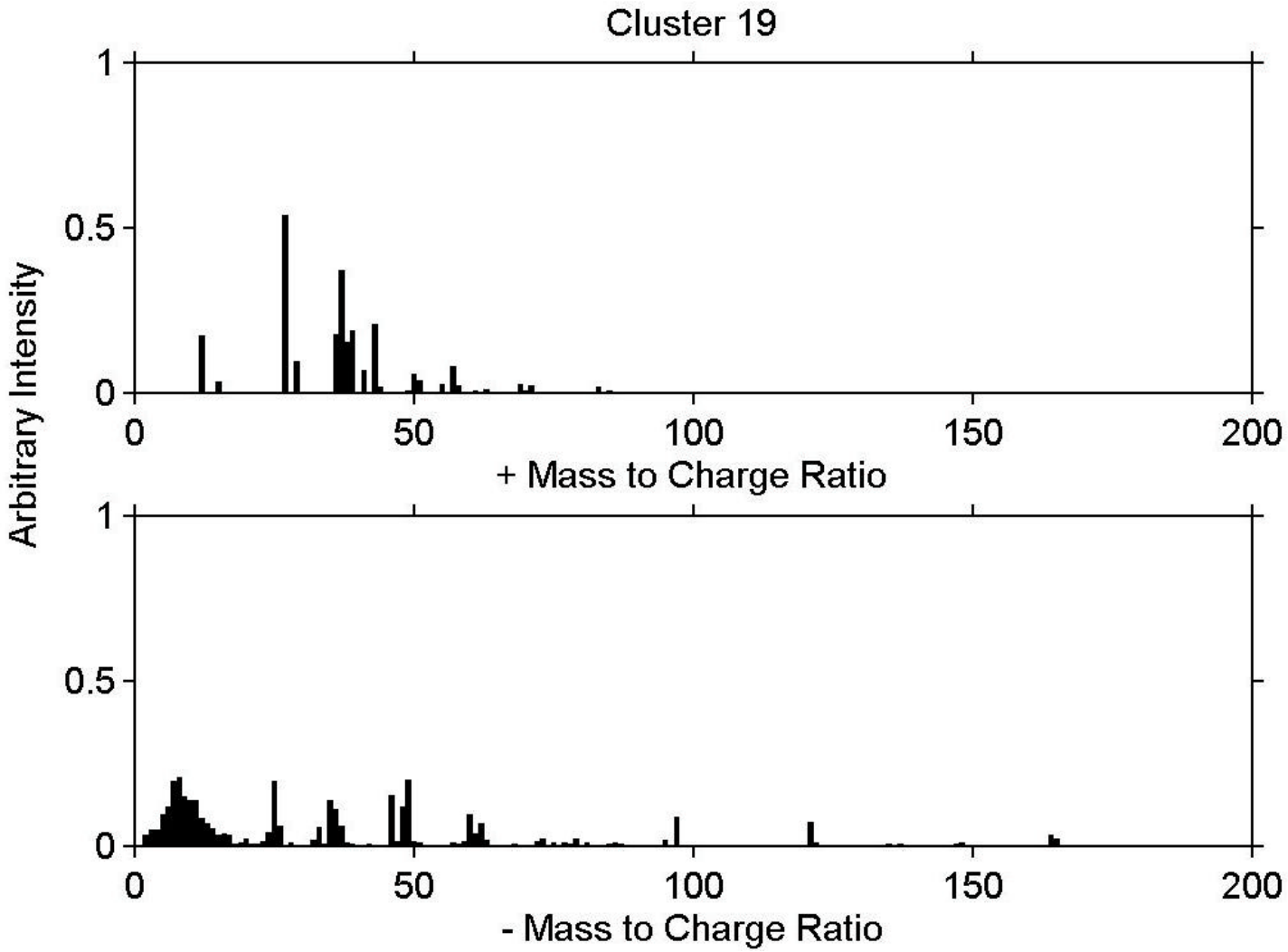
Cluster 19
Arbitrary Intensity
1
0.5
0
0
50
100
150
200
+ Mass to Charge Ratio
1
0.5
0
0
50
100
150
200
- Mass to Charge Ratio

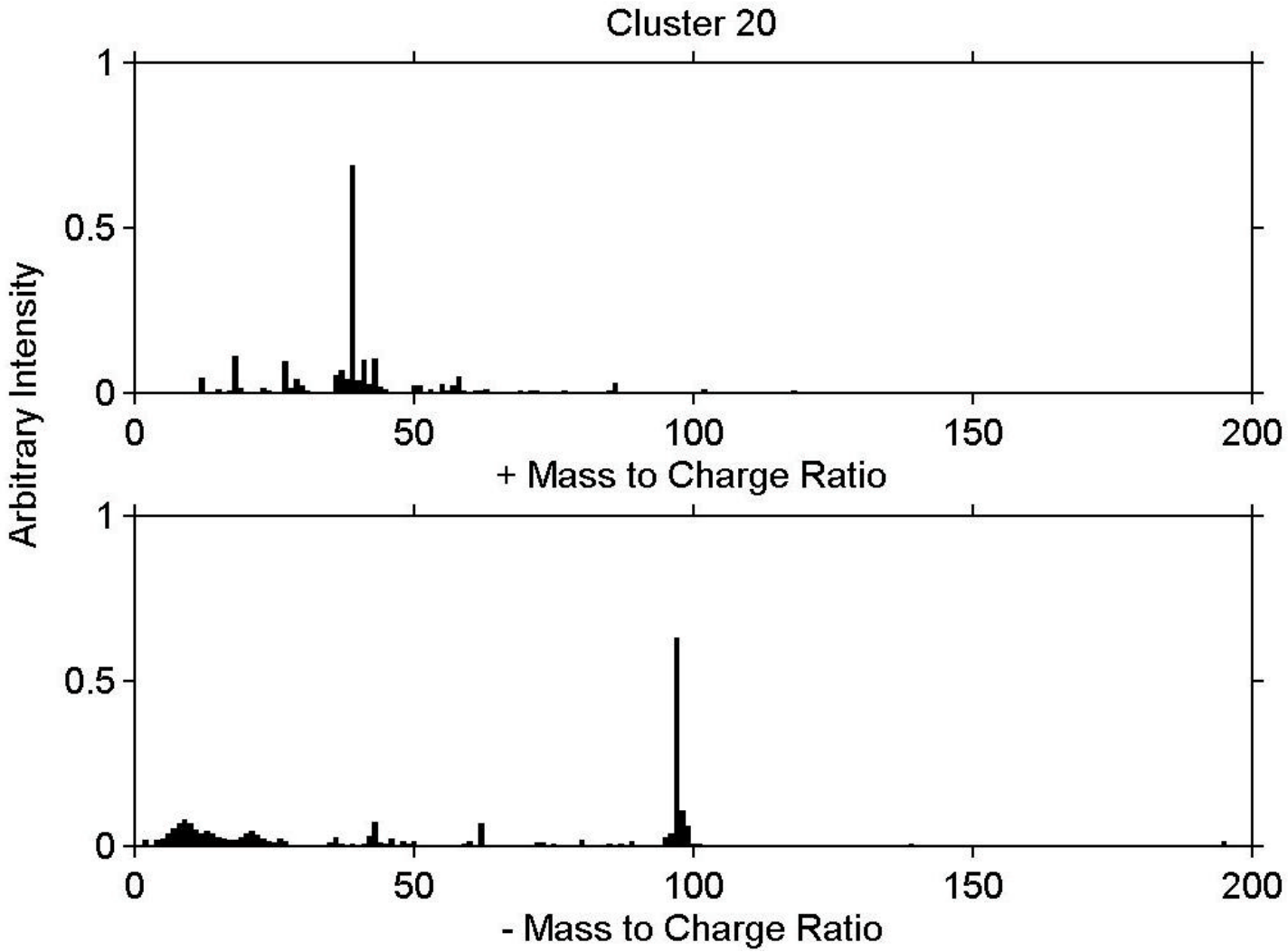
Cluster 20
Arbitrary Intensity
1
0.5
0
0
50
100
150
200
+ Mass to Charge Ratio
1
0.5
0
0
50
100
150
200
- Mass to Charge Ratio

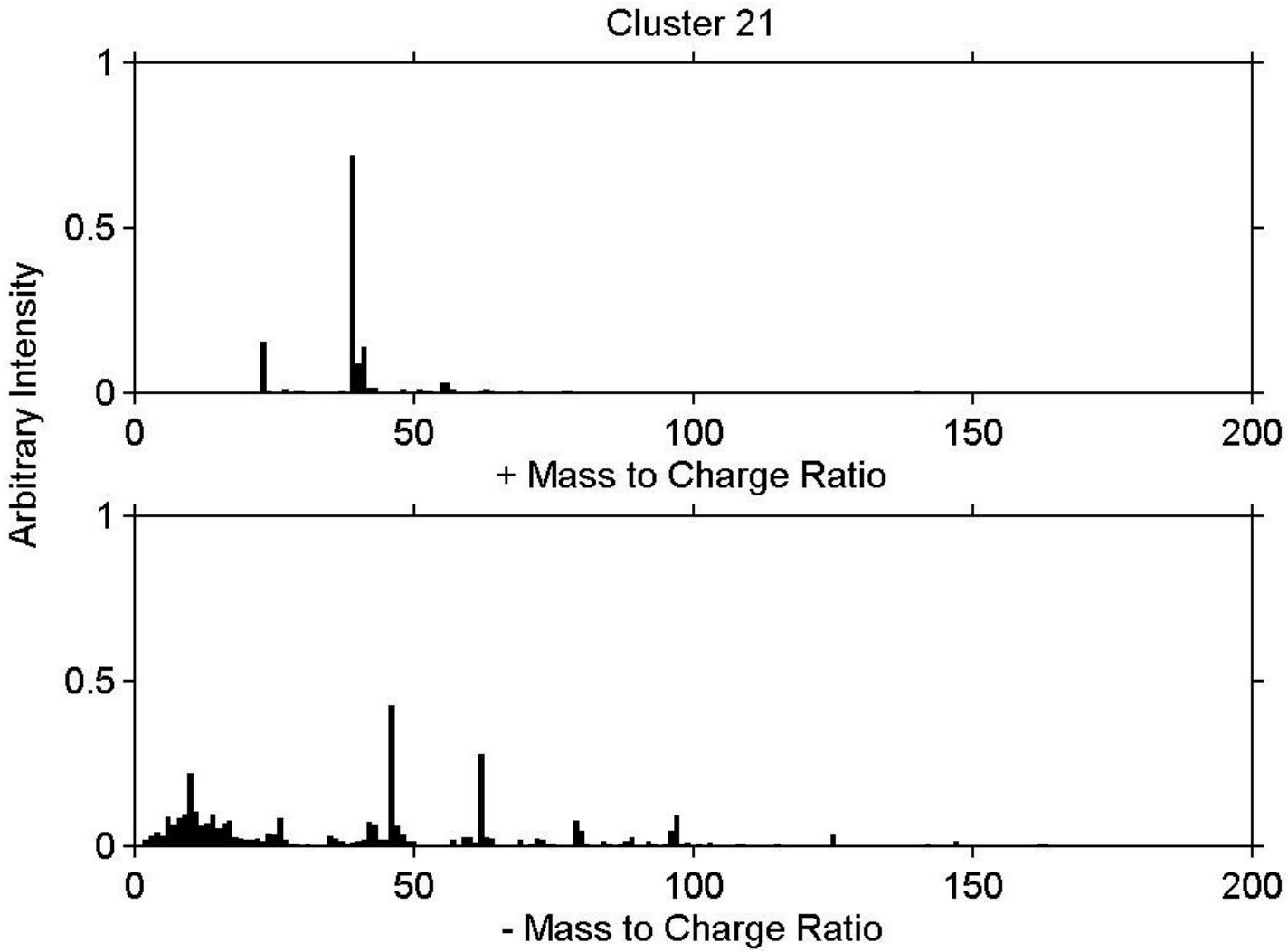
Cluster 21
Arbitrary Intensity
1
0.5
0
0
50
100
150
200
+ Mass to Charge Ratio
1
0.5
0
0
50
100
150
200
- Mass to Charge Ratio

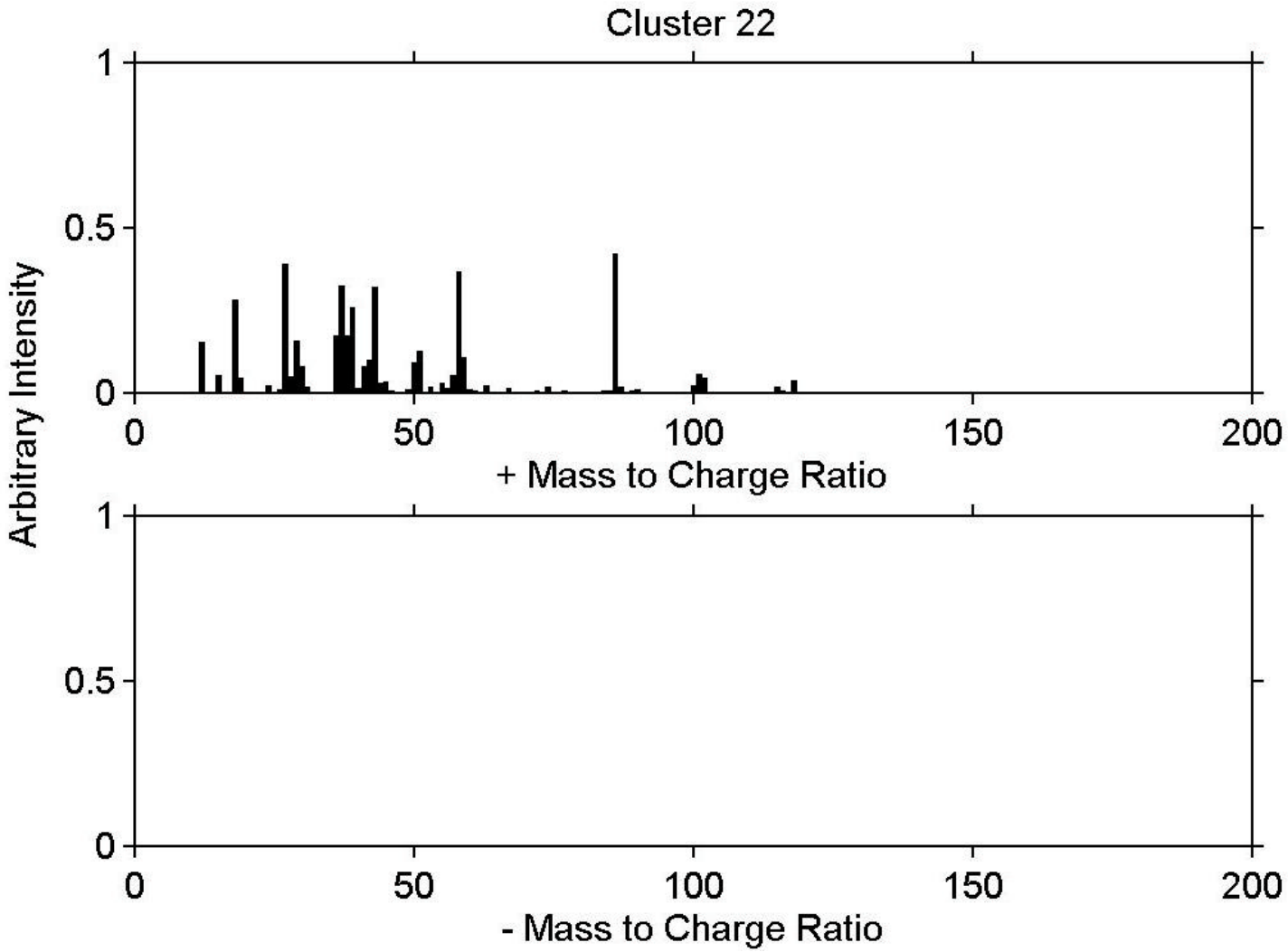
Cluster 22
Arbitrary Intensity
1
0.5
0
0
50
100
150
200
+ Mass to Charge Ratio
1
0.5
0
0
50
100
150
200
- Mass to Charge Ratio

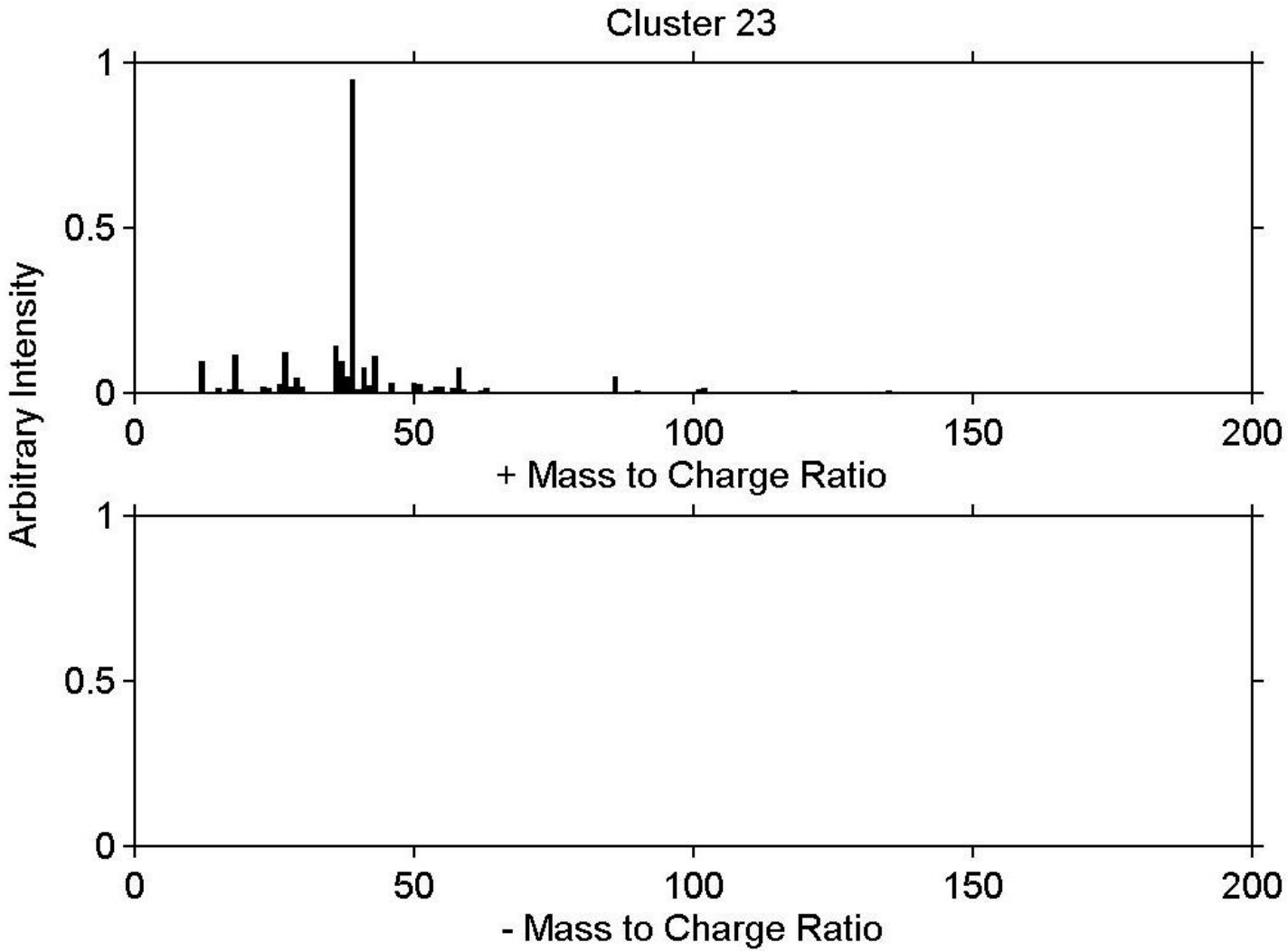
Cluster 23
Arbitrary Intensity
1
0.5
0
0
50
100
150
200
+ Mass to Charge Ratio
1
0.5
0
0
50
100
150
200
- Mass to Charge Ratio

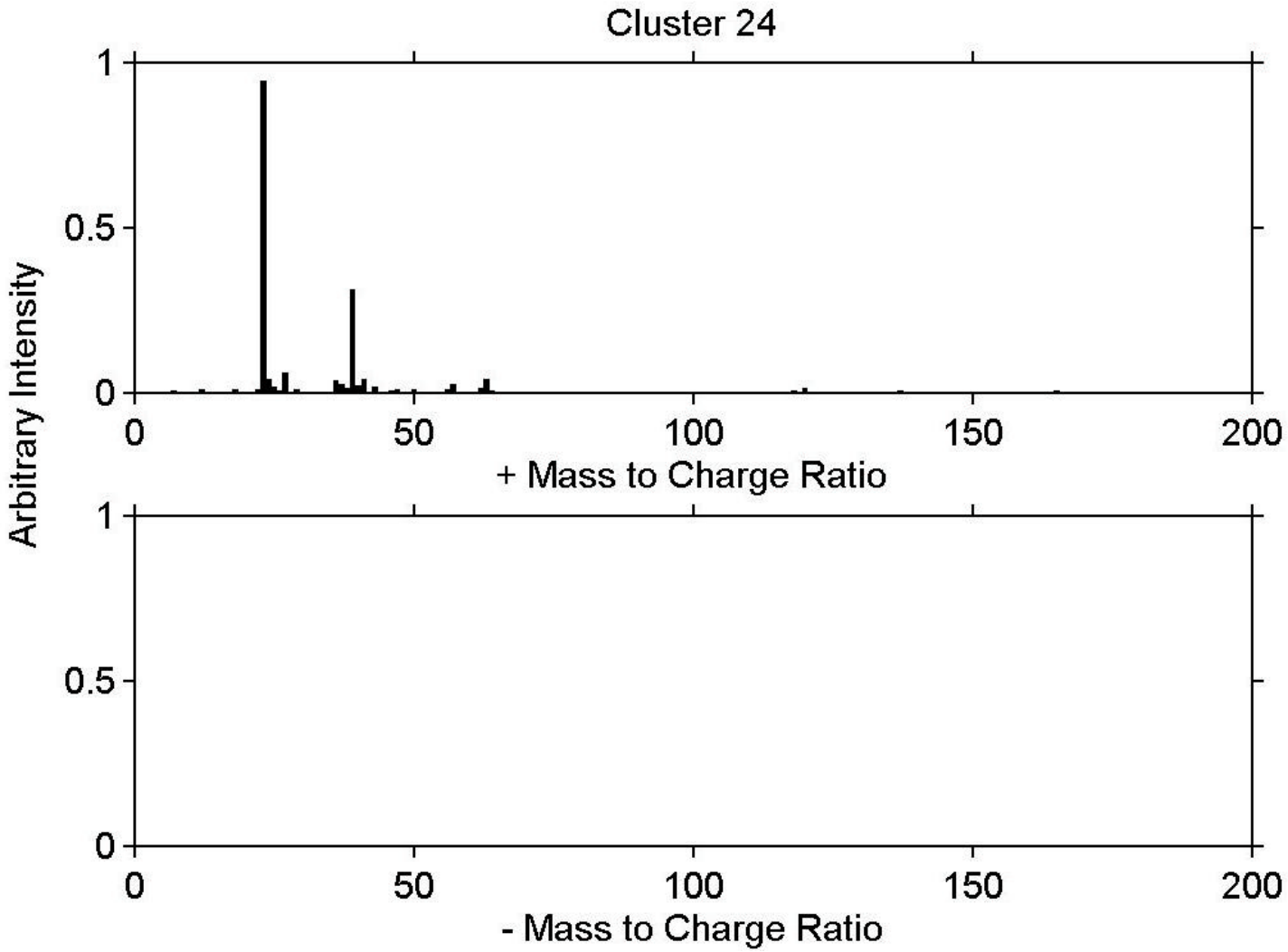
Cluster 24
Arbitrary Intensity
1
0.5
0
0
50
100
150
200
+ Mass to Charge Ratio
1
0.5
0
0
50
100
150
200
- Mass to Charge Ratio

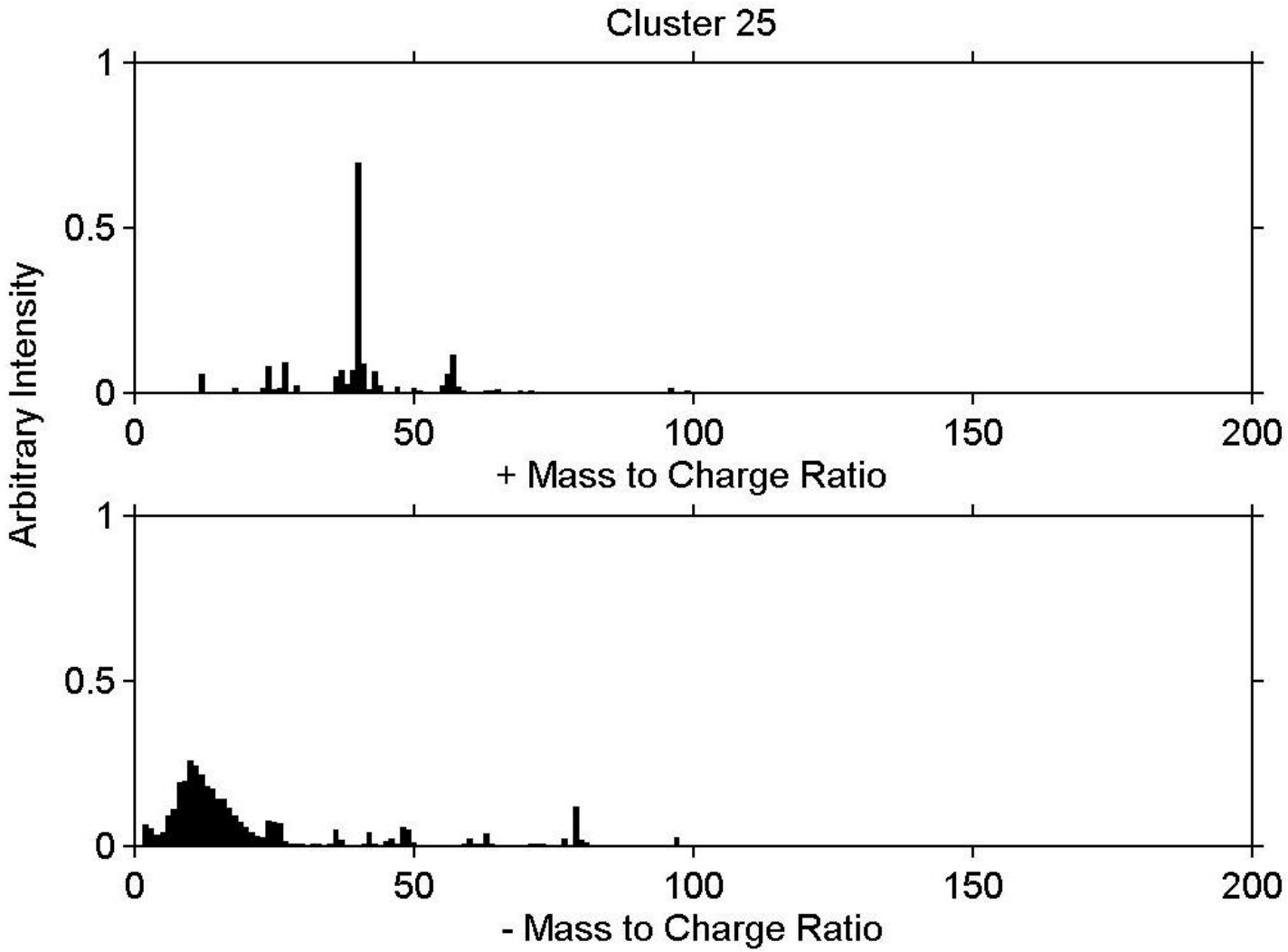
Cluster 25
Arbitrary Intensity
1
0.5
0
0
50
100
150
200
+ Mass to Charge Ratio
1
0.5
0
0
50
100
150
200
- Mass to Charge Ratio

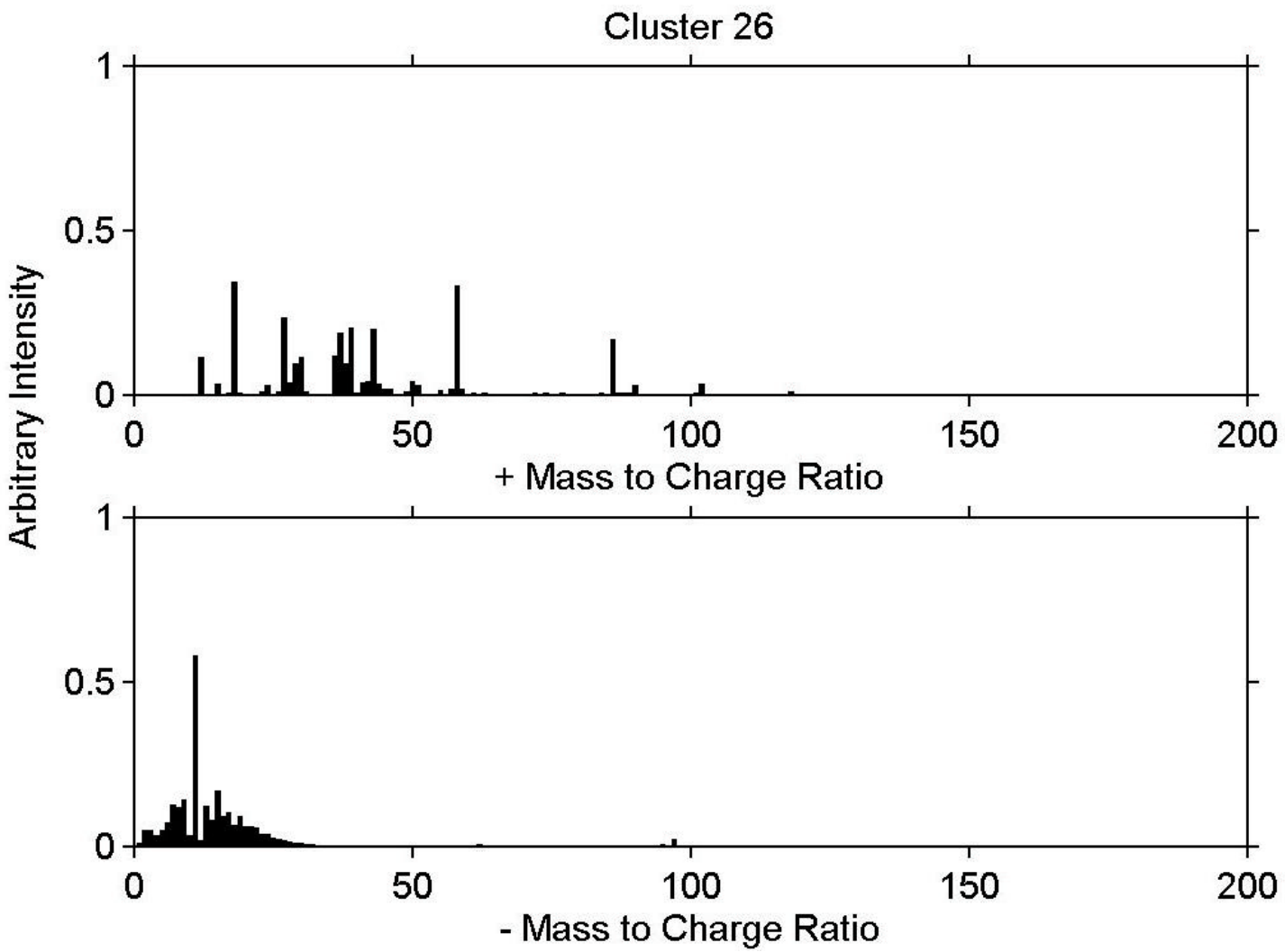
Cluster 26
Arbitrary Intensity
1
0.5
0
0
50
100
150
200
+ Mass to Charge Ratio
1
0.5
0
0
50
100
150
200
- Mass to Charge Ratio

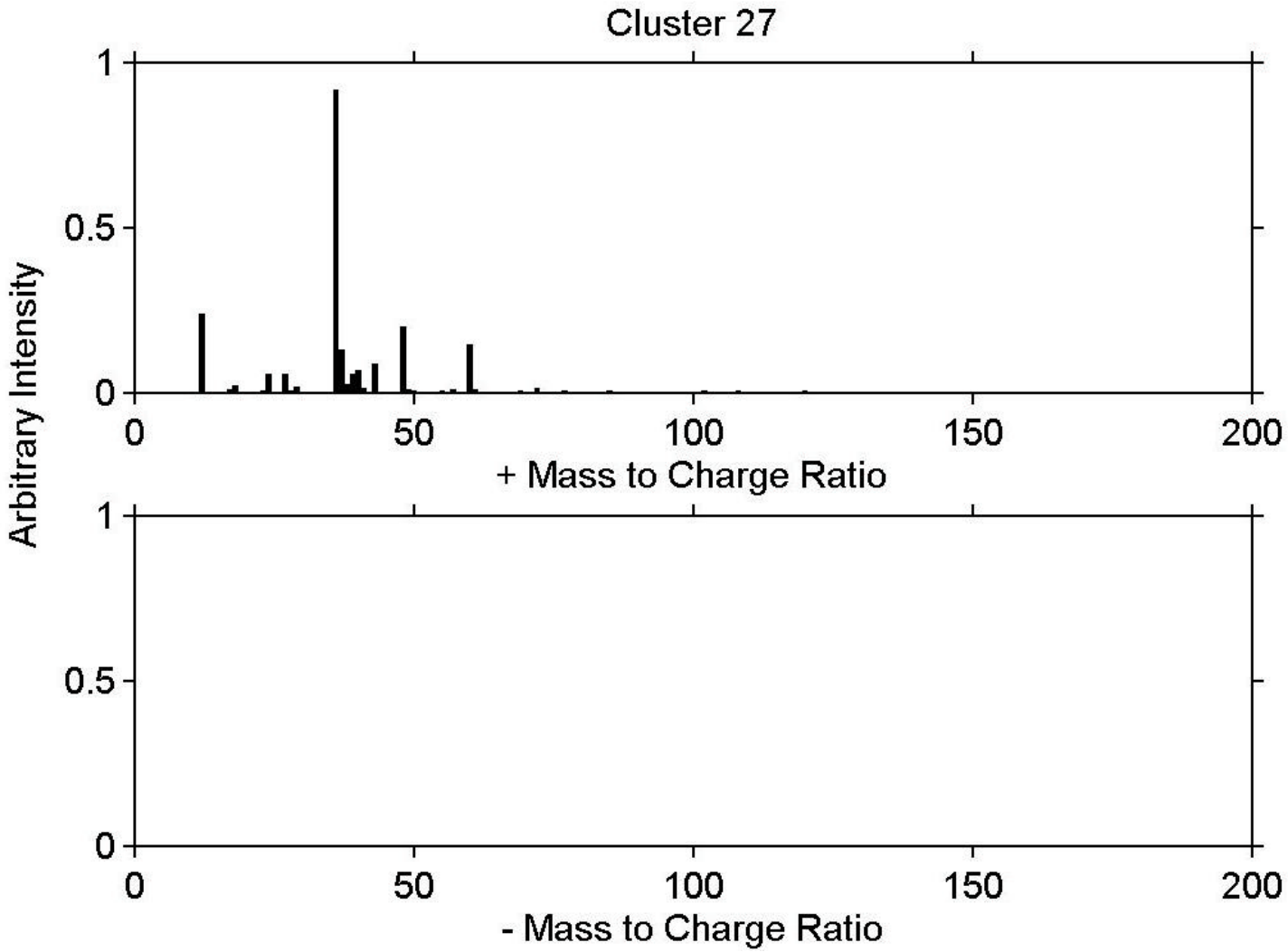
Cluster 27
Arbitrary Intensity
1
0.5
0
0
50
100
150
200
+ Mass to Charge Ratio
1
0.5
0
0
50
100
150
200
- Mass to Charge Ratio

Appendix N: Table showing matching of Azusa to ART-2a dual-ion weight vectors for car vehicle dynamometer: m/z ratio and normalized intensity (vigilance factor = 0.7; 27 clusters)

Class #	Number of particles in the class Cars	Number of particles matched to the class Azusa
1	141	35
2	122	348
3	83	0
4	65	0
5	47	0
6	44	28
7	42	441
8	39	22
9	38	284
10	35	4
11	28	146
12	27	9
13	27	0
14	22	0
15	22	34
16	21	1
17	19	4
18	19	32
19	18	3
20	18	12
21	18	39
22	17	268
23	17	27
24	16	329
25	14	0
26	12	0
27	11	106

Appendix O: ART-2a positive-ion weight vectors for Diamond Bar, Mira Loma, and Riverside ambient during trajectory-matched times September 27-29, 1997: m/z ratio and normalized intensity (vigilance factor = 0.7; 57 clusters)

Class #	Number of particles matched to the class Diamond Bar	Number of particles matched to the class Mira Loma	Number of particles matched to the class Riverside
1	10,175	437	4320
2	3825	71	62
3	5779	910	37,075
4	2946	172	836
5	2222	253	14,181
6	2102	218	454
7	895	154	88
8	1033	202	238
9	718	312	256
10	529	141	428
11	728	442	836
12	540	331	759
13	638	72	66
14	745	1584	2169
15	428	198	272
16	686	102	922
17	713	64	2756
18	591	893	267
19	614	277	520
20	492	1065	80
21	502	479	1255
22	391	238	1521
23	565	229	40
24	310	147	1006
25	384	445	423
26	211	174	301
27	374	178	594
28	317	316	560
29	365	219	597
30	259	153	149
31	264	90	157
32	72	249	10
33	24	67	1
34	209	204	167
35	49	78	10

Class #	Number of particles matched to the class Diamond Bar	Number of particles matched to the class Mira Loma	Number of particles matched to the class Riverside
36	227	45	108
37	57	35	0
38	134	39	431
39	30	56	9
40	50	24	70
41	171	22	16
42	39	50	179
43	1	0	967
44	0	4	894
45	6	9	1444
46	3	0	753
47	1	0	289
48	3	0	357
49	0	2	434
50	0	0	752
51	3	12	528
52	24	19	509
53	3	0	384
54	1	2	358
55	44	17	216
56	9	0	346
57	2	6	257

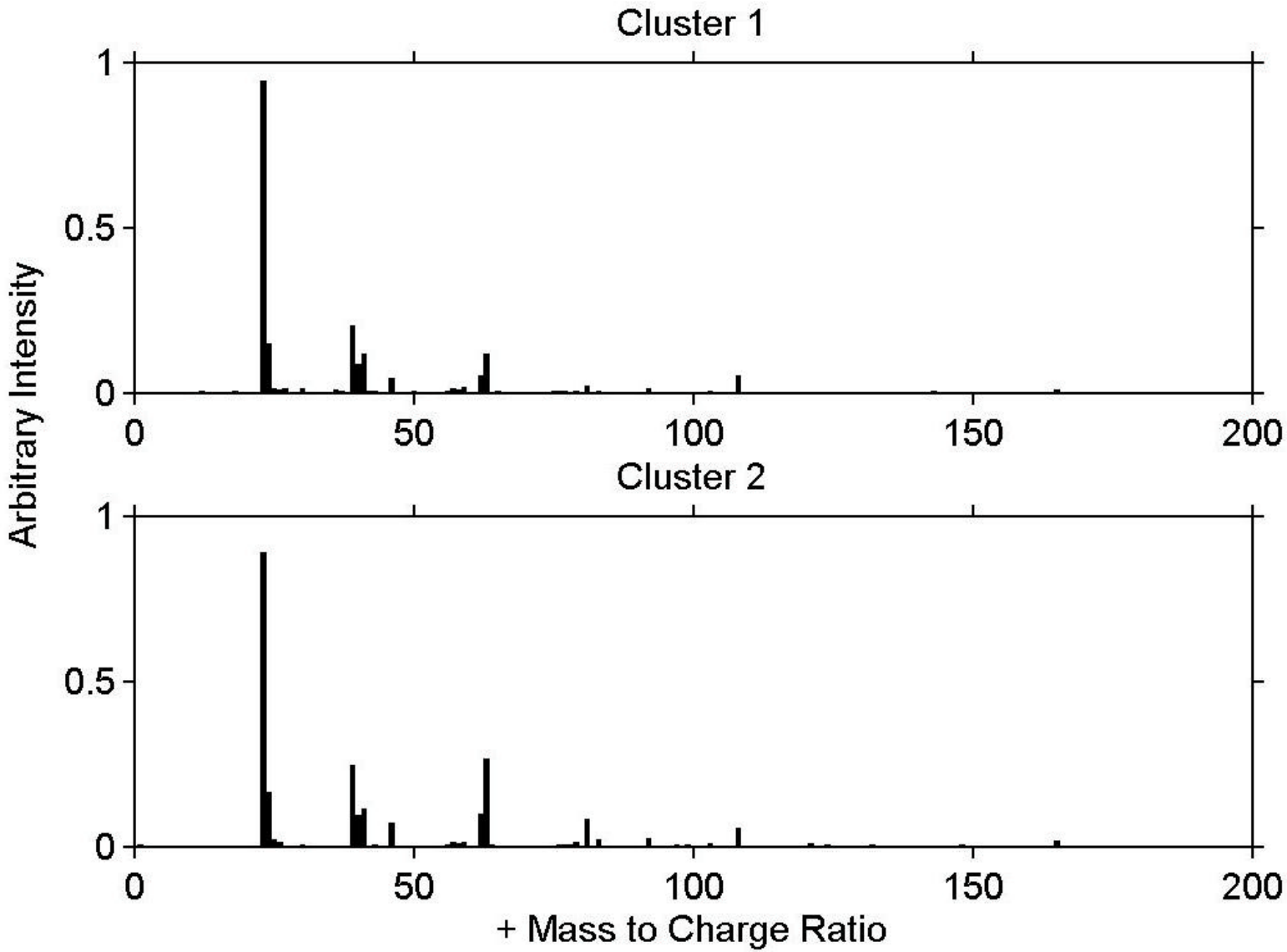
Cluster 1
Cluster 2
Arbitrary Intensity
1
0.5
0
0
50
100
150
200
+ Mass to Charge Ratio

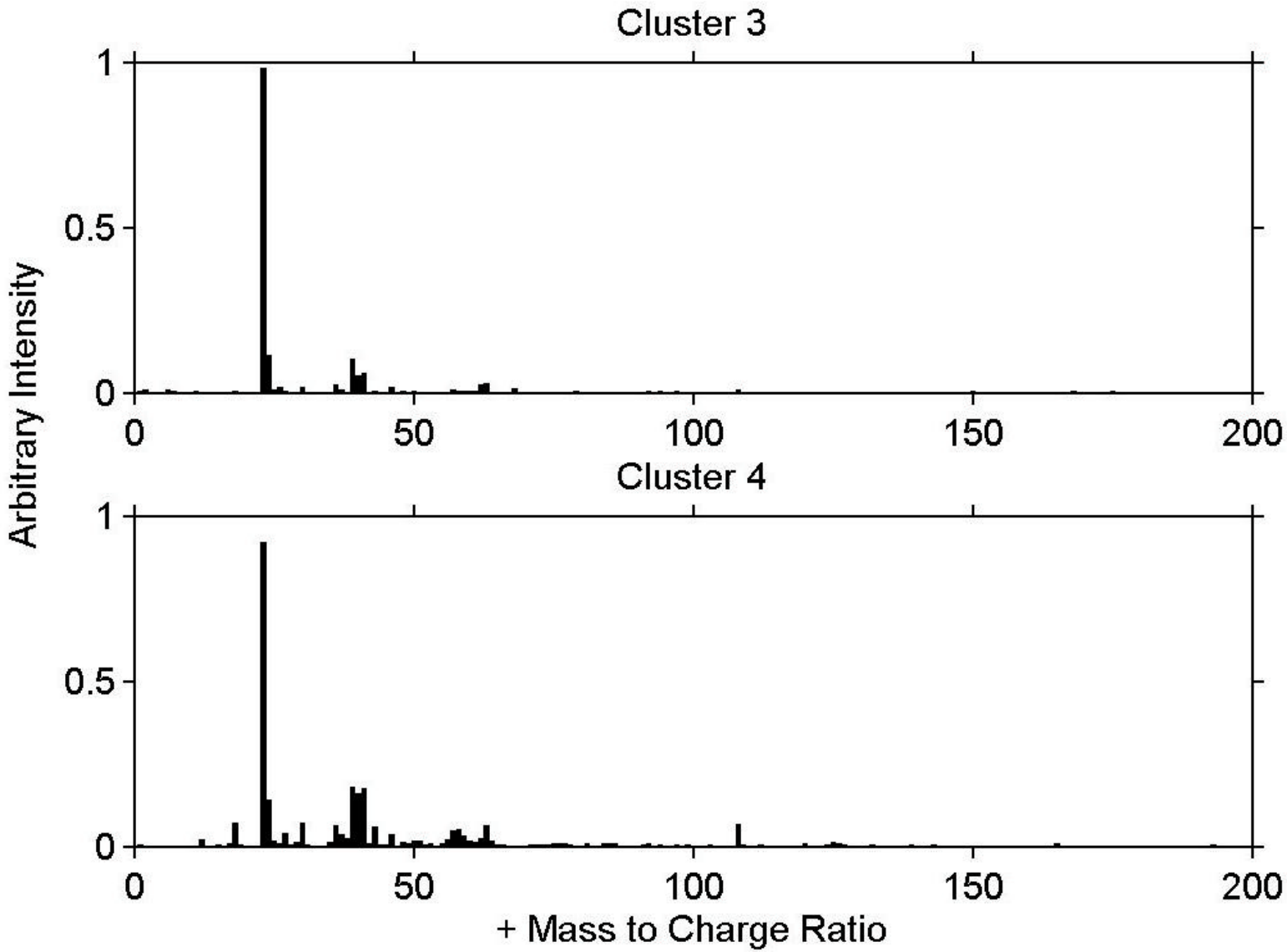
Cluster 3
Cluster 4
Arbitrary Intensity
+ Mass to Charge Ratio
0
0.5
1
0
50
100
150
200

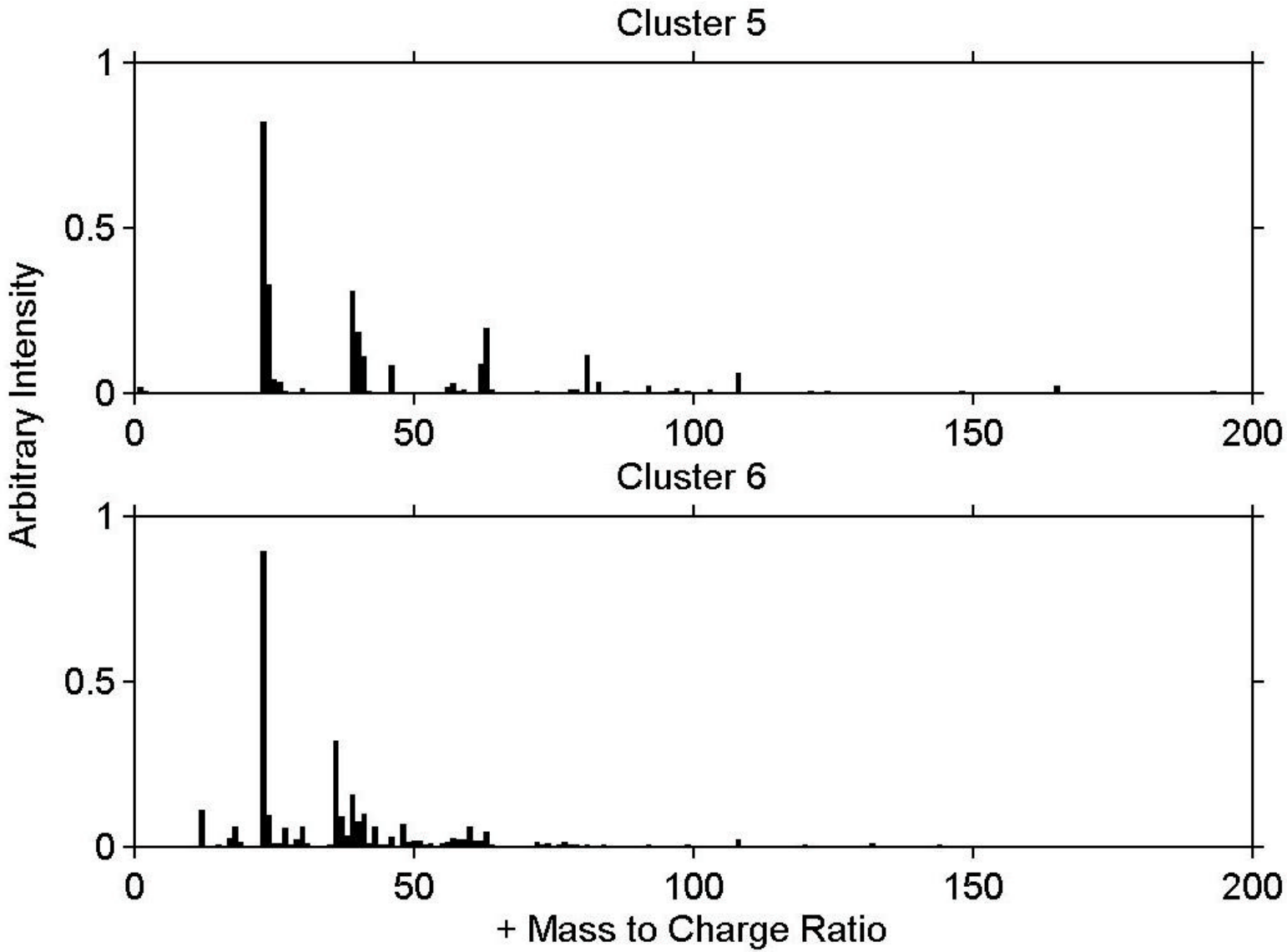
Cluster 5
Cluster 6
Arbitrary Intensity
1
0.5
0
0
50
100
150
200
+ Mass to Charge Ratio

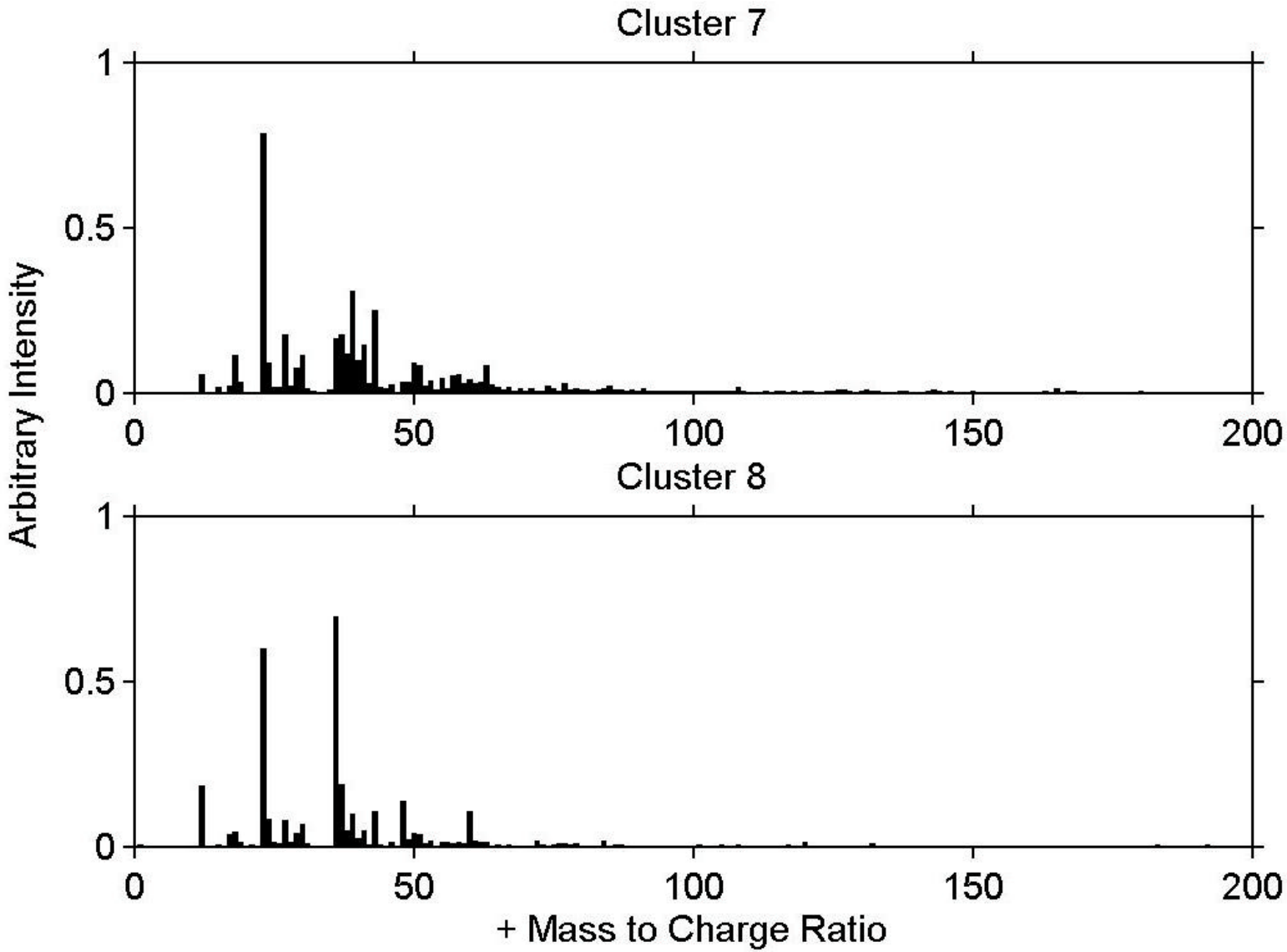
Cluster 7
Cluster 8
Arbitrary Intensity
+ Mass to Charge Ratio
0
0.5
1
0
50
100
150
200

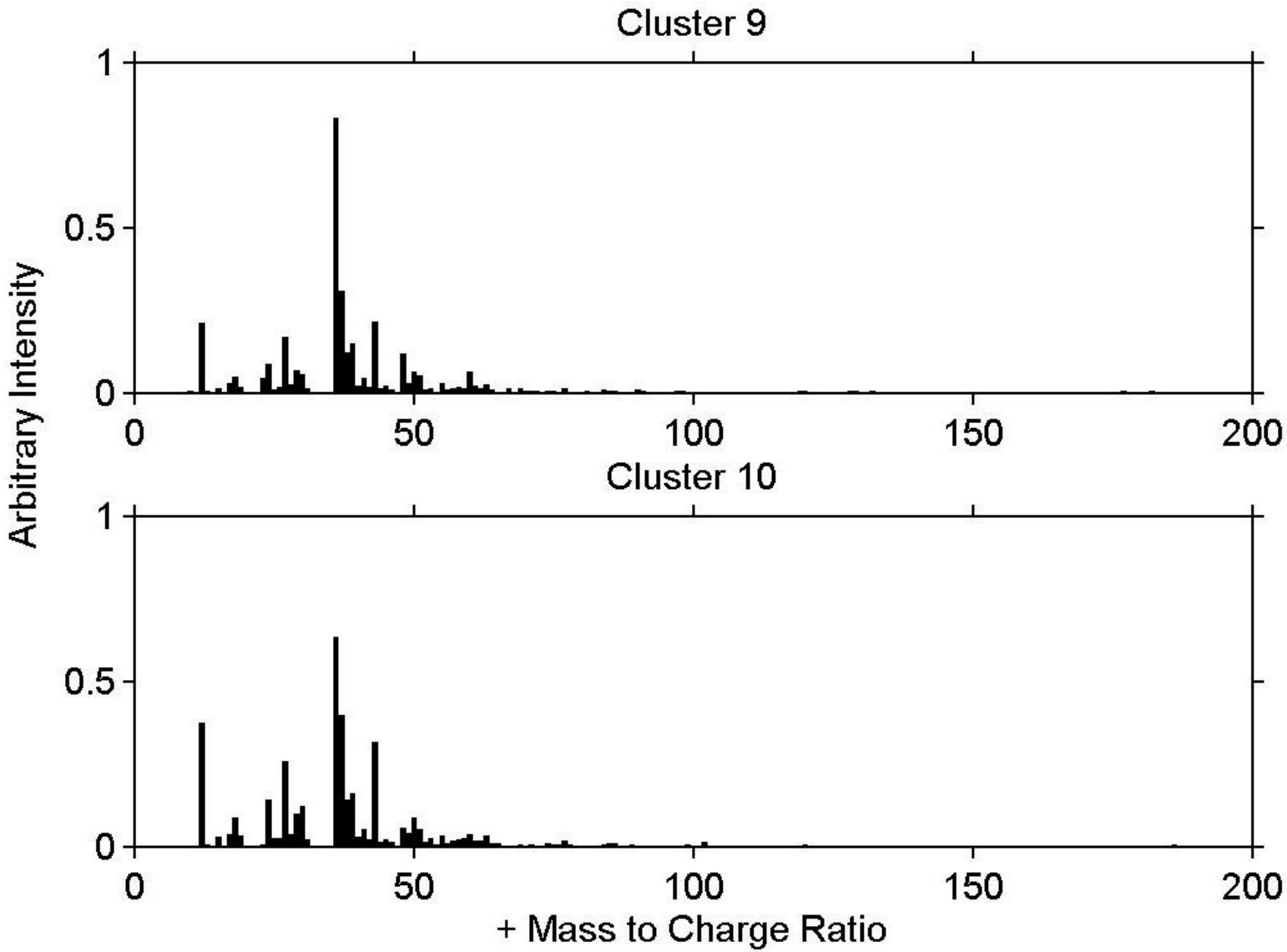
Cluster 9
Cluster 10
Arbitrary Intensity
1
0.5
0
0
50
100
150
200
+ Mass to Charge Ratio

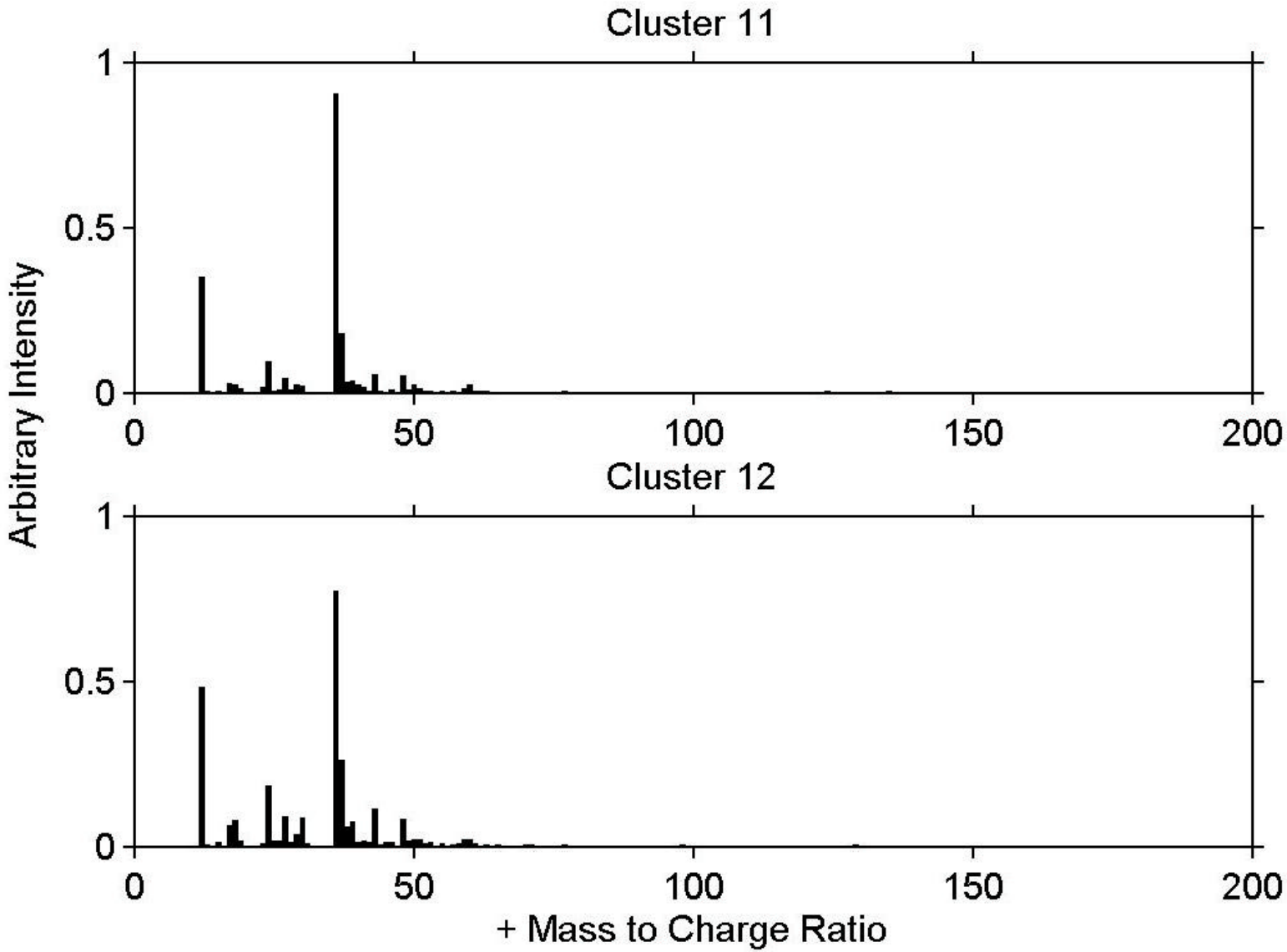
Cluster 11
Cluster 12
Arbitrary Intensity
1
0.5
0
0
50
100
150
200
+ Mass to Charge Ratio

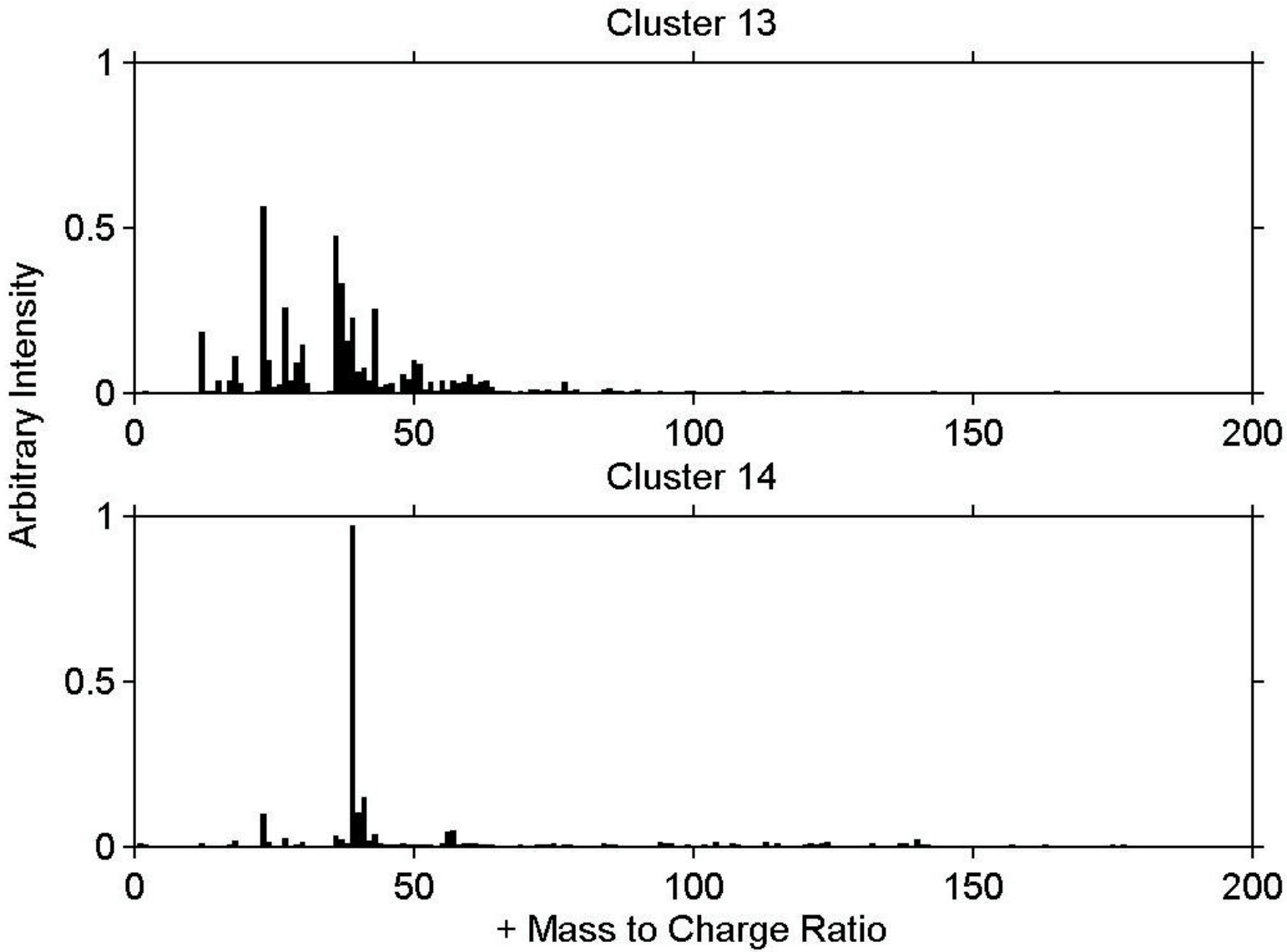
Cluster 13
Cluster 14
Arbitrary Intensity
+ Mass to Charge Ratio
0
0.5
1
0
50
100
150
200

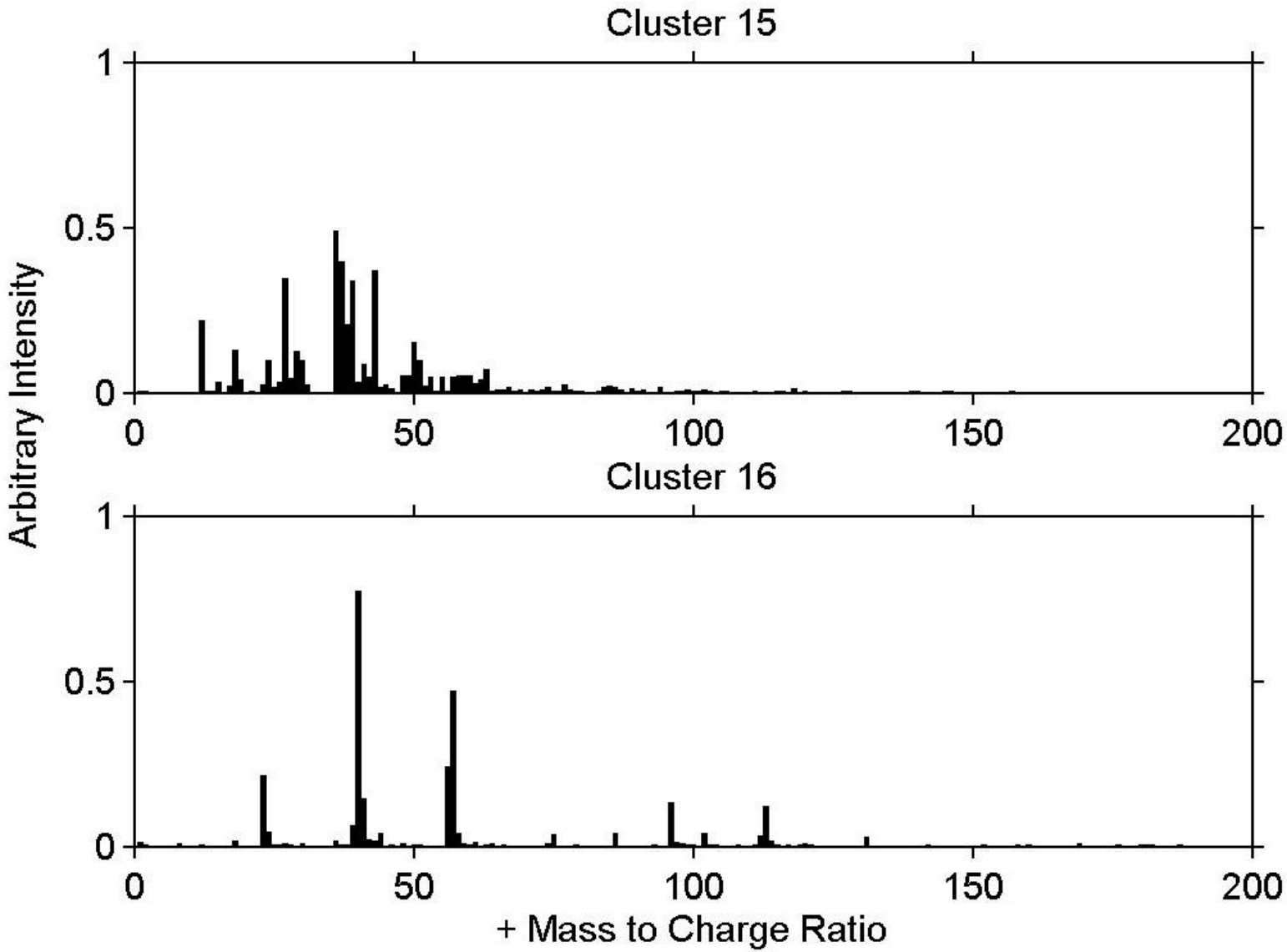
Cluster 15
Cluster 16
Arbitrary Intensity
+ Mass to Charge Ratio
0
0.5
1
0
50
100
150
200

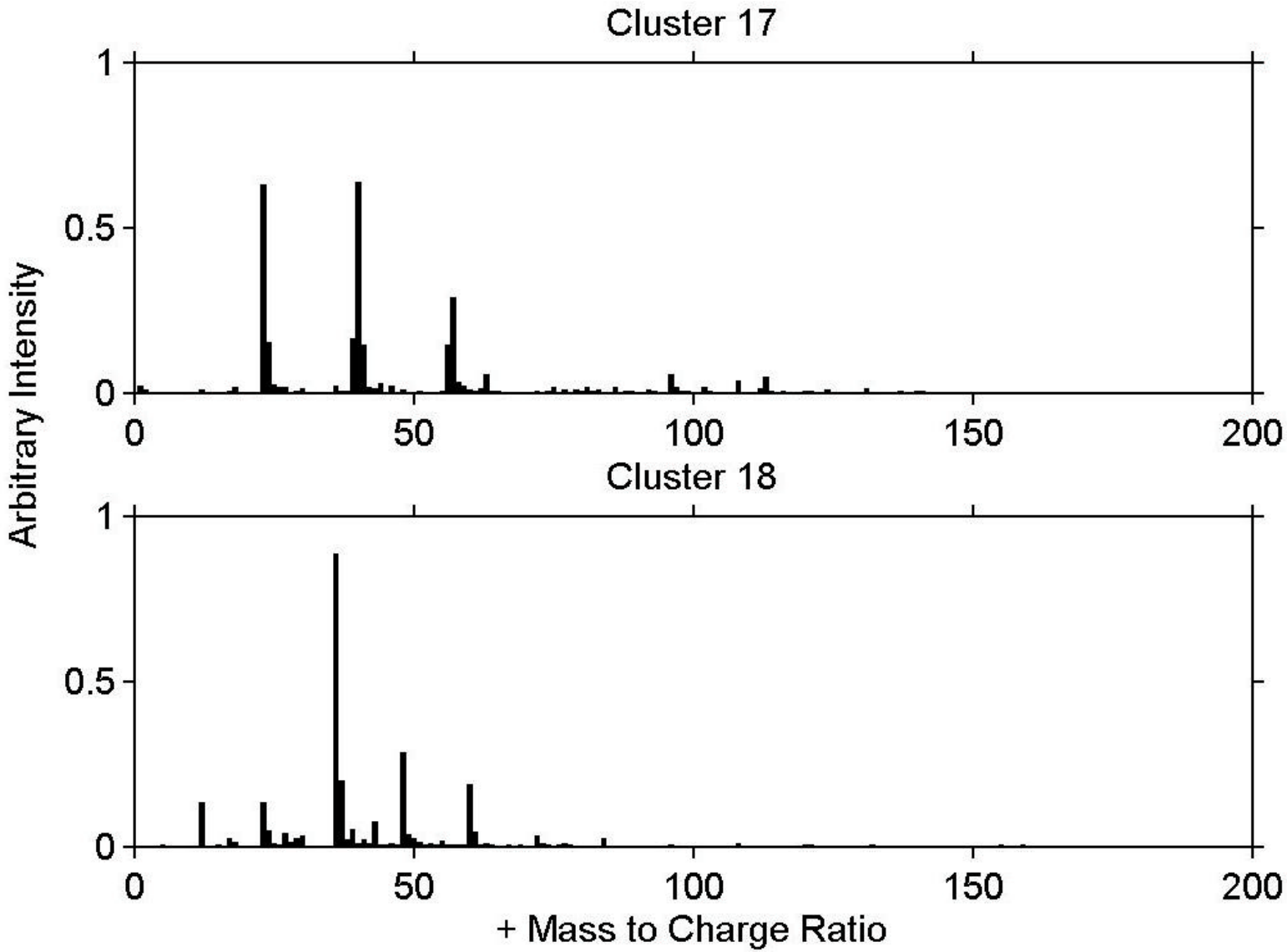
Cluster 17
Cluster 18
Arbitrary Intensity
+ Mass to Charge Ratio
0
0.5
1
0
50
100
150
200

300

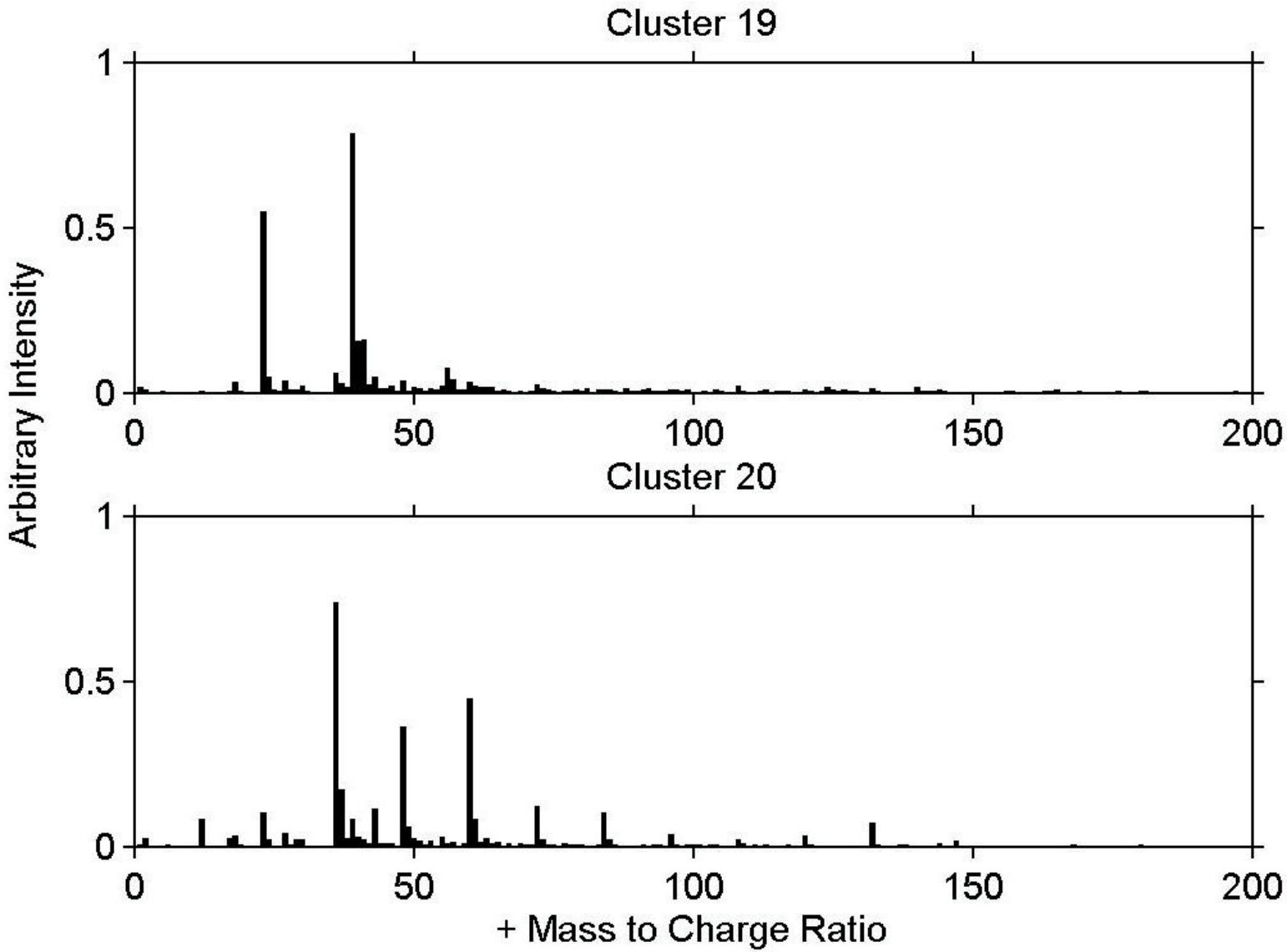
Cluster 19
Cluster 20
Arbitrary Intensity
+ Mass to Charge Ratio
0
0.5
1
0
50
100
150
200

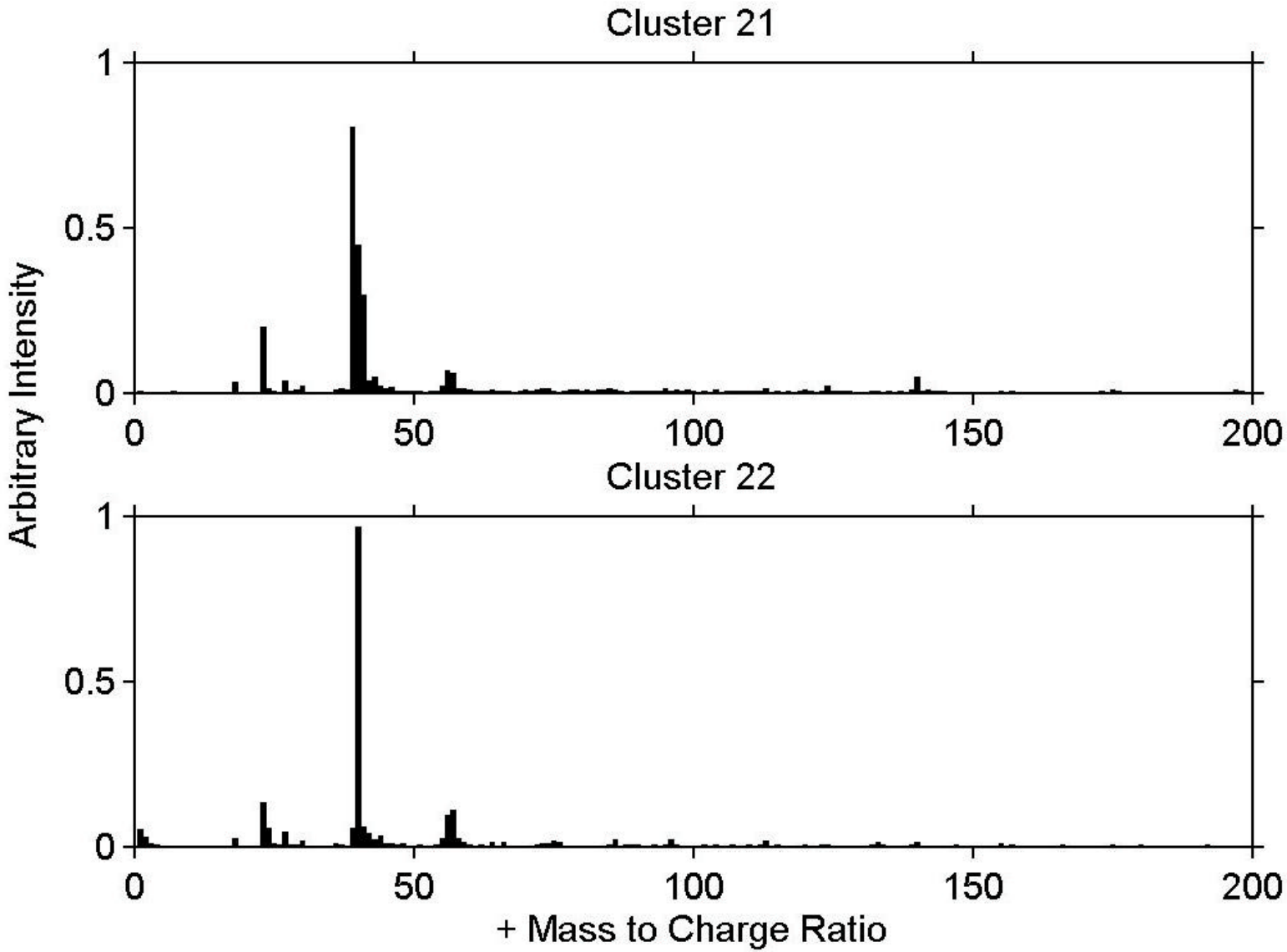
Cluster 21
Cluster 22
Arbitrary Intensity
1
0.5
0
0
50
100
150
200
+ Mass to Charge Ratio

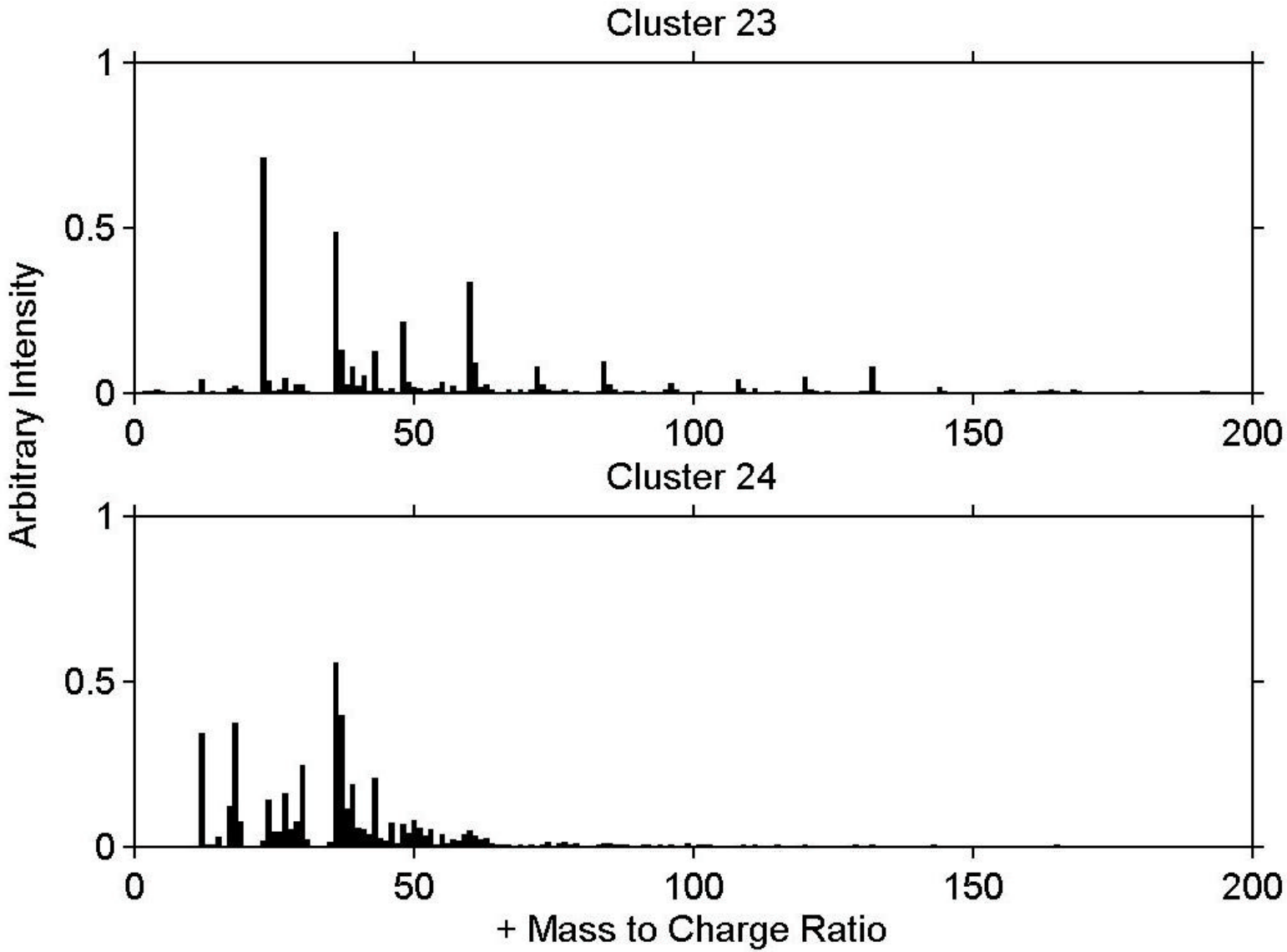
Cluster 23
Cluster 24
Arbitrary Intensity
+ Mass to Charge Ratio
0
0.5
1
0
50
100
150
200

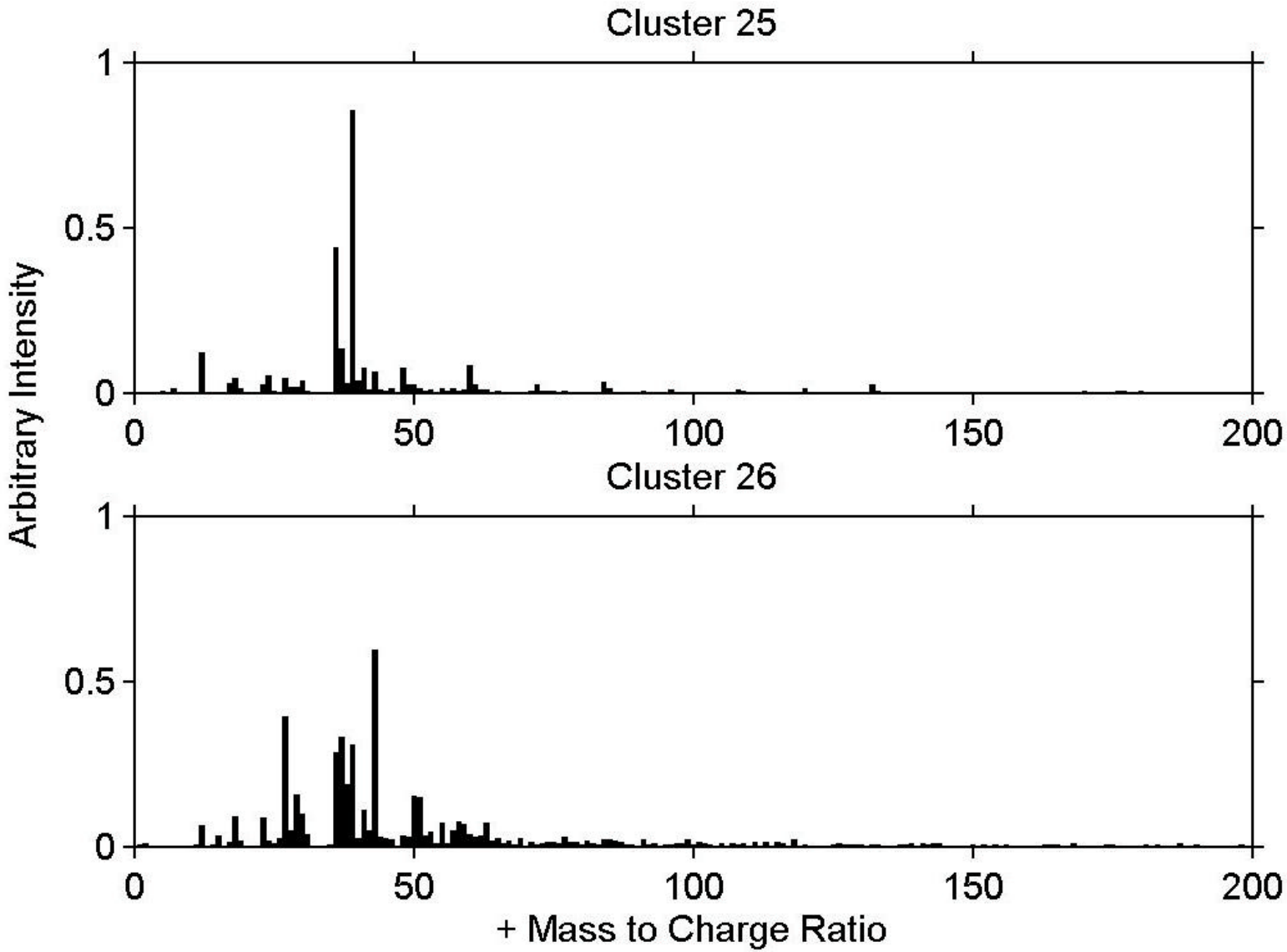
Cluster 25
Cluster 26
Arbitrary Intensity
+ Mass to Charge Ratio
0
0.5
1
0
50
100
150
200

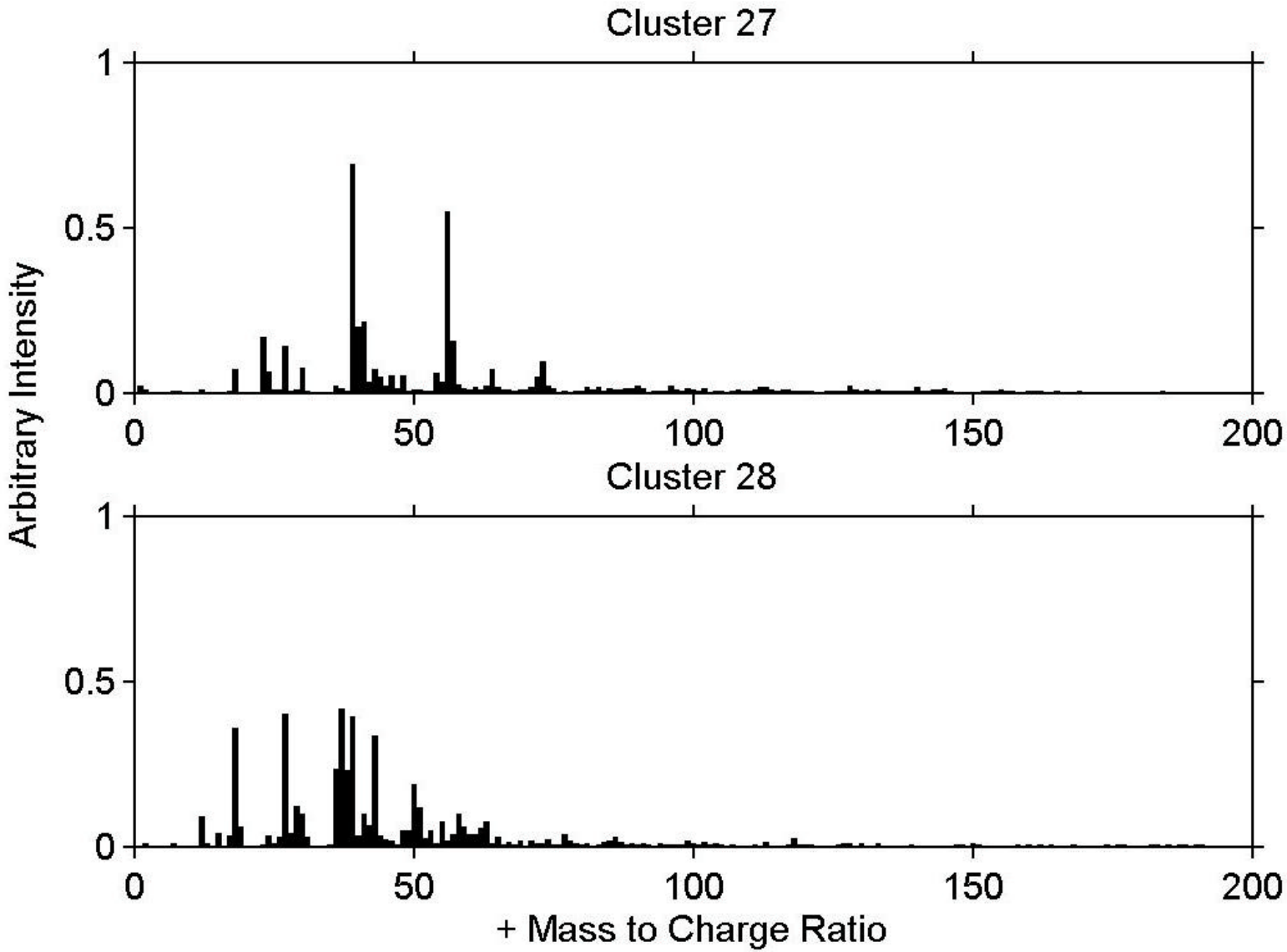
Cluster 27
Cluster 28
Arbitrary Intensity
+ Mass to Charge Ratio
0
0.5
1
0
50
100
150
200

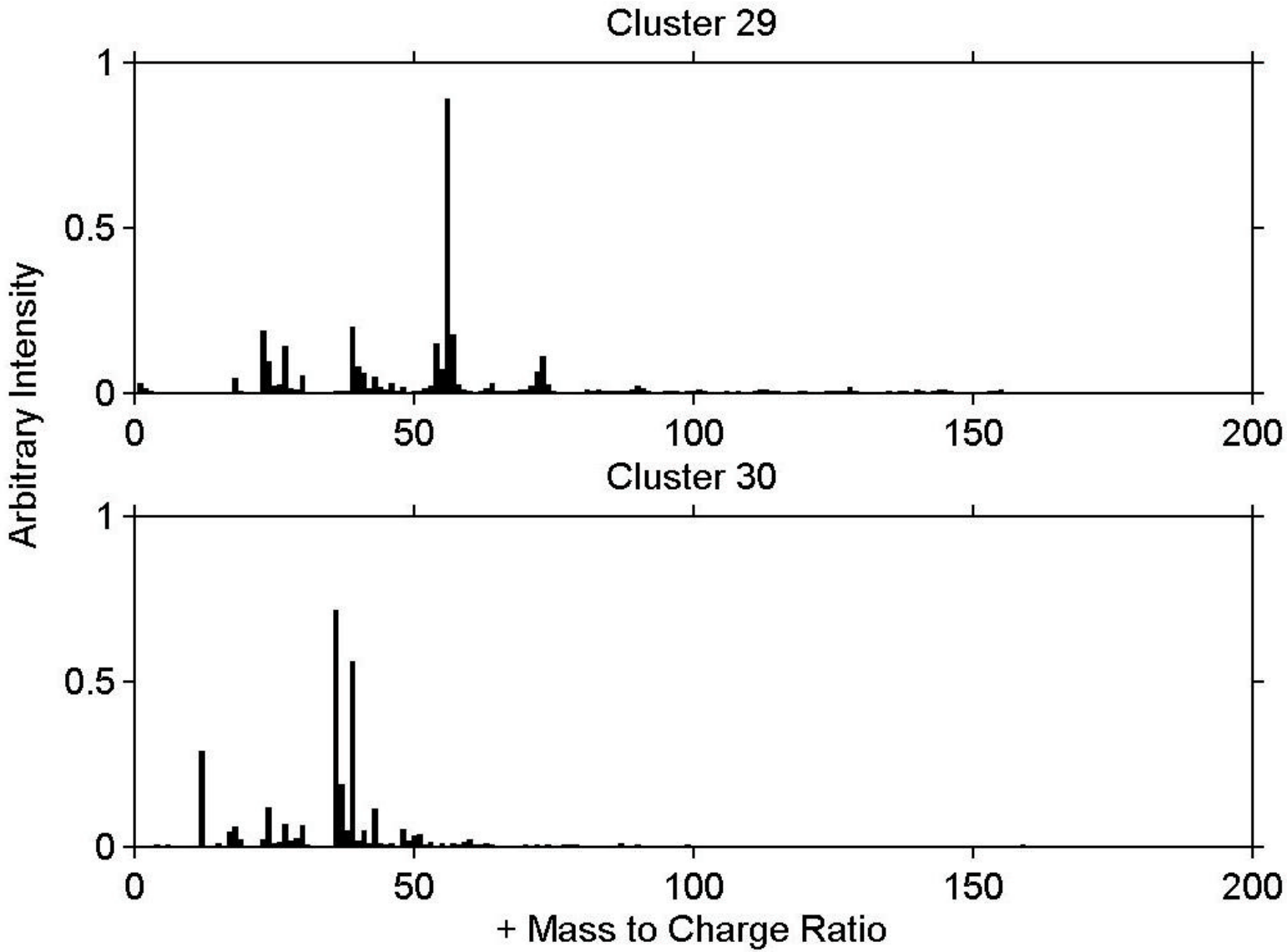
Cluster 29
Cluster 30
Arbitrary Intensity
+ Mass to Charge Ratio
0
0.5
1
0
50
100
150
200

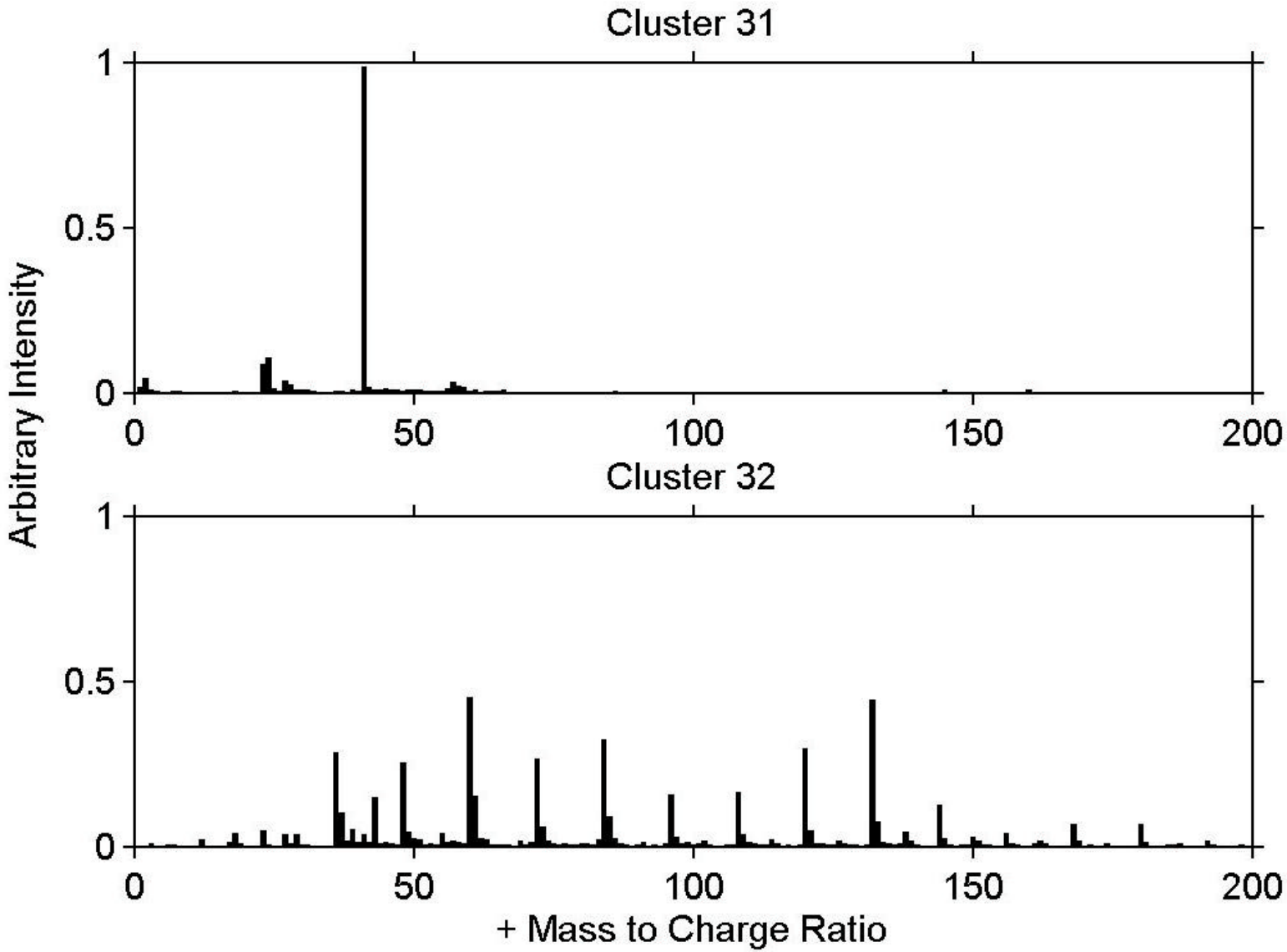
Cluster 31
Cluster 32
Arbitrary Intensity
1
0.5
0
0
50
100
150
200
+ Mass to Charge Ratio

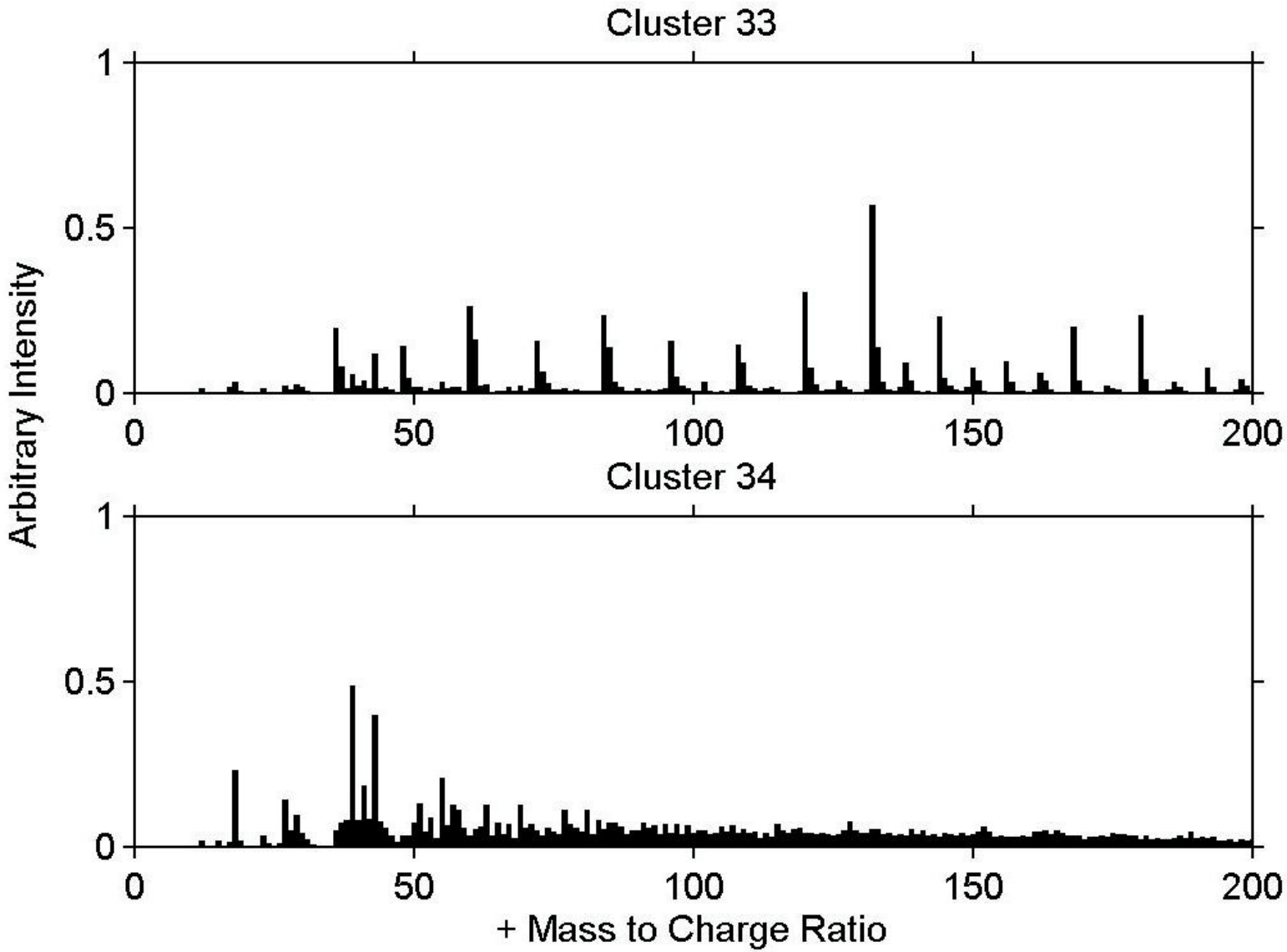
Cluster 33
Cluster 34
Arbitrary Intensity
+ Mass to Charge Ratio
0
0.5
1
0
50
100
150
200

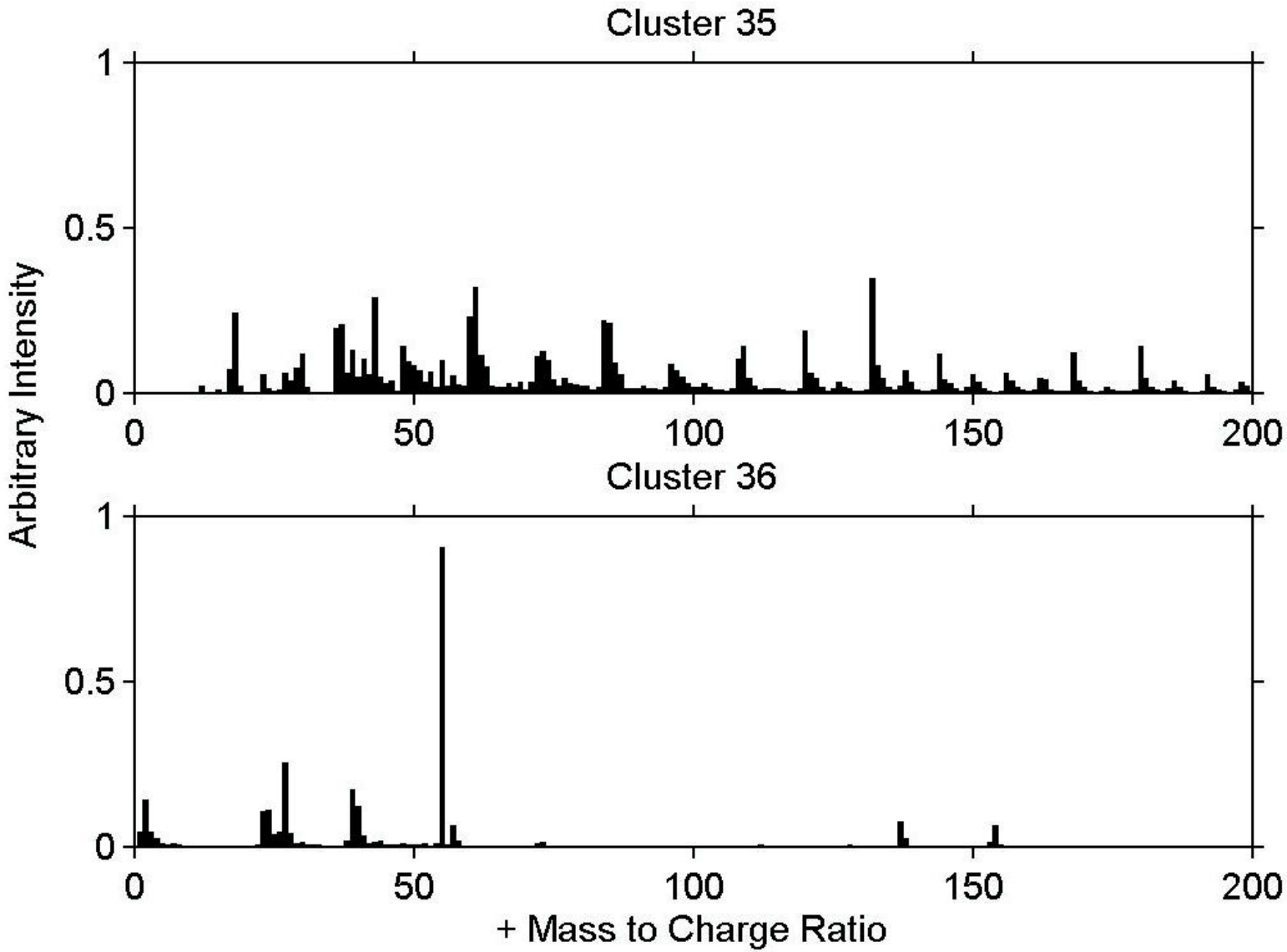
Cluster 35
Cluster 36
Arbitrary Intensity
+ Mass to Charge Ratio
0
0.5
1
0
50
100
150
200

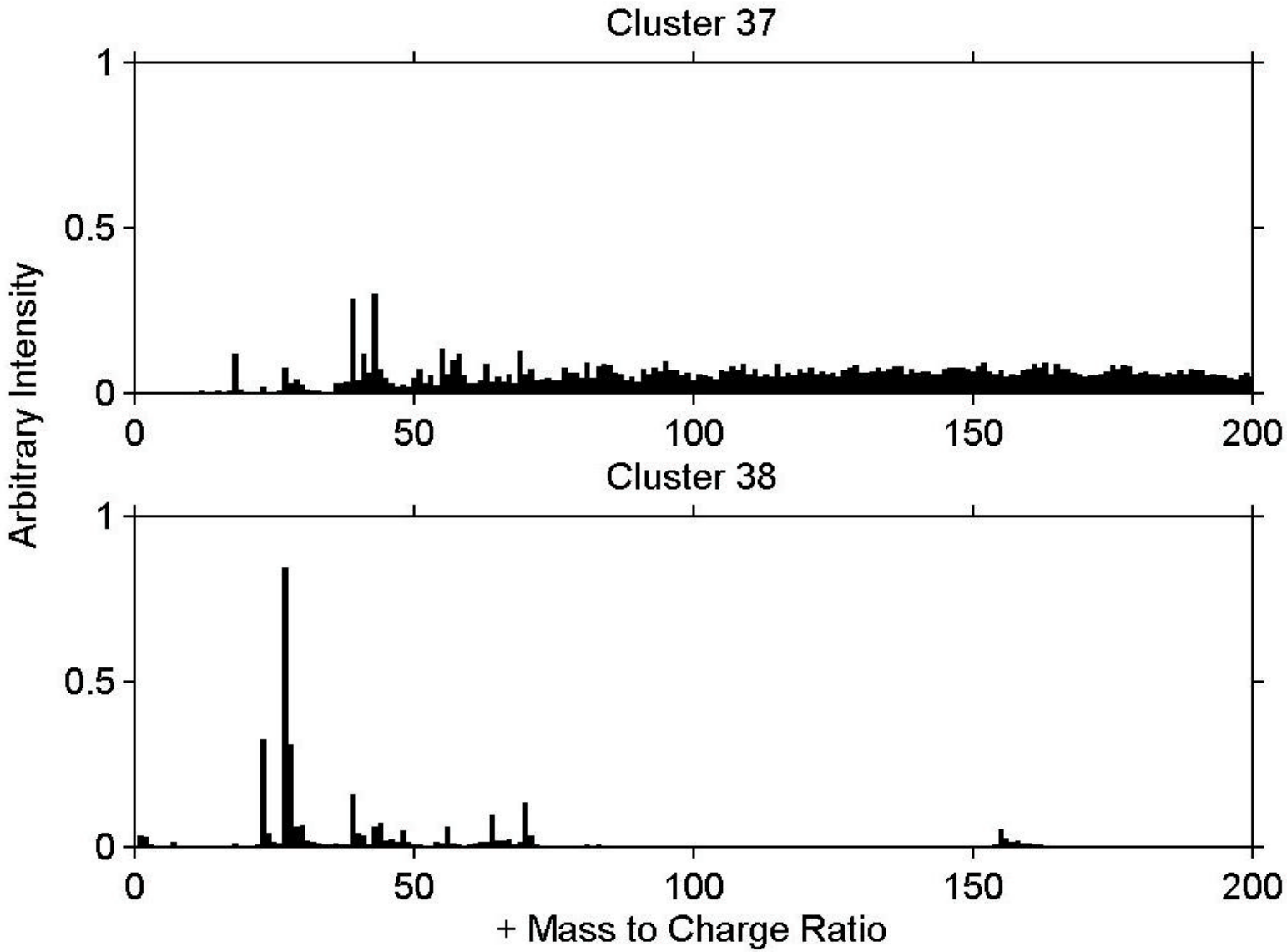
Cluster 37
Cluster 38
Arbitrary Intensity
+ Mass to Charge Ratio
0
0.5
1
0
50
100
150
200

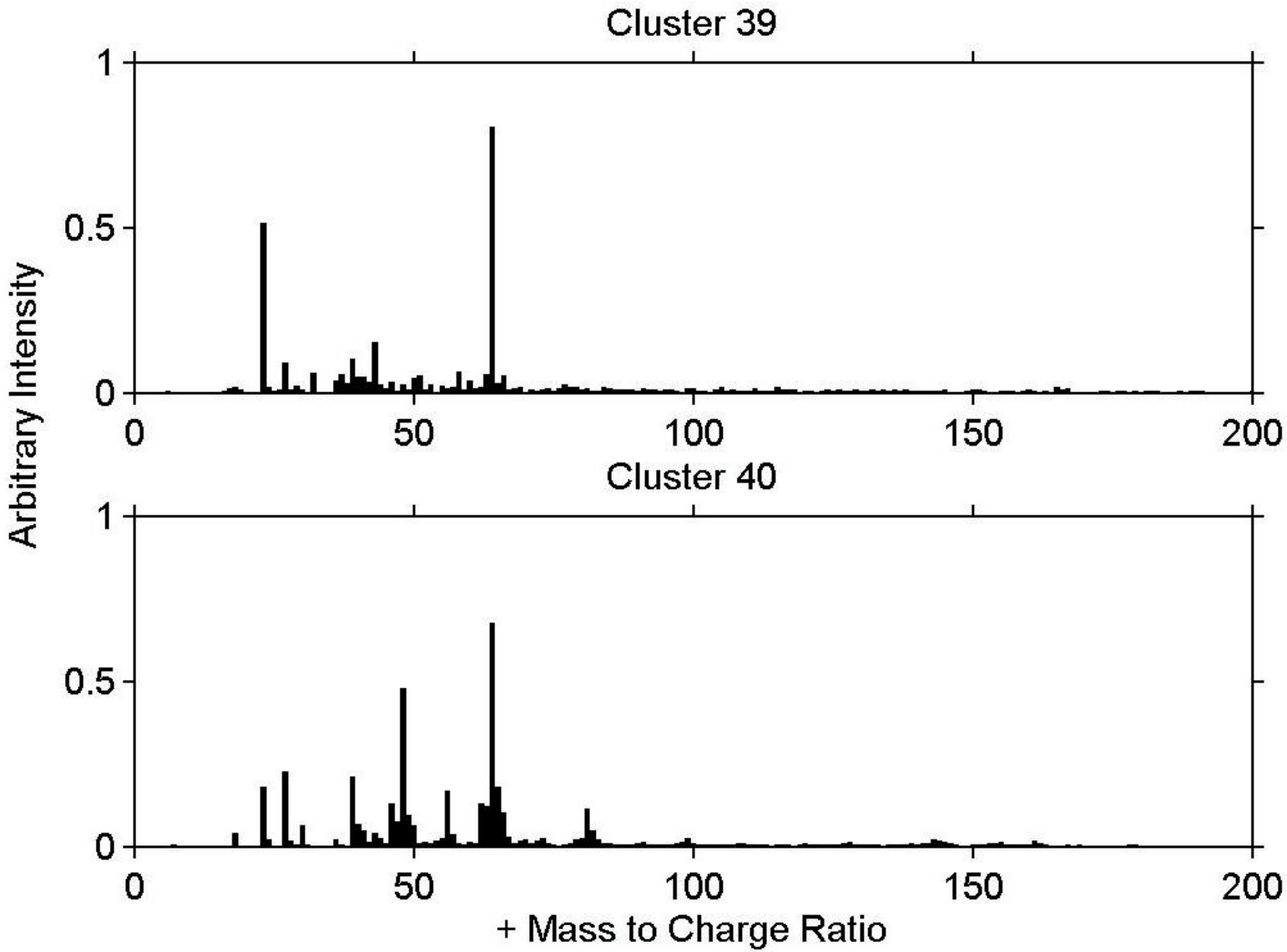
Cluster 39
Cluster 40
Arbitrary Intensity
+ Mass to Charge Ratio
0
0.5
1
0
50
100
150
200

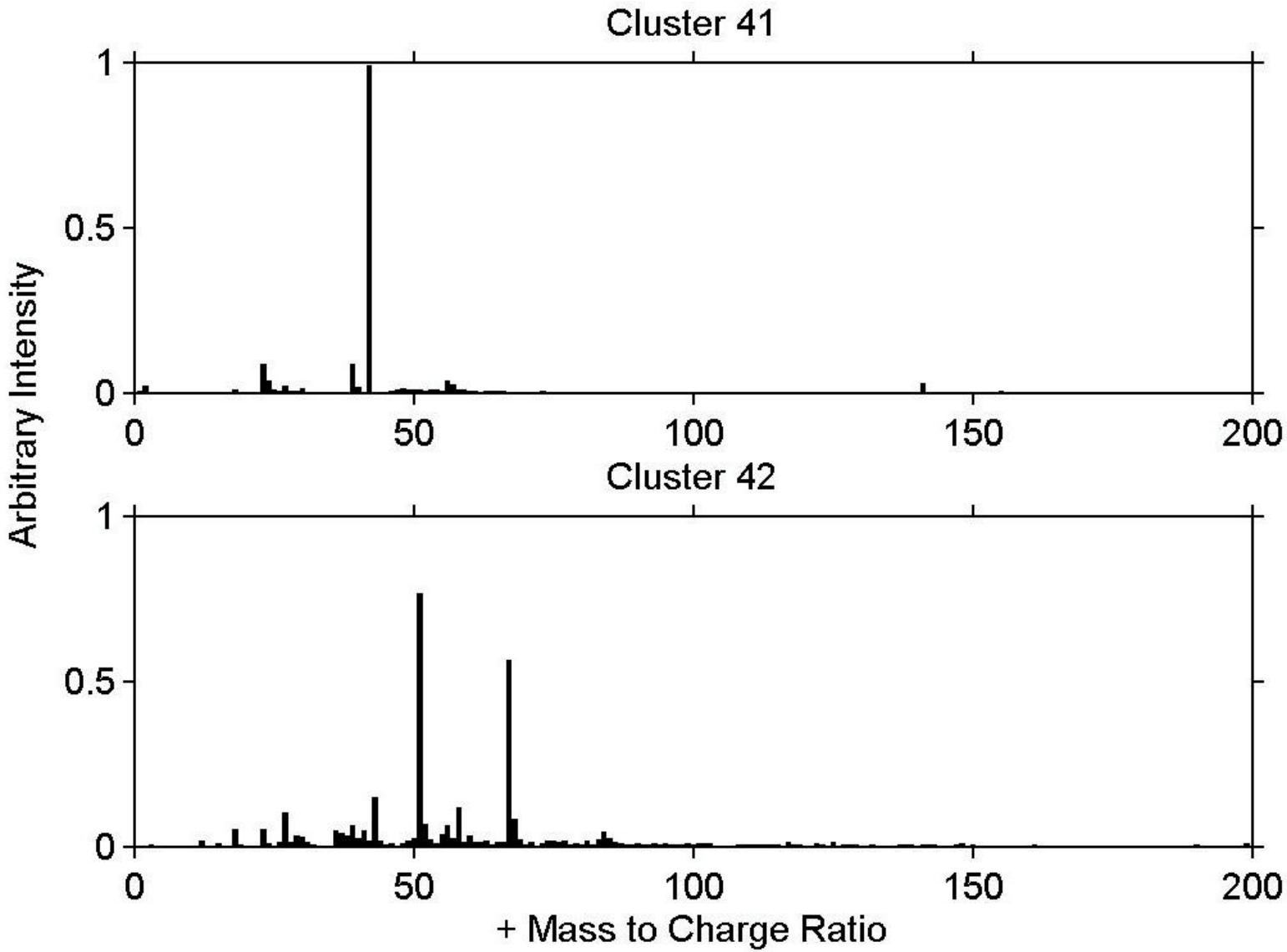
Cluster 41
Cluster 42
Arbitrary Intensity
+ Mass to Charge Ratio
0
0.5
1
0
50
100
150
200

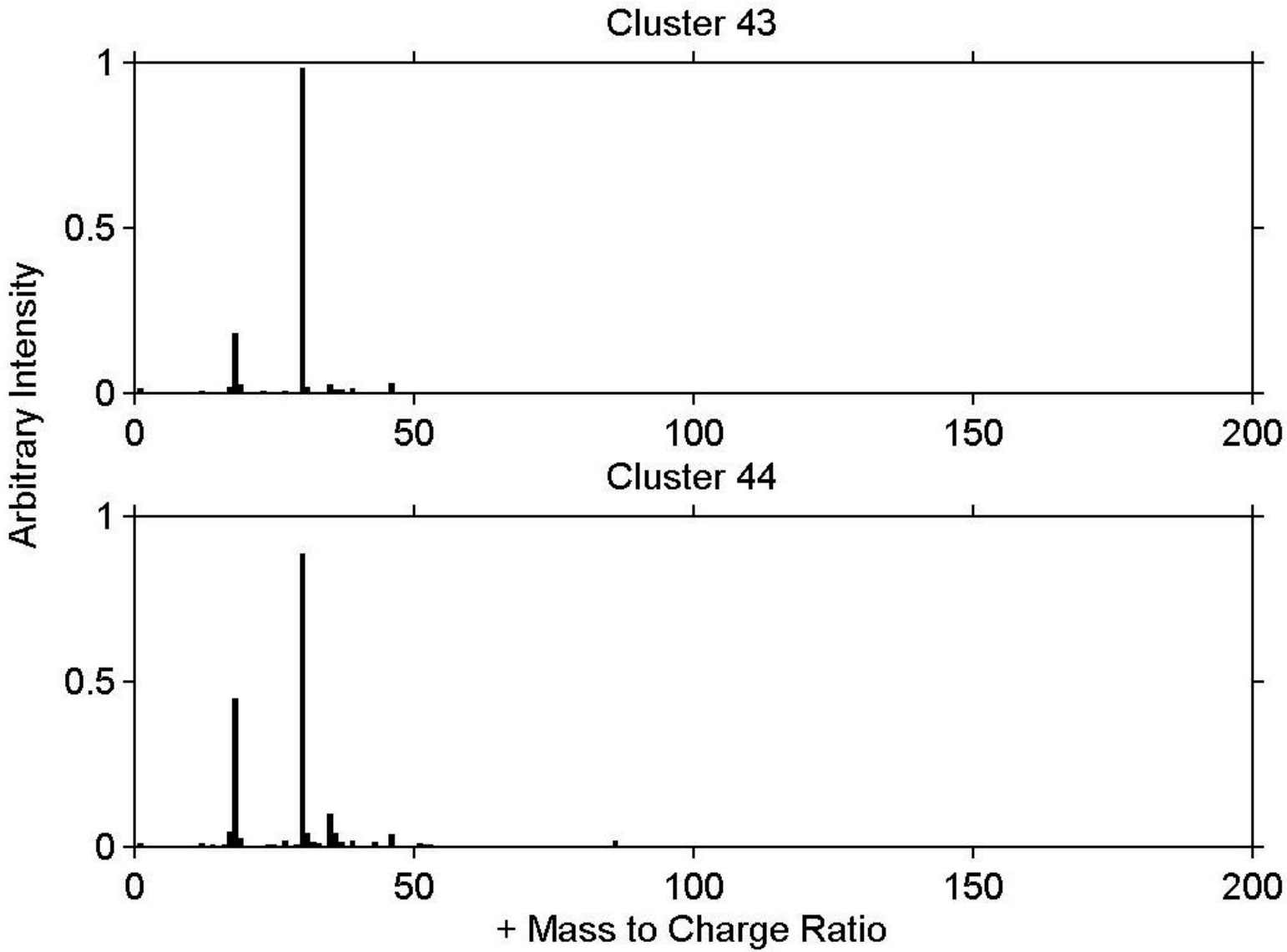
Cluster 43
Cluster 44
Arbitrary Intensity
1
0.5
0
0
50
100
150
200
+ Mass to Charge Ratio

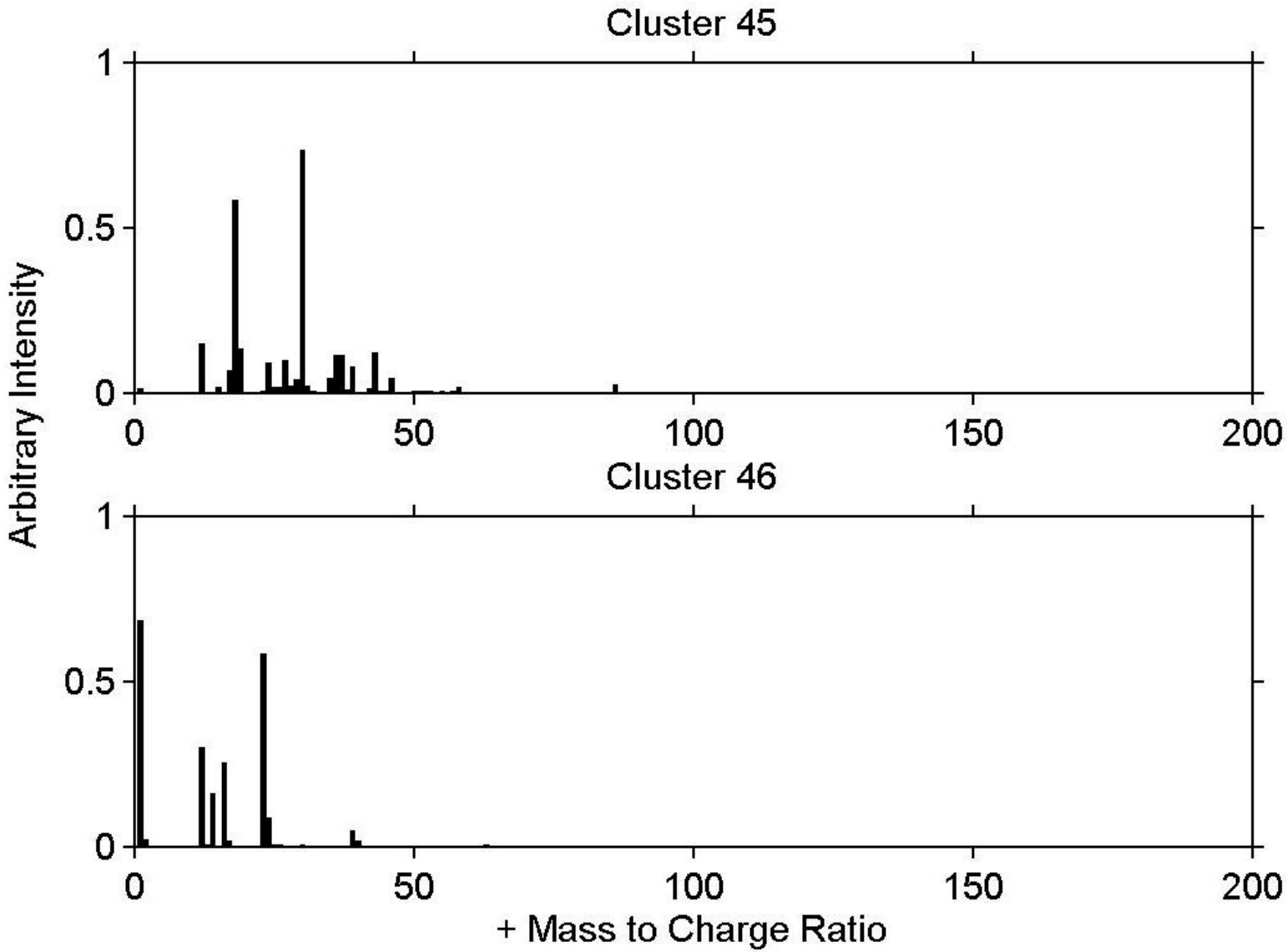
Cluster 45
Cluster 46
Arbitrary Intensity
+ Mass to Charge Ratio
0
0.5
1
0
50
100
150
200

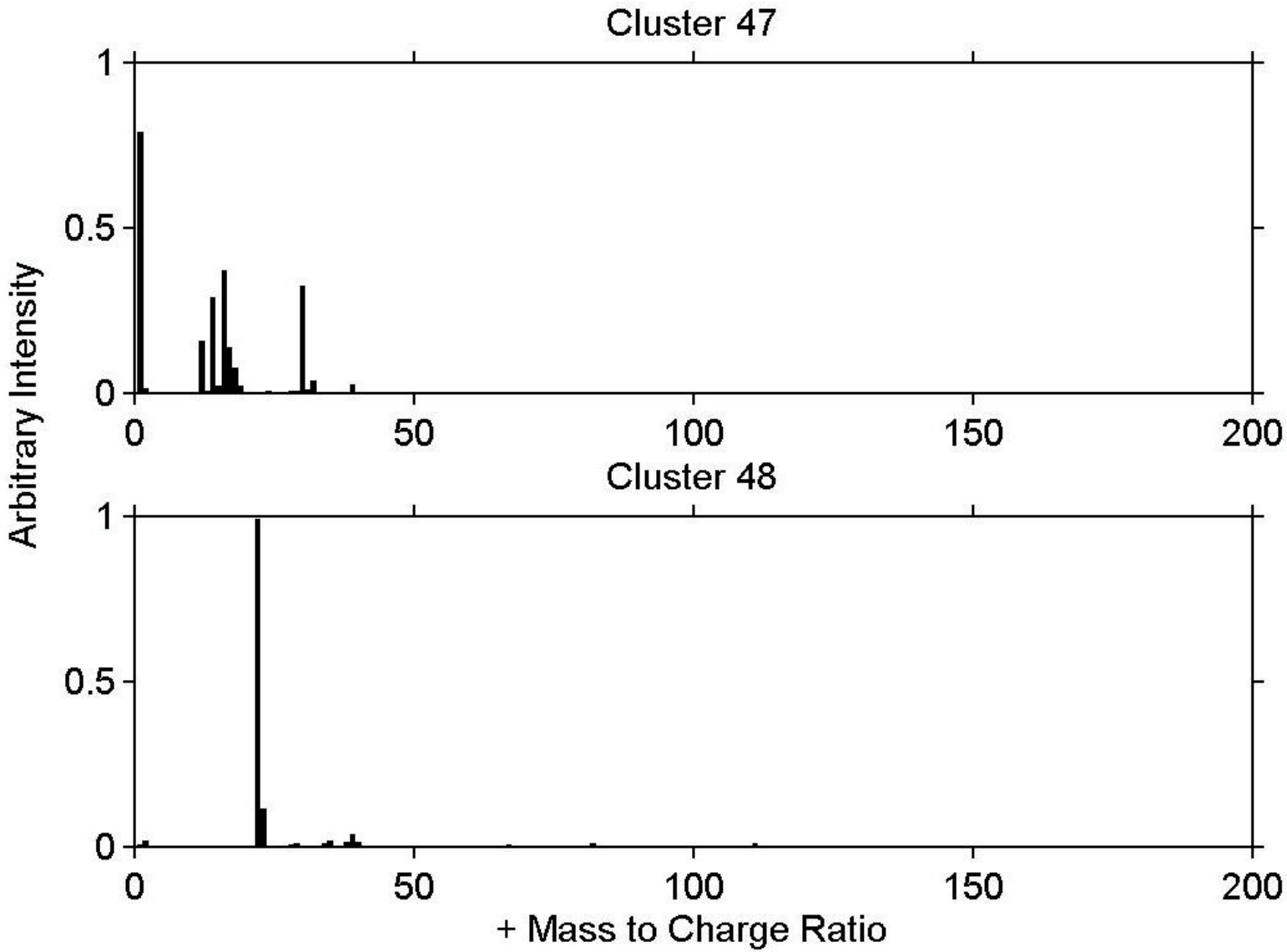
Cluster 47
Cluster 48
Arbitrary Intensity
1
0.5
0
0
50
100
150
200
+ Mass to Charge Ratio

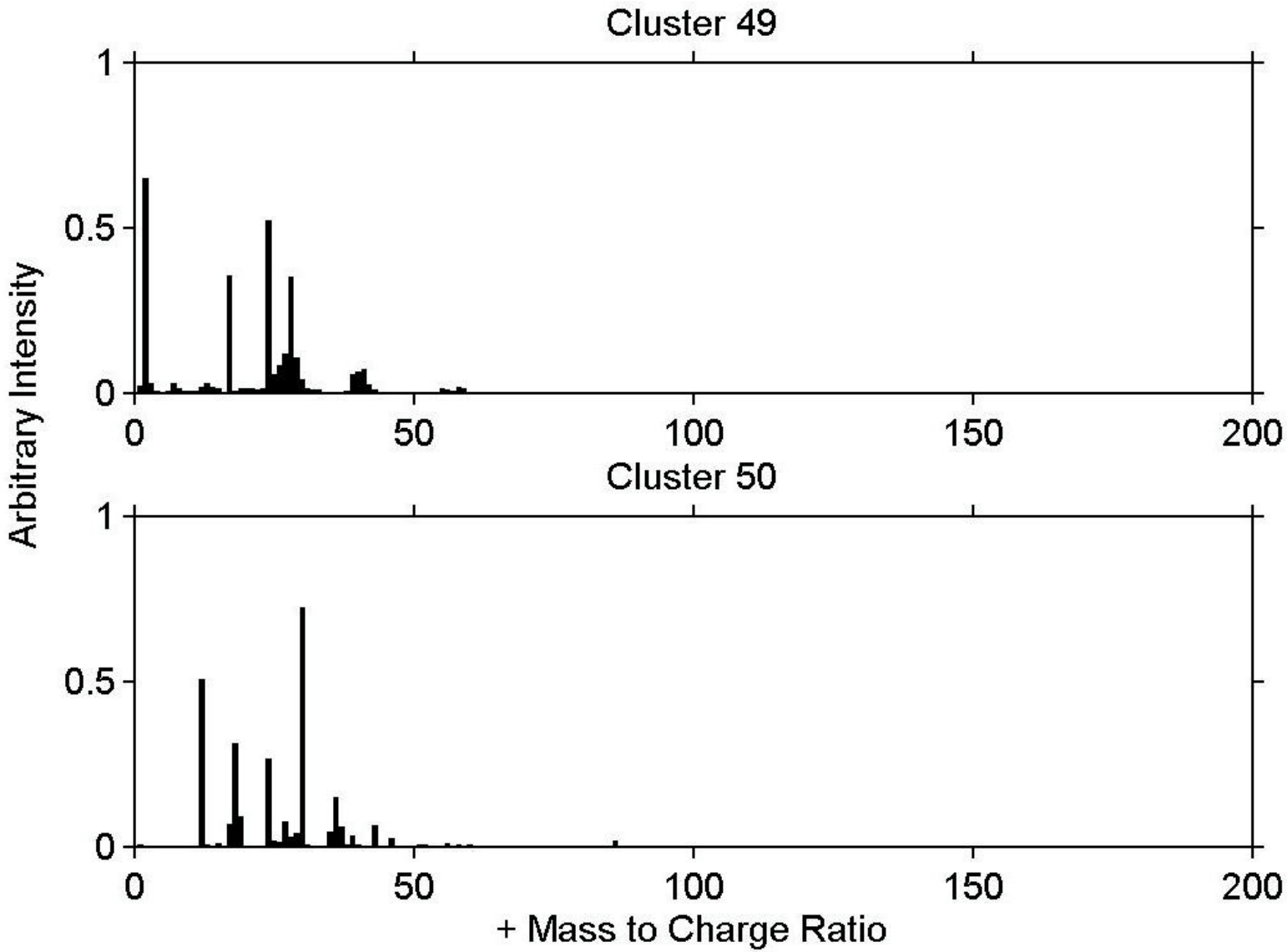
Cluster 49
Cluster 50
Arbitrary Intensity
1
0.5
0
0
50
100
150
200
+ Mass to Charge Ratio

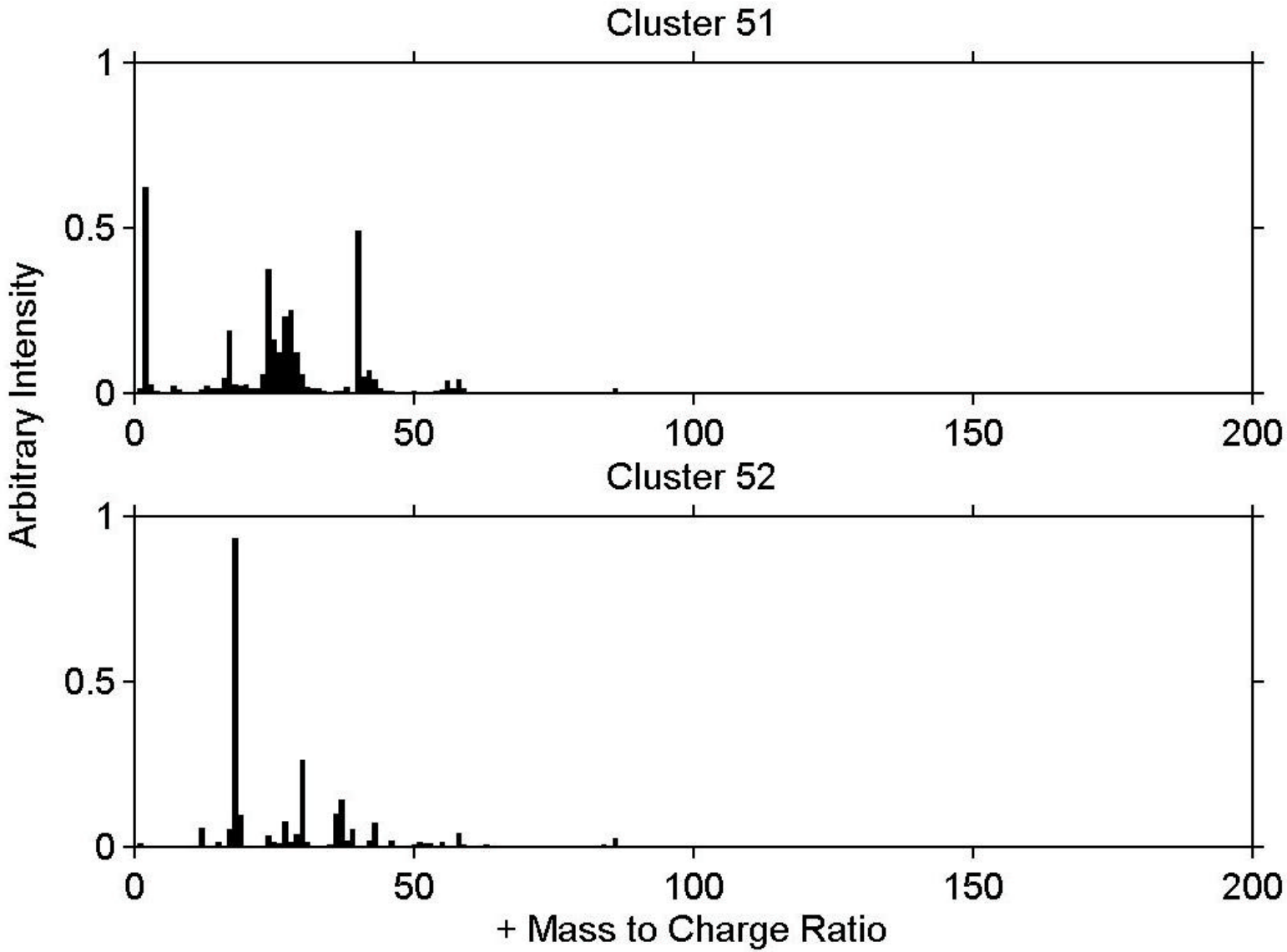
Cluster 51
Cluster 52
Arbitrary Intensity
+ Mass to Charge Ratio
0
0.5
1
0
50
100
150
200

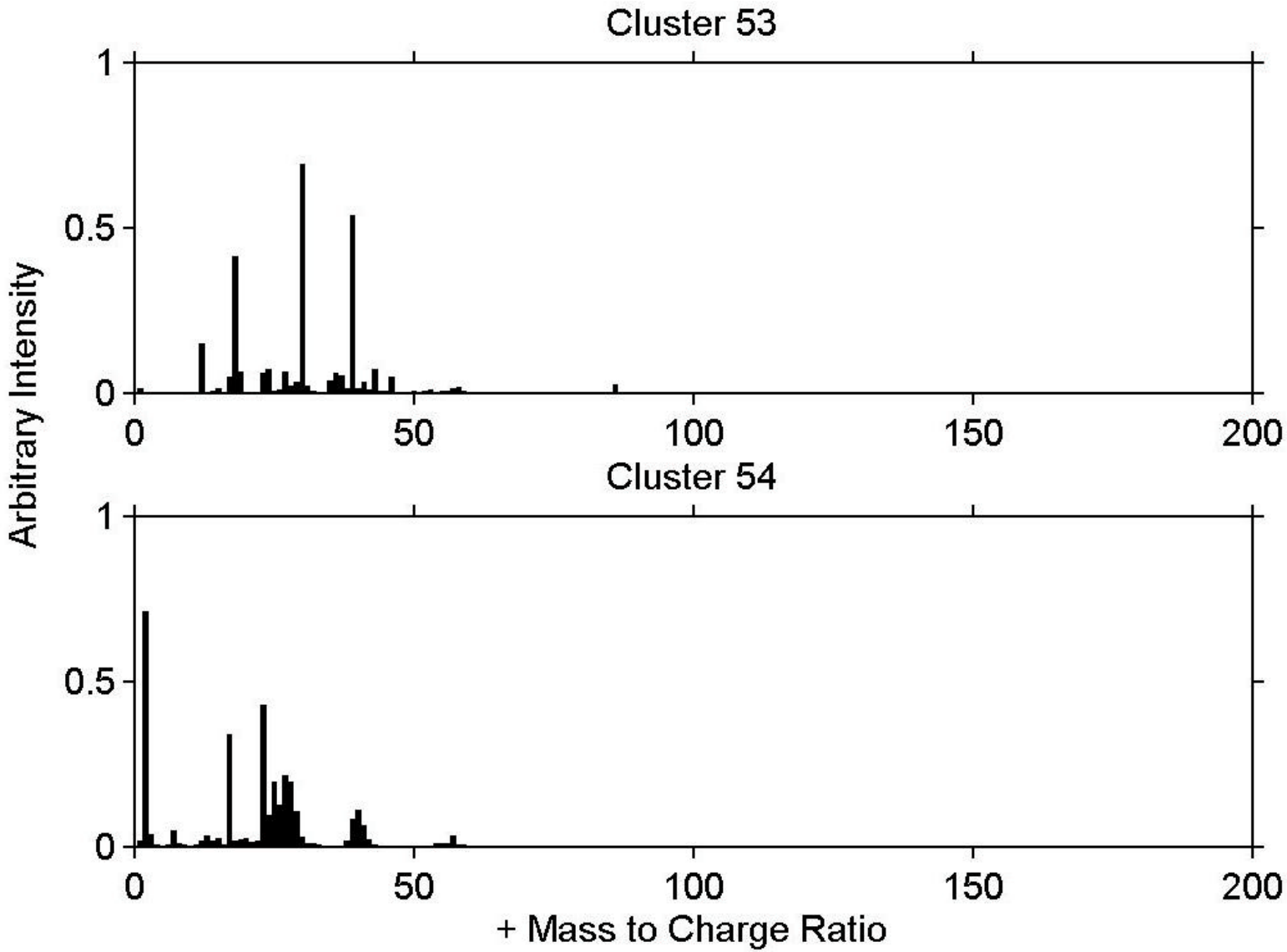
Cluster 53
Cluster 54
Arbitrary Intensity
+ Mass to Charge Ratio
0
0.5
1
0
50
100
150
200

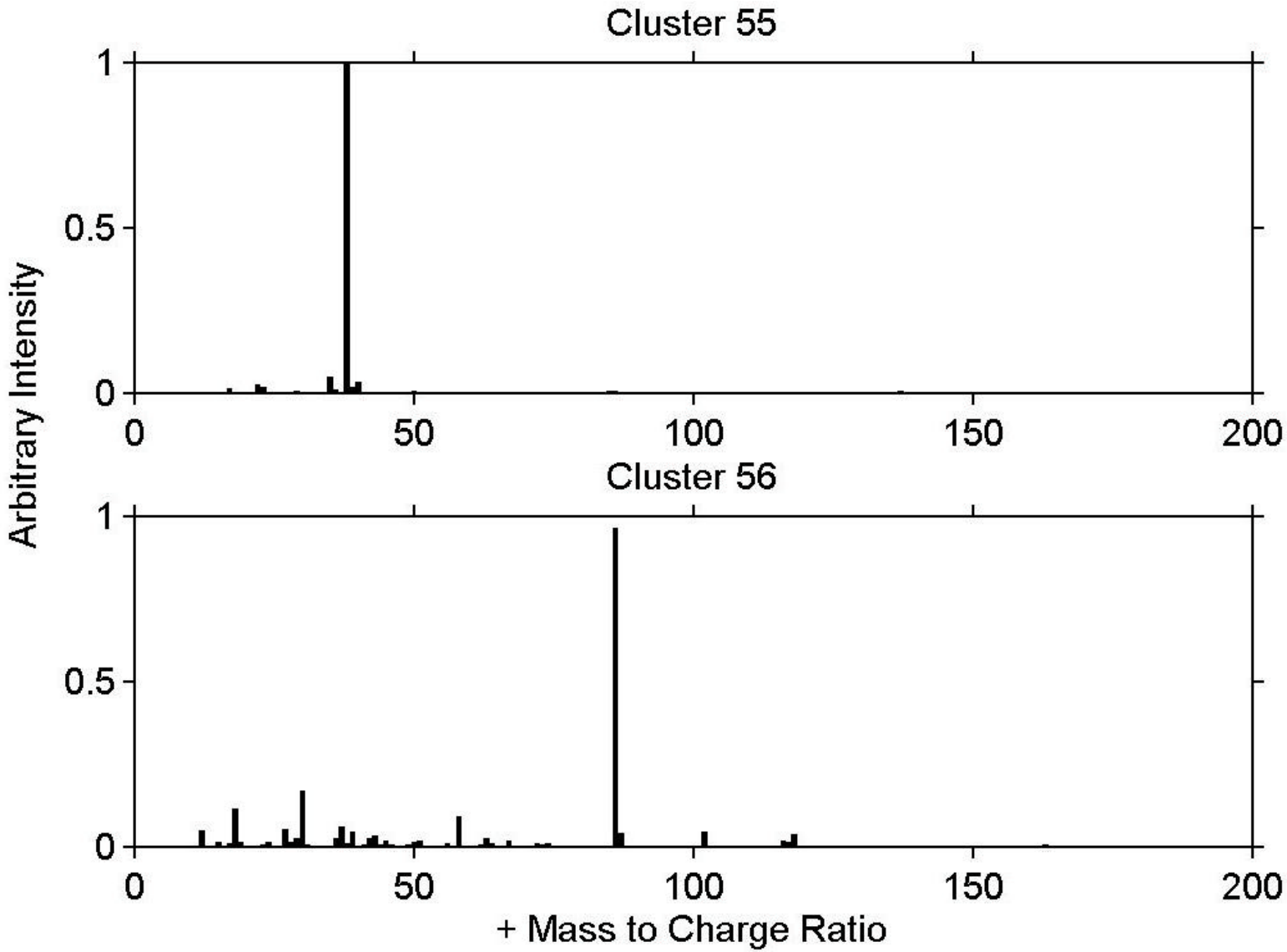
Cluster 55
Cluster 56
Arbitrary Intensity
+ Mass to Charge Ratio
0
0.5
1
0
50
100
150
200

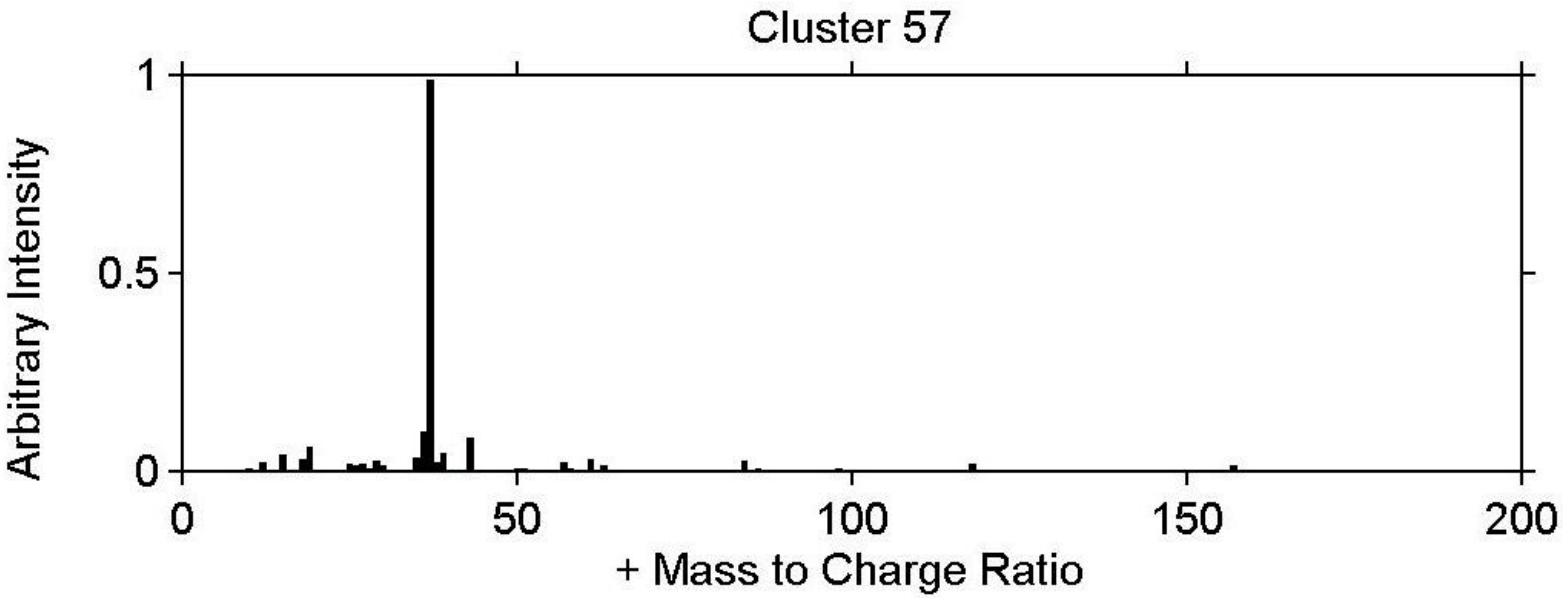
Cluster 57
Arbitrary Intensity
1
0.5
0
0
50
100
150
200
+ Mass to Charge Ratio

Appendix P: Color versions of similarity plots presented in the body of the report in grayscale. A red to blue color-coding replaces the white to black grayscale coding. See the body of the report for captions and additional information.

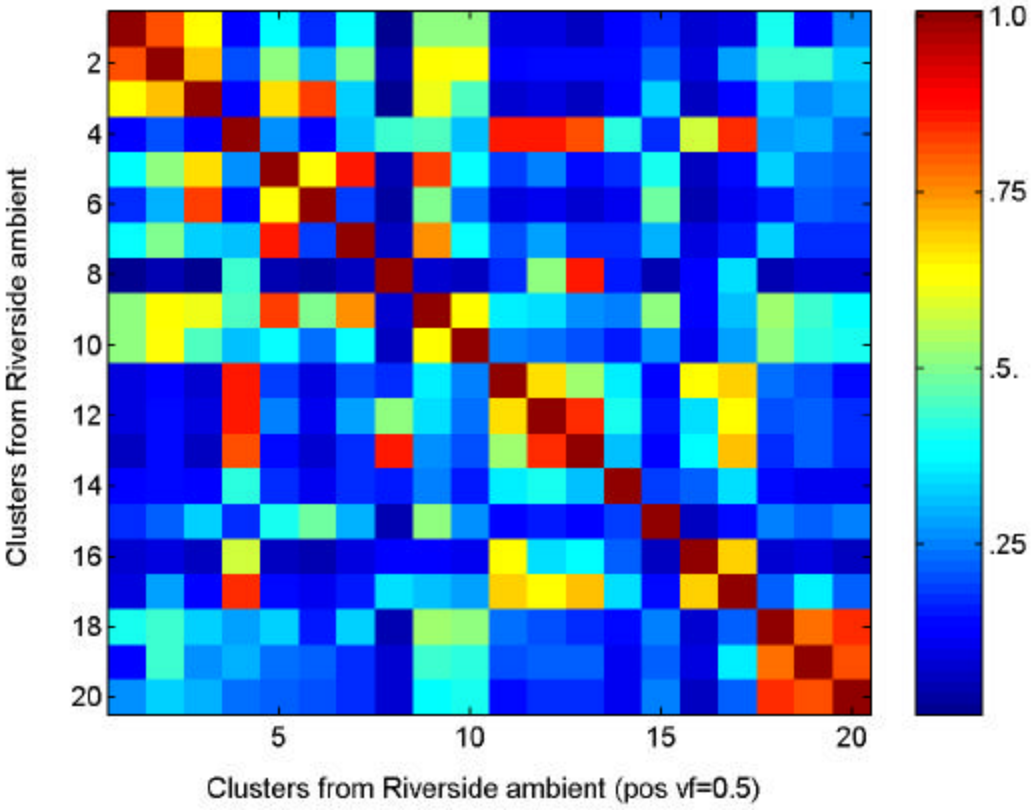

Figure 2.5

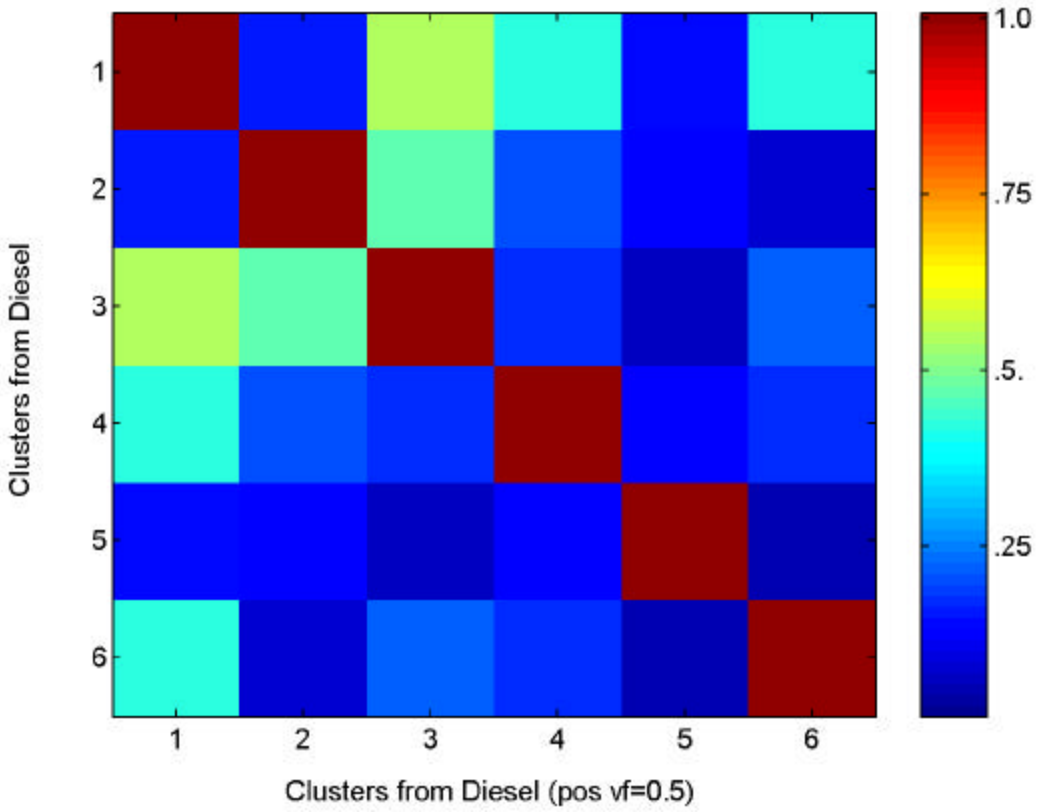
Clusters from Diesel
1
2
3
4
5
6
1
2
3
4
5
6
Clusters from Diesel (pos vf=0.5)
1.0
.75
.5.
.25

Figure 4.1

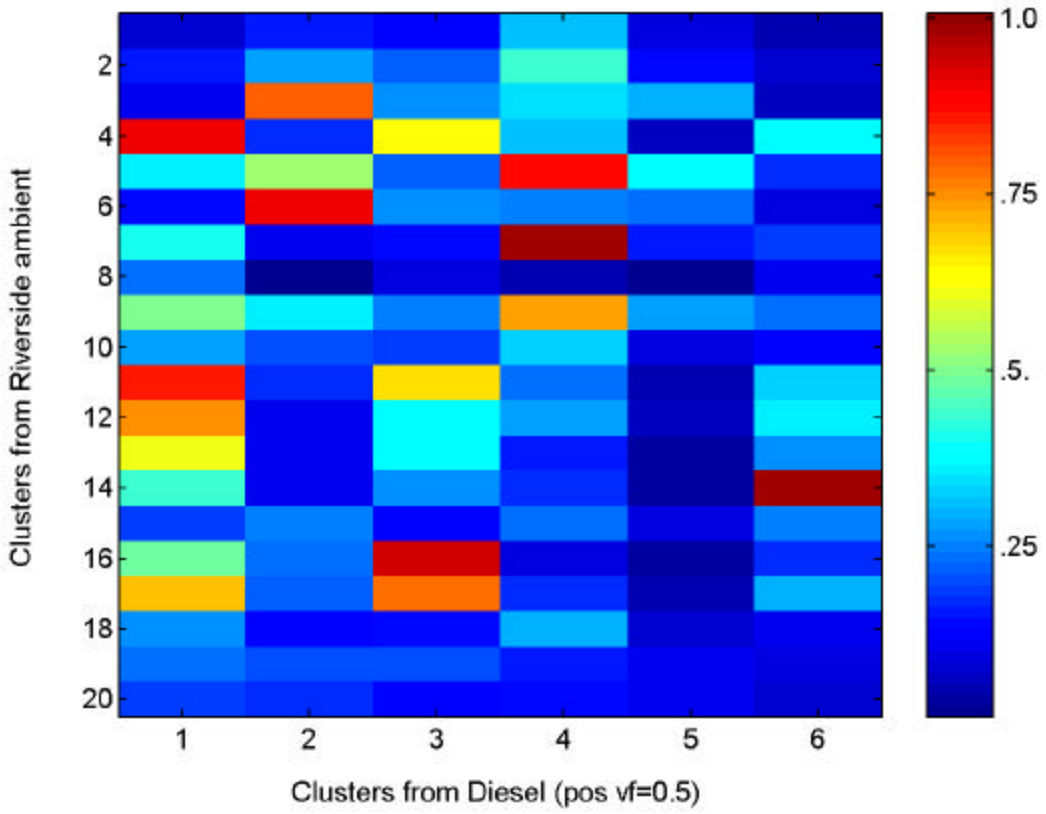
Clusters from Riverside ambient
2
4
6
8
10
12
14
16
18
20
1
2
3
4
5
6
Clusters from Diesel (pos vf=0.5)
1.0
.75
.5.
.25

Figure 4.2

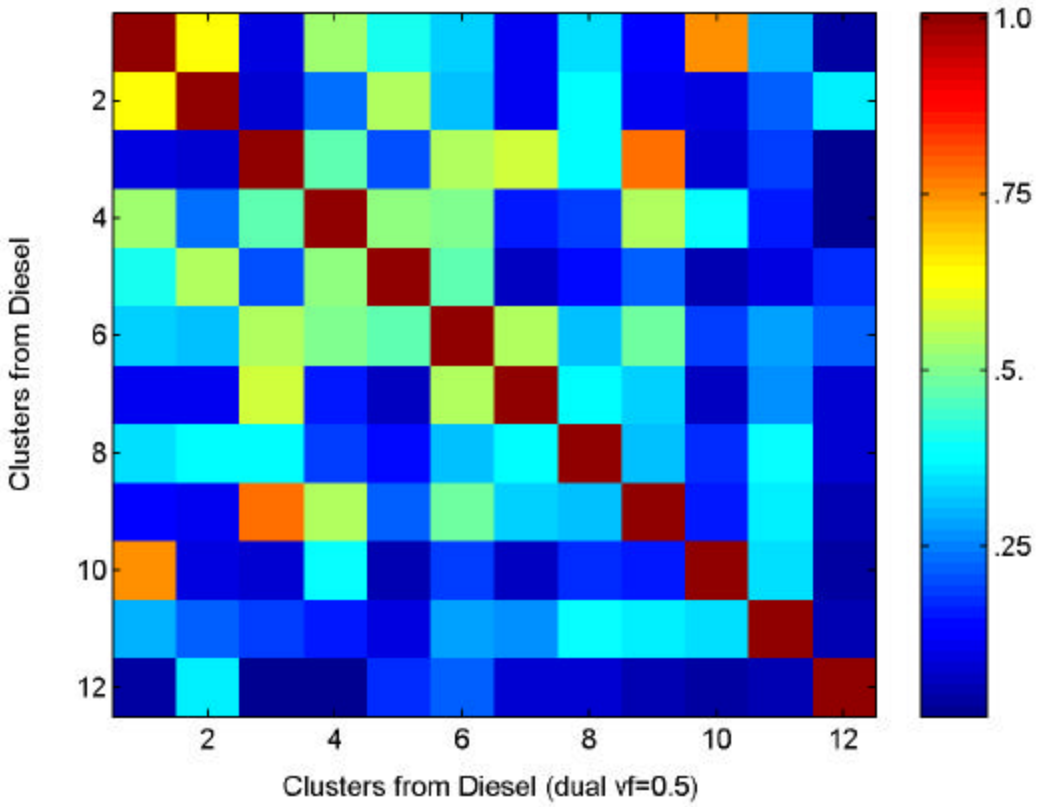
Clusters from Diesel
2
4
6
8
10
12
2
4
6
8
10
12
Clusters from Diesel (dual vf=0.5)
1.0
.75
.5.
.25

Figure 4.3

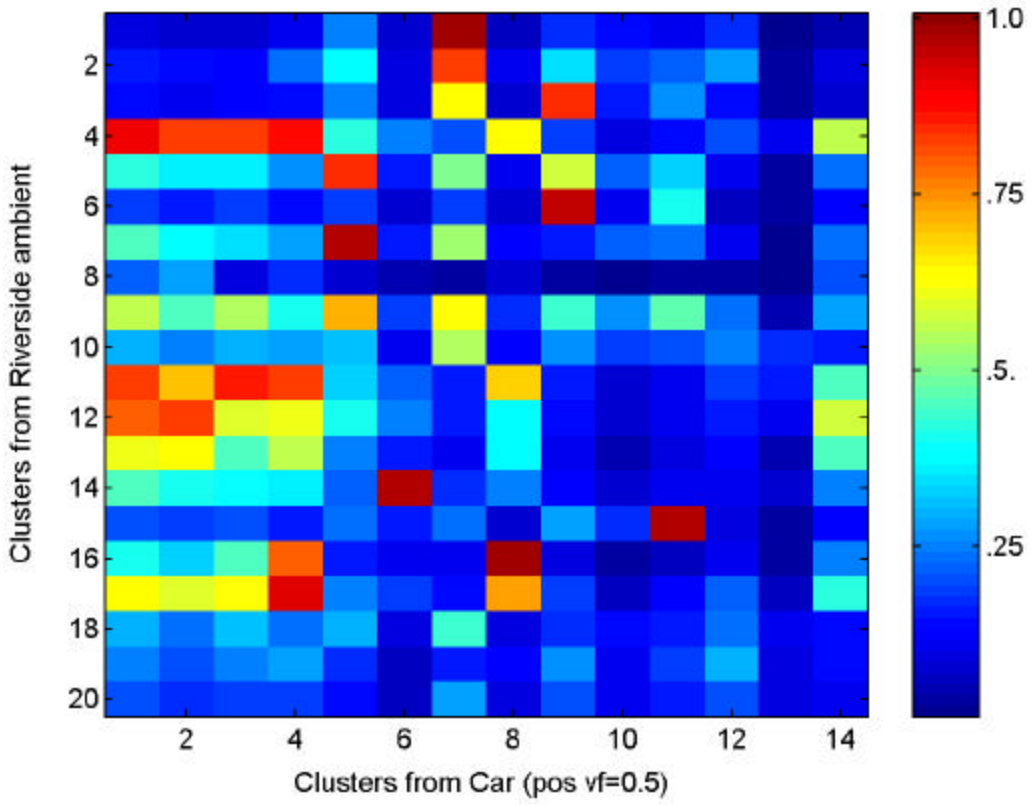
Clusters from Riverside ambient
2
4
6
8
10
12
14
16
18
20
2
4
6
8
10
12
14
Clusters from Car (pos vf=0.5)
1.0
.75
.5.
.25

Figure 4.4

Appendix Q: Temporal plots of clusters #1-20 in Riverside over 40 consecutive days between August 19, 1997 and September 27, 1997 during SCOS97-NARSTO.

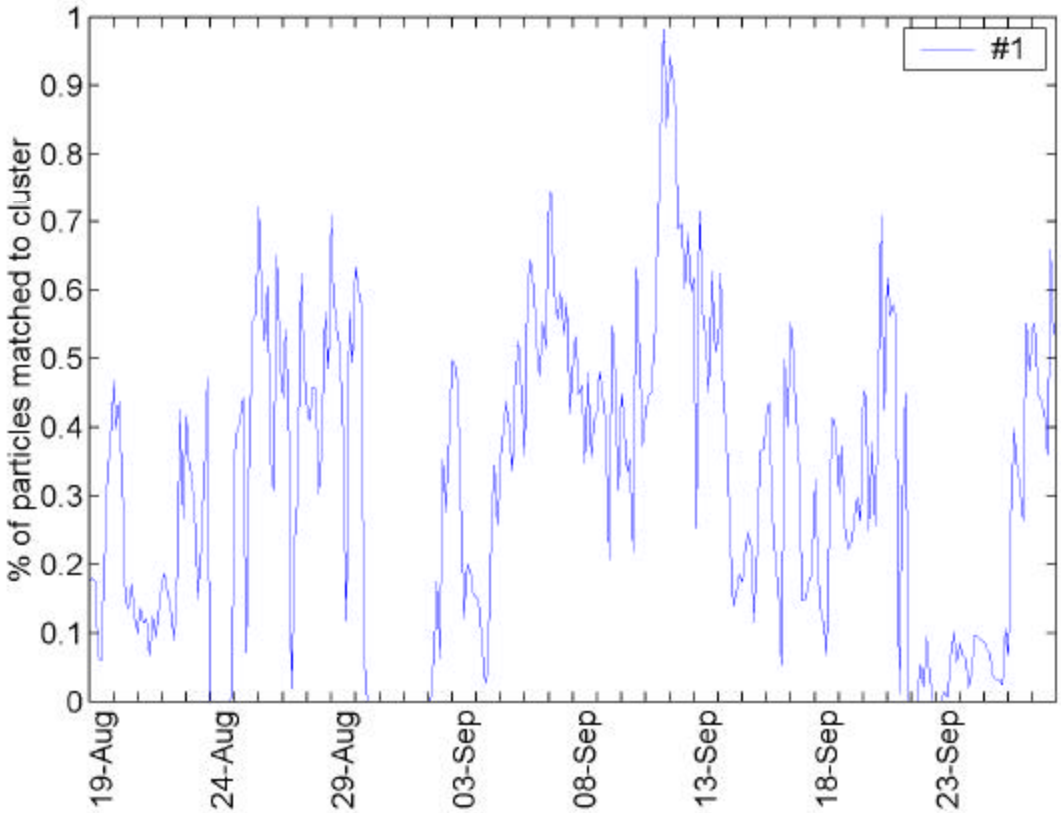

Temporal plot of cluster #1 in Riverside over 40 consecutive days between August 19, 1997 and September 27, 1997 during SCOS97.

August 19, 1997 and September 27, 1997 during SCOS97.

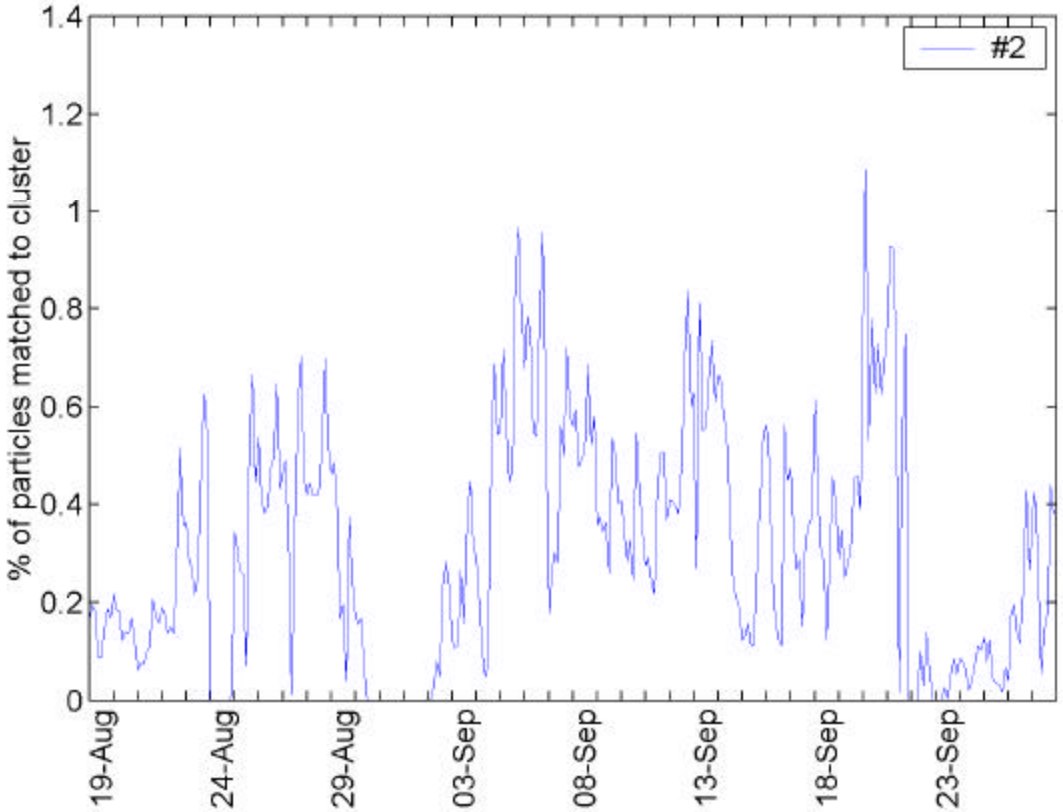

Temporal plot of cluster #3 in Riverside over 40 consecutive days between August 19, 1997 and September 27, 1997 during SCOS97.

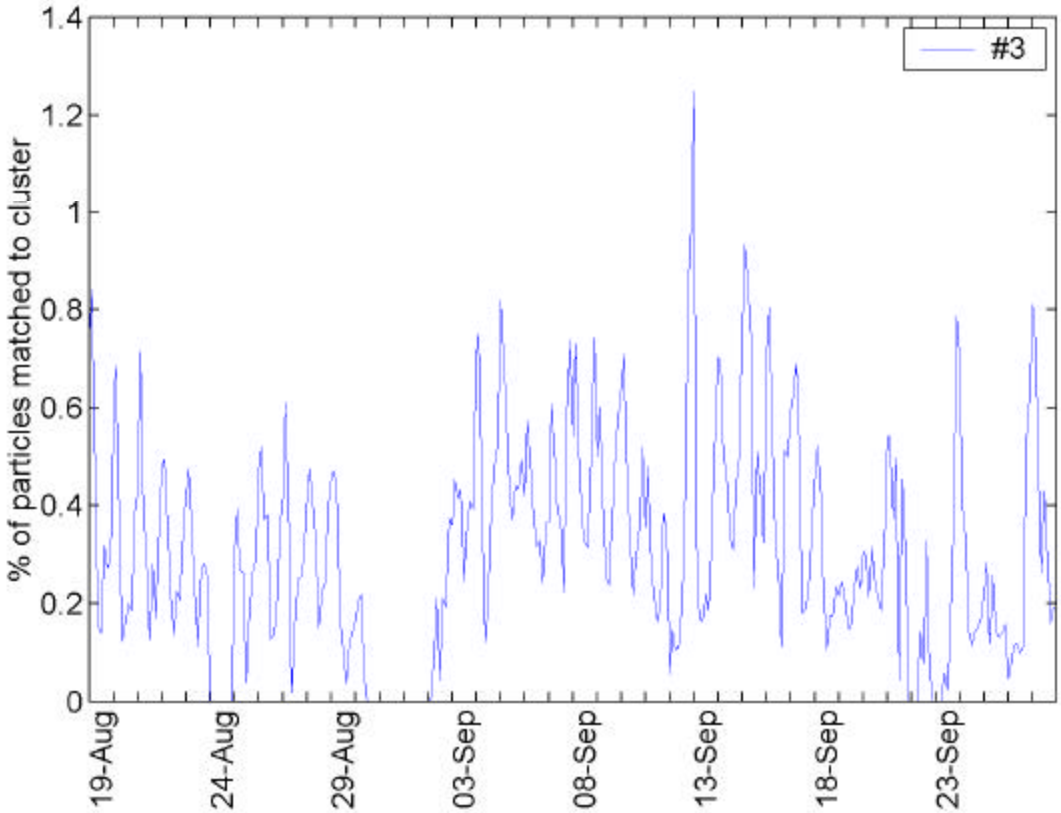

Temporal plot of cluster #4 in Riverside over 40 consecutive days between August 19, 1997 and September 27, 1997 during SCOS97.

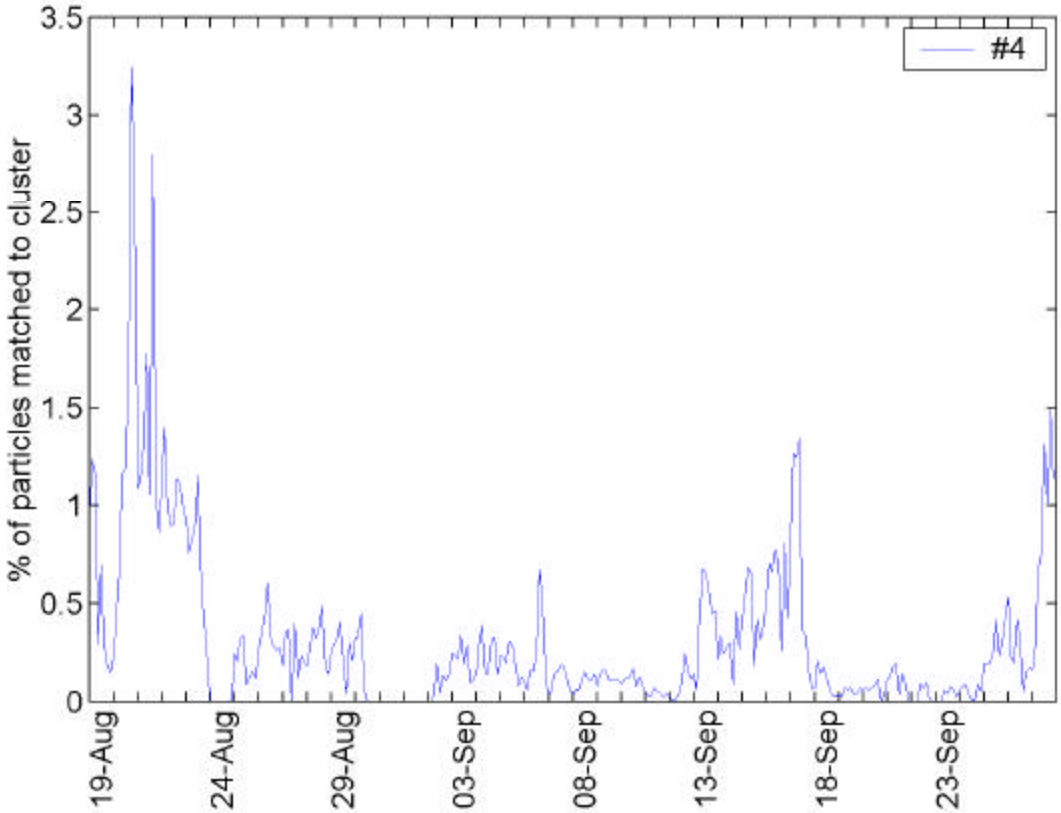

Temporal plot of cluster #5 in Riverside over 40 consecutive days between August 19, 1997 and September 27, 1997 during SCOS97.

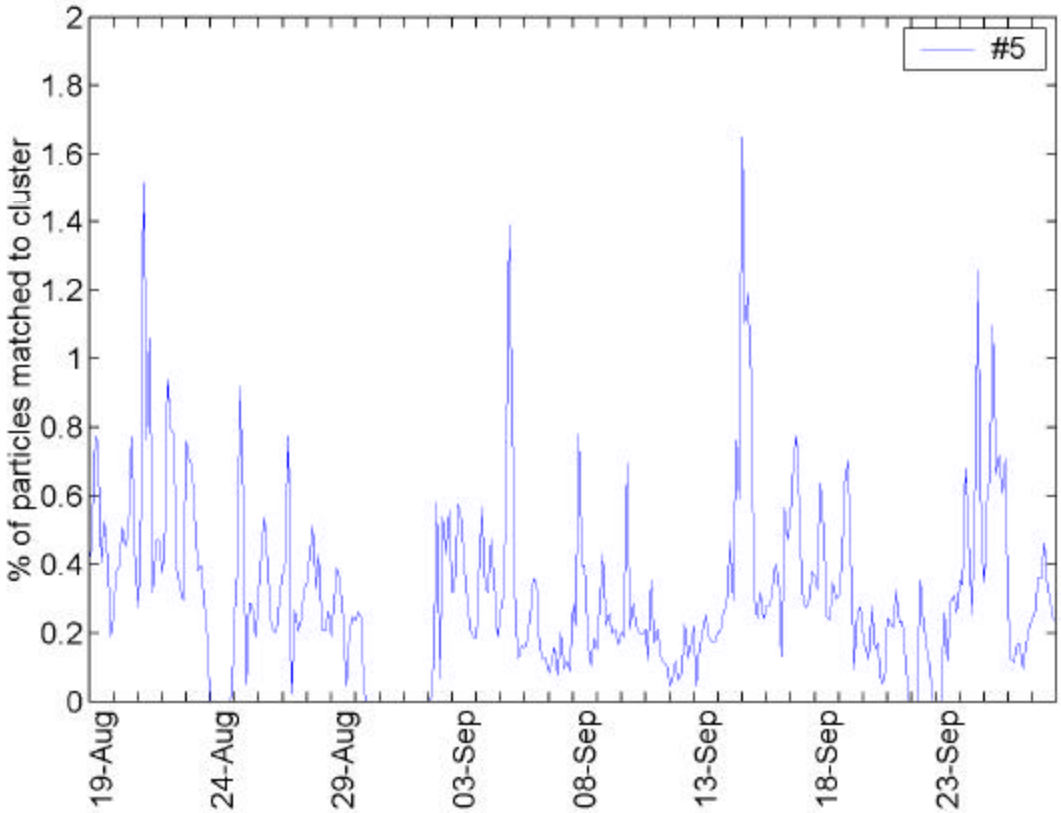

Temporal plot of cluster #6 in Riverside over 40 consecutive days between August 19, 1997 and September 27, 1997 during SCOS97.

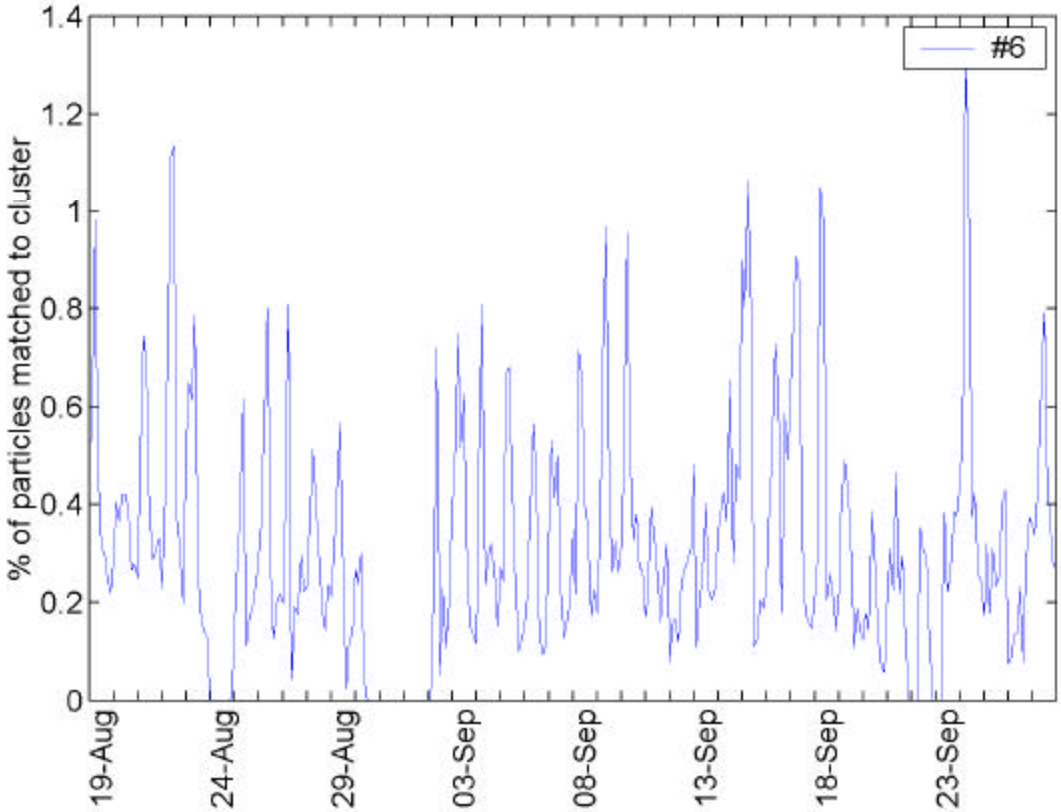

Temporal plot of cluster #7 in Riverside over 40 consecutive days between August 19, 1997 and September 27, 1997 during SCOS97.

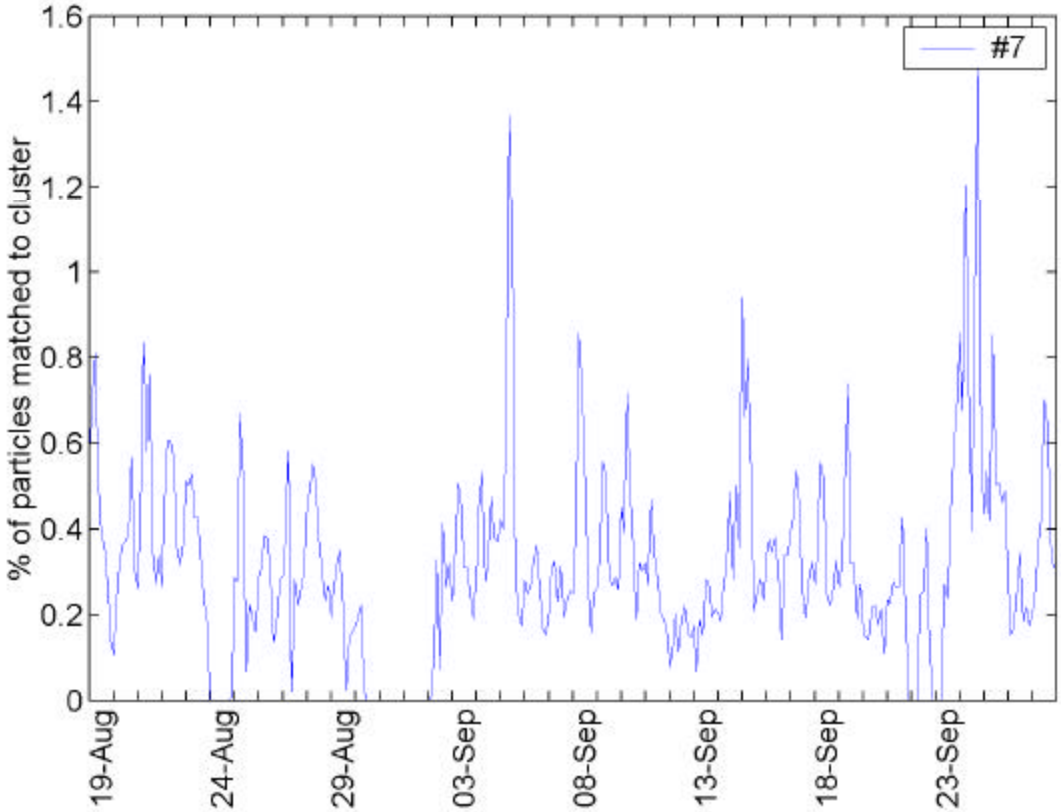

Temporal plot of cluster #8 in Riverside over 40 consecutive days between August 19, 1997 and September 27, 1997 during SCOS97.

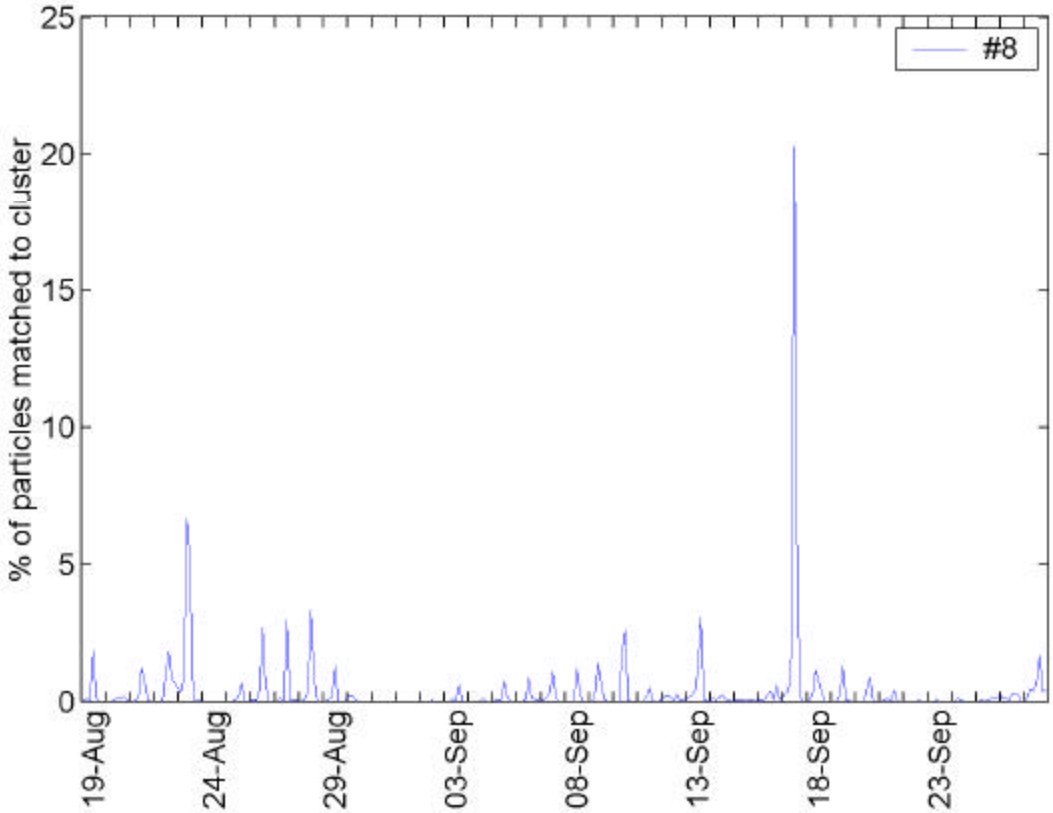

Temporal plot of cluster #9 in Riverside over 40 consecutive days between August 19, 1997 and September 27, 1997 during SCOS97.

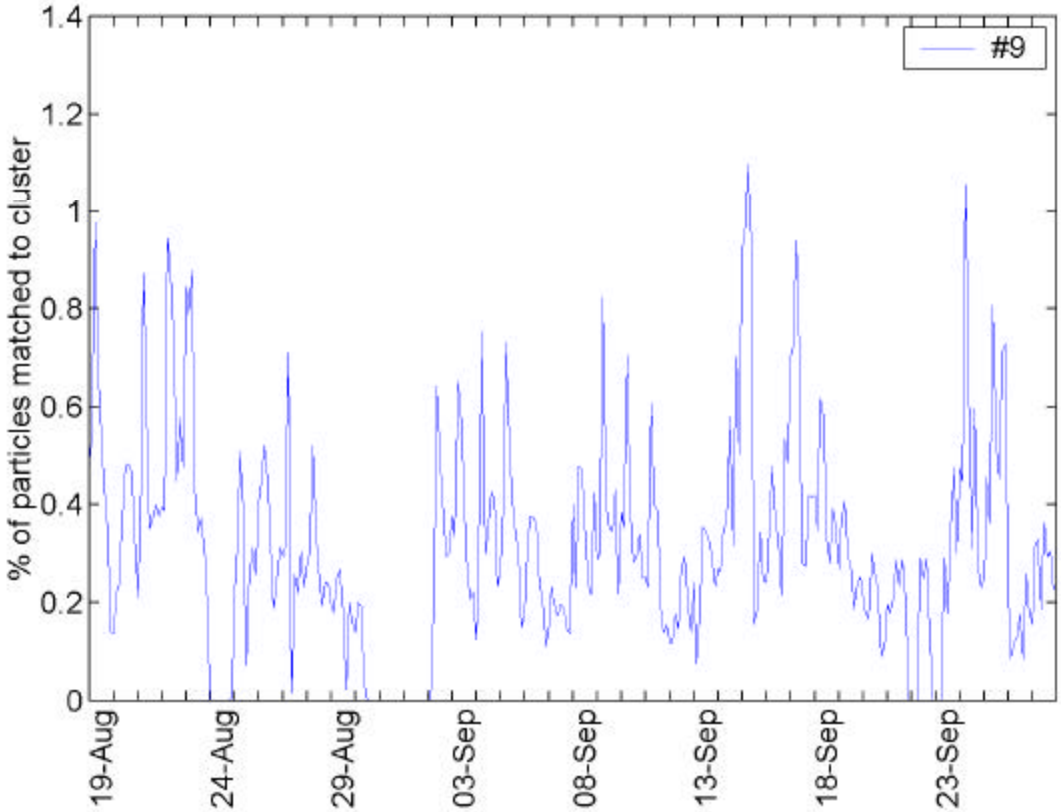

Temporal plot of cluster #10 in Riverside over 40 consecutive days between August 19, 1997 and September 27, 1997 during SCOS97.

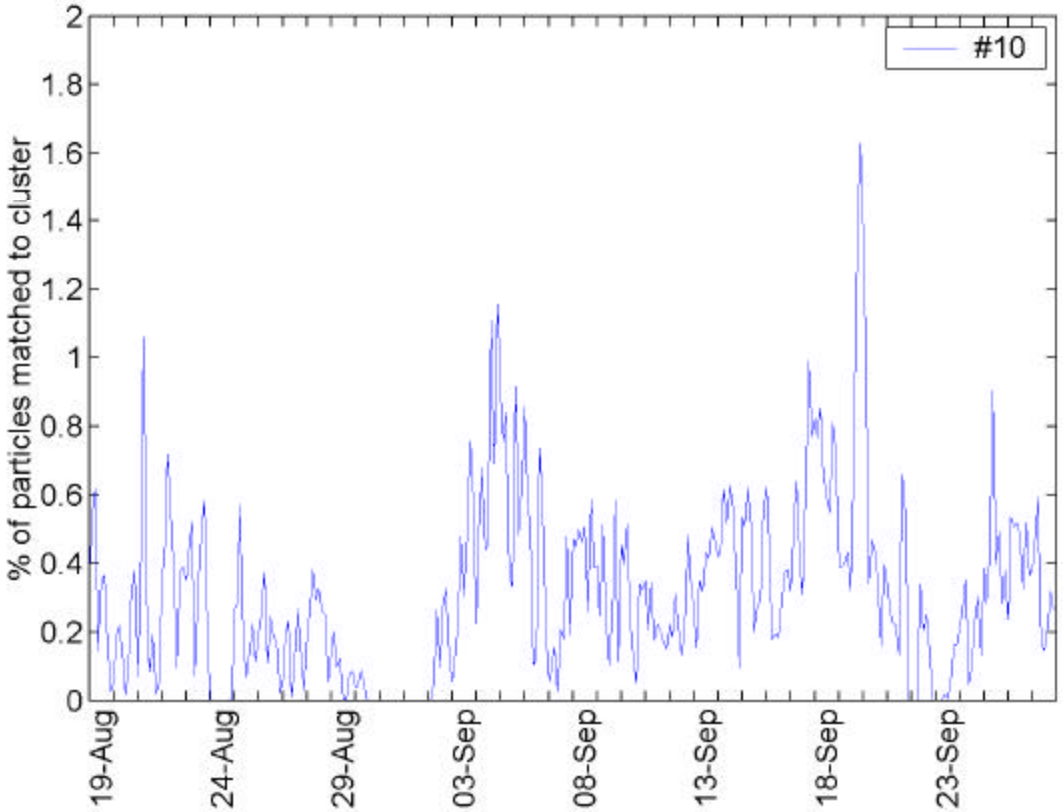
#10
% of particles matched to cluster
2
1.8
1.6
1.4
1.2
1
0.8
0.6
0.4
0.2
0
19-Aug
24-Aug
29-Aug
03-Sep
08-Sep
13-Sep
18-Sep
23-Sep

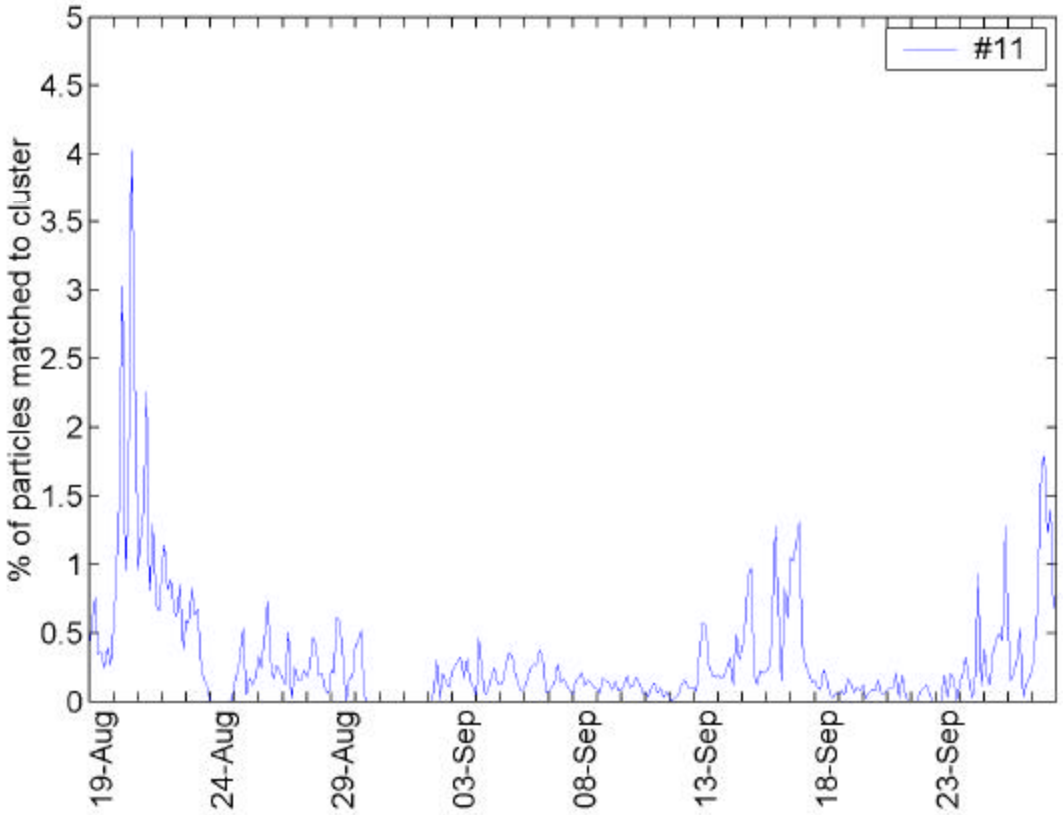

Temporal plot of cluster #11 in Riverside over 40 consecutive days between August 19, 1997 and September 27, 1997 during SCOS97.

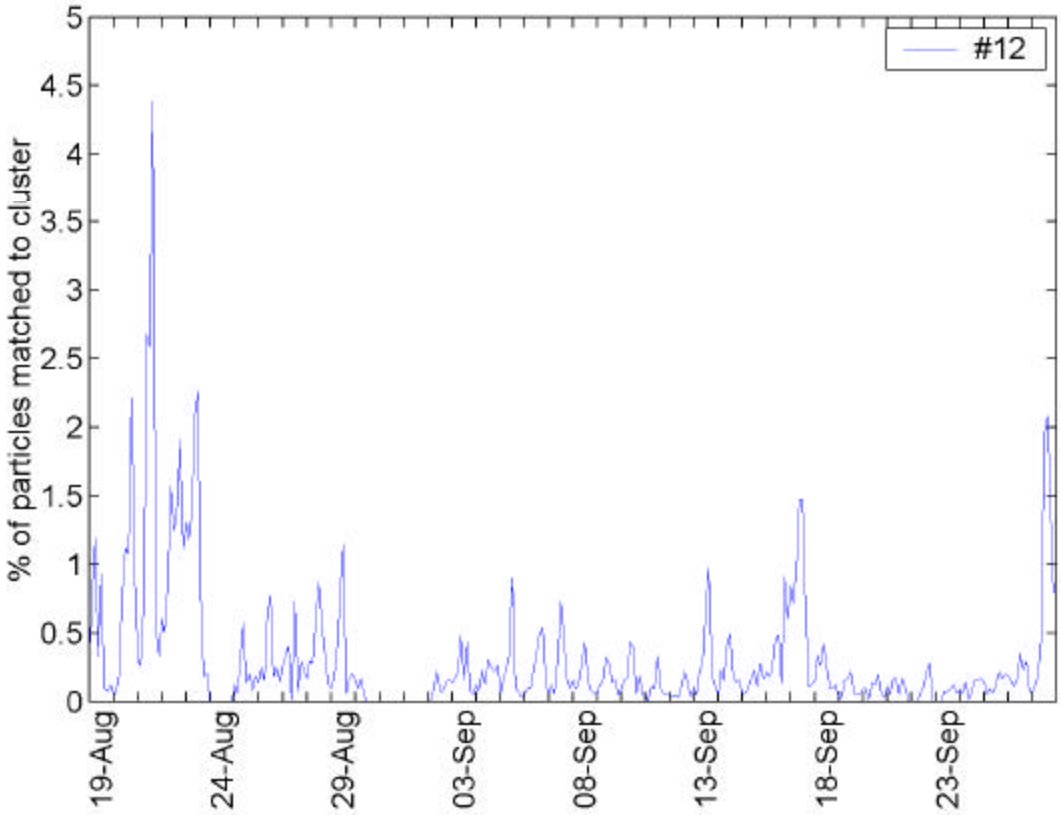

Temporal plot of cluster #13 in Riverside over 40 consecutive days between August 19, 1997 and September 27, 1997 during SCOS97.

August 19, 1997 and September 27, 1997 during SCOS97.

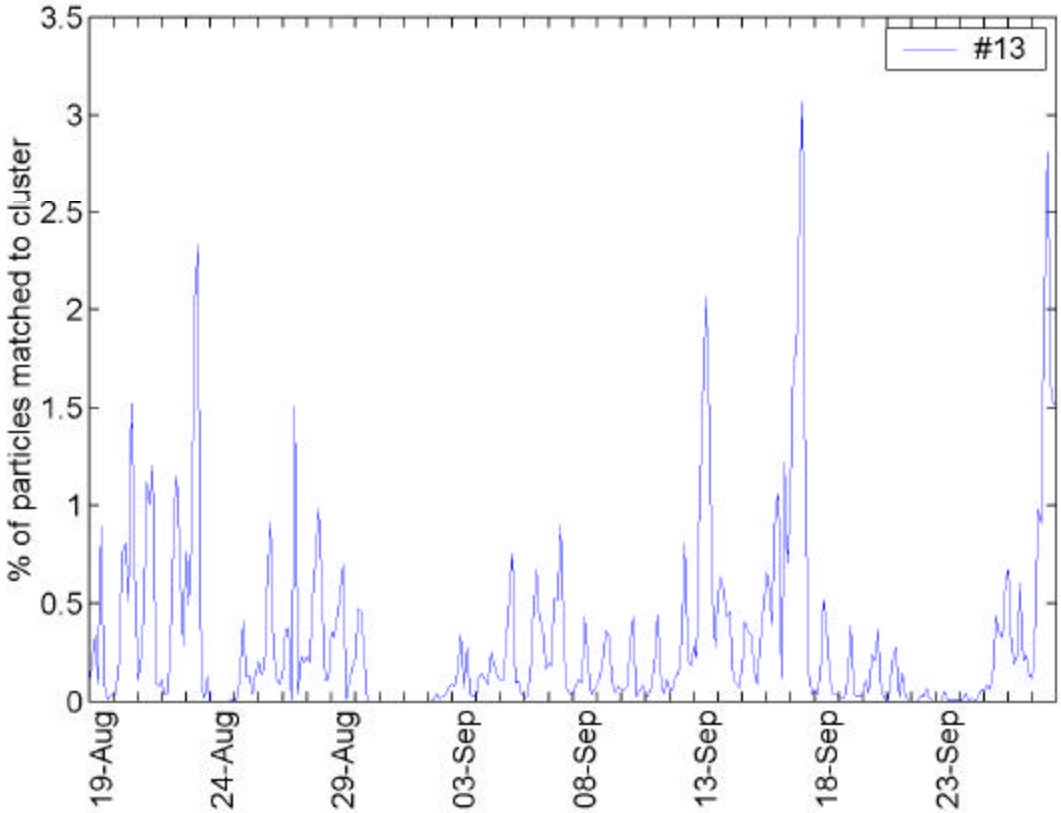

Temporal plot of cluster #14 in Riverside over 40 consecutive days between August 19, 1997 and September 27, 1997 during SCOS97.

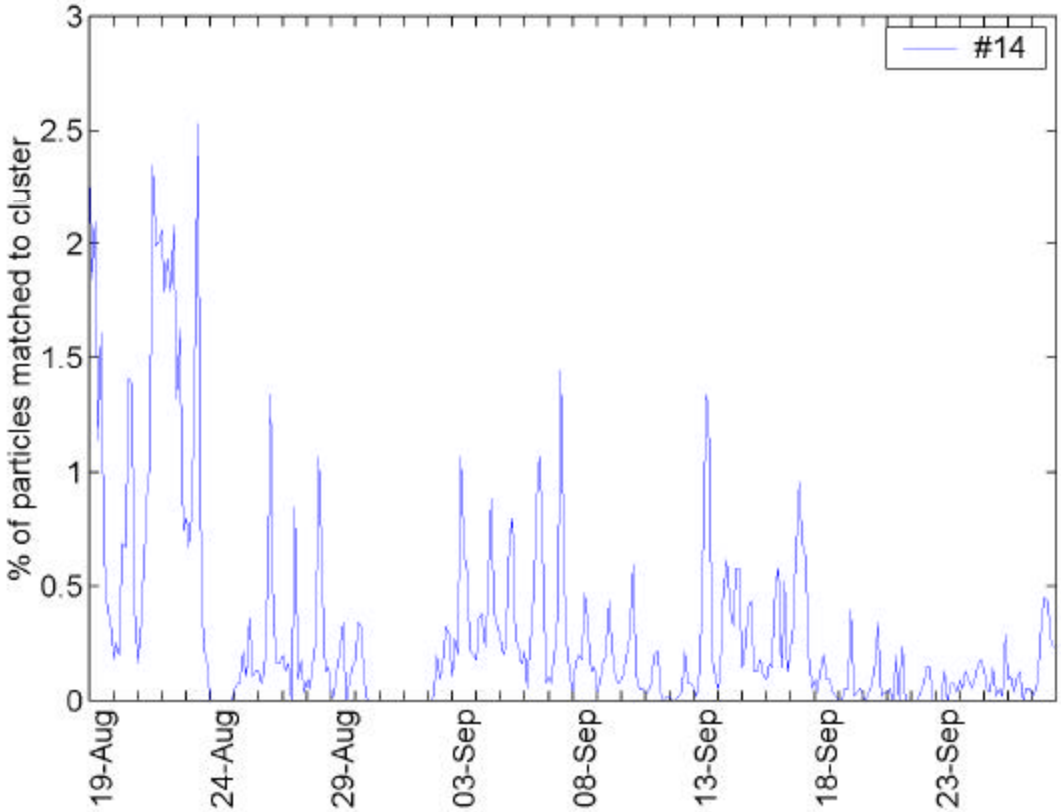

Temporal plot of cluster #15 in Riverside over 40 consecutive days between August 19, 1997 and September 27, 1997 during SCOS97.

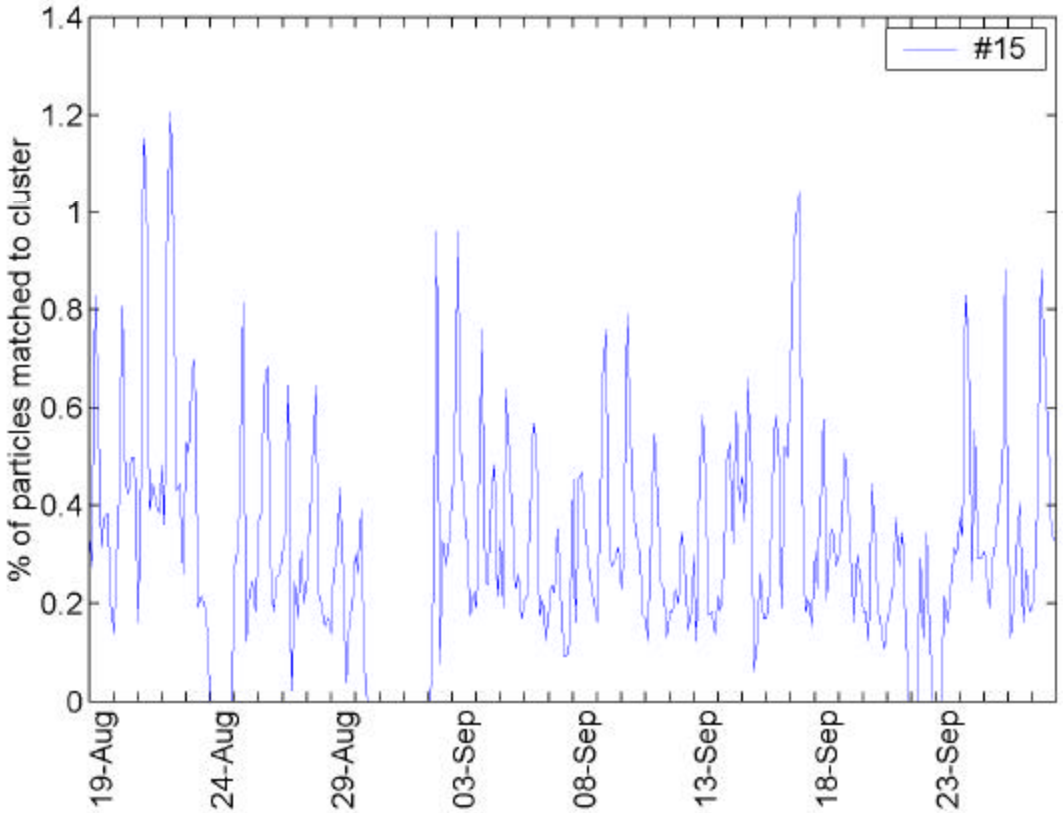

Temporal plot of cluster #16 in Riverside over 40 consecutive days between August 19, 1997 and September 27, 1997 during SCOS97.

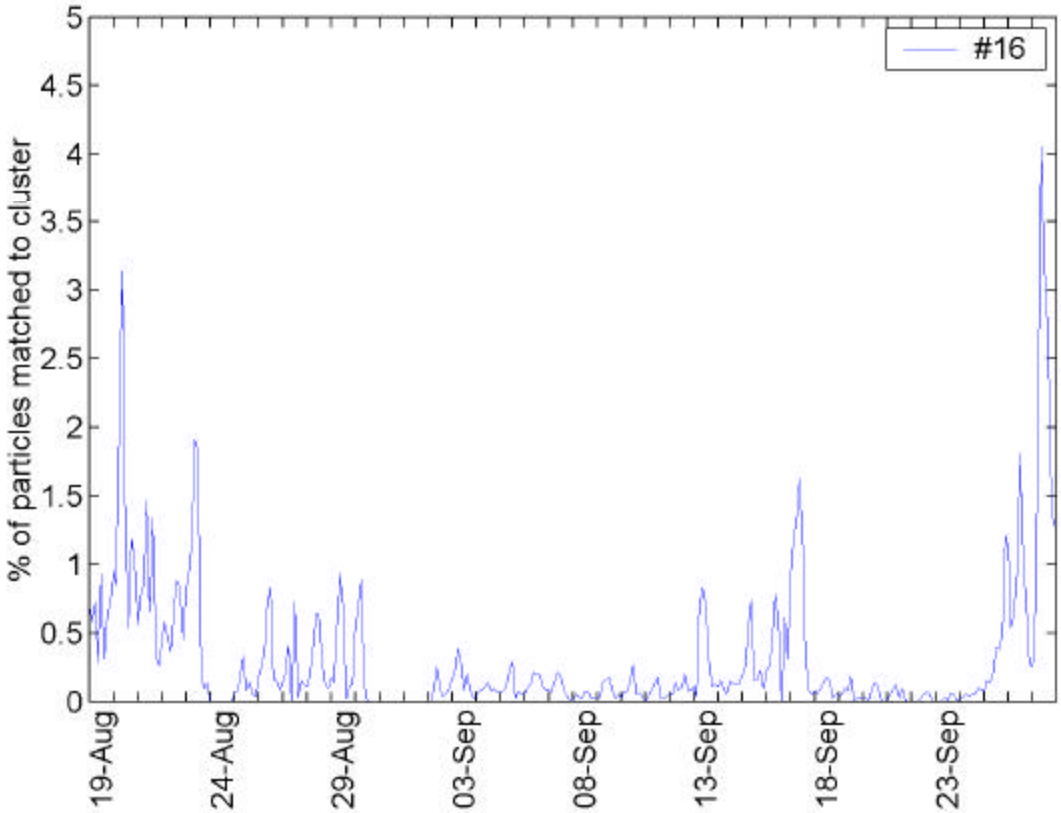

Temporal plot of cluster #17 in Riverside over 40 consecutive days between August 19, 1997 and September 27, 1997 during SCOS97.

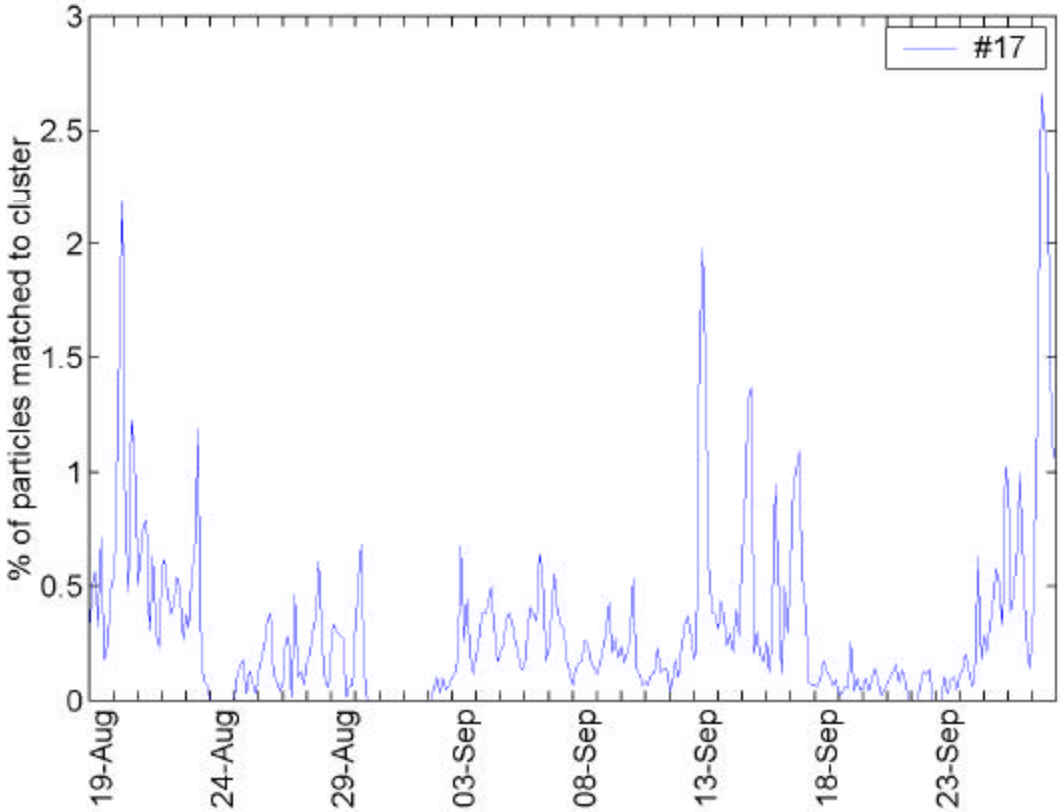

Temporal plot of cluster #18 in Riverside over 40 consecutive days between August 19, 1997 and September 27, 1997 during SCOS97.

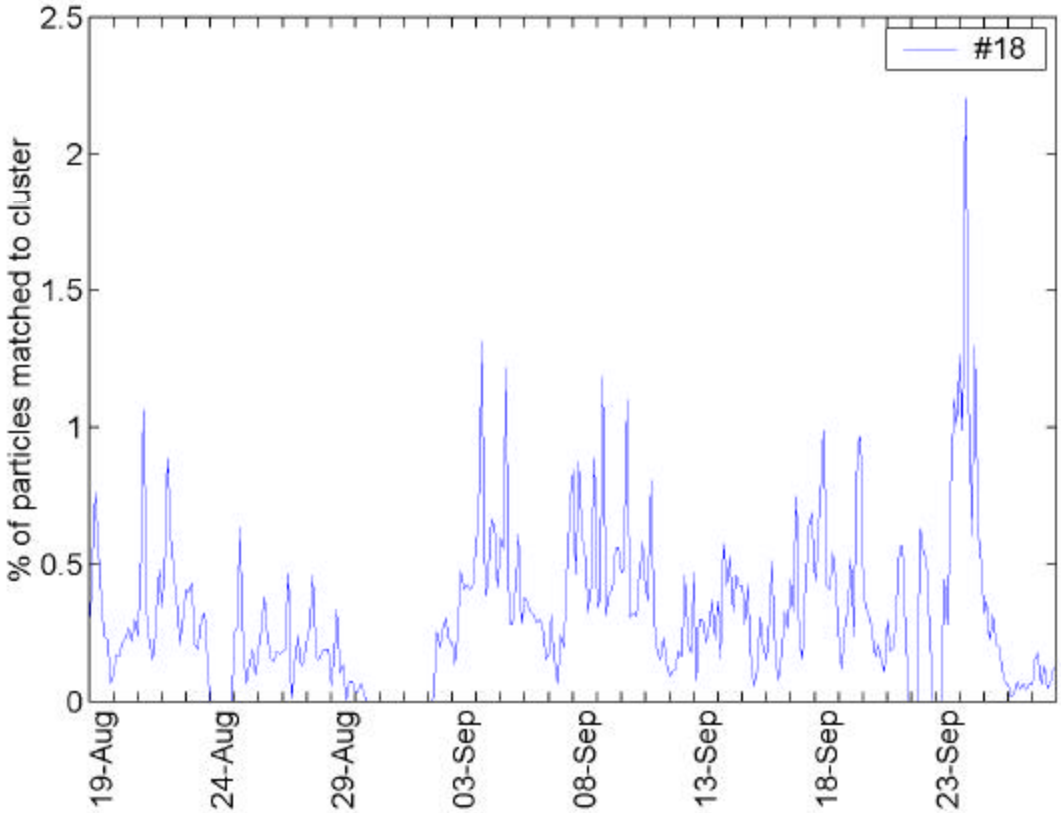

Temporal plot of cluster #19 in Riverside over 40 consecutive days between August 19, 1997 and September 27, 1997 during SCOS97.

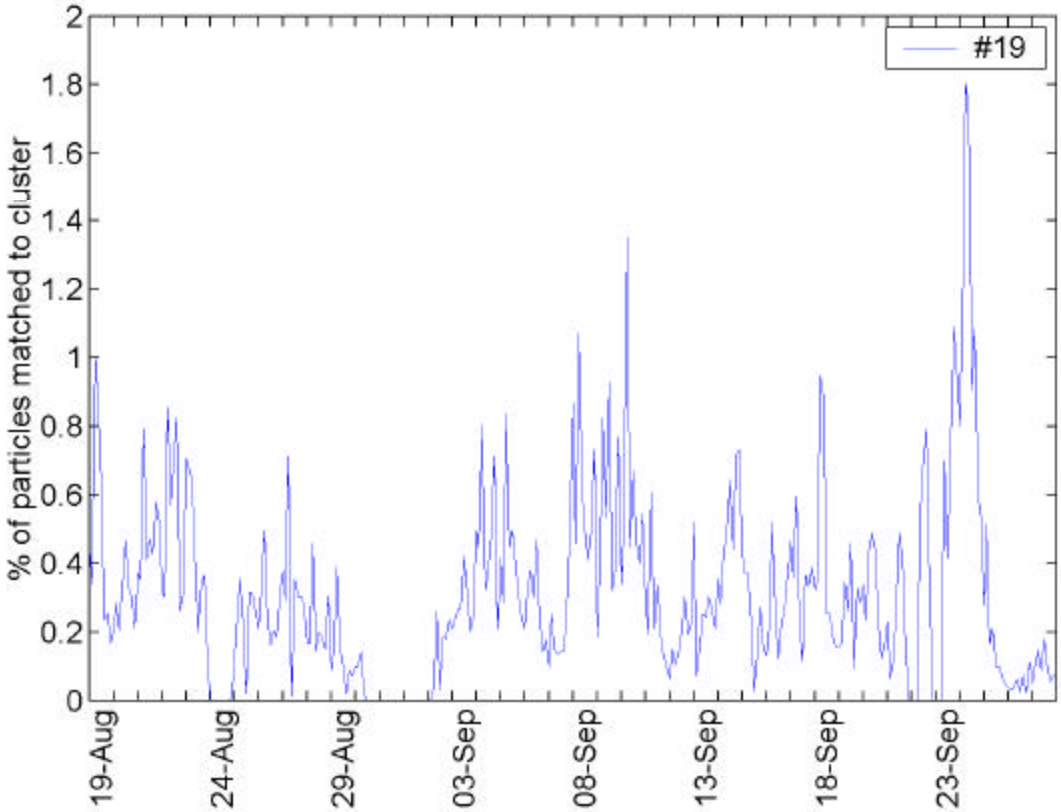
#19
% of particles matched to cluster
2
1.8
1.6
1.4
1.2
1
0.8
0.6
0.4
0.2
0
19-Aug
24-Aug
29-Aug
03-Sep
08-Sep
13-Sep
18-Sep
23-Sep

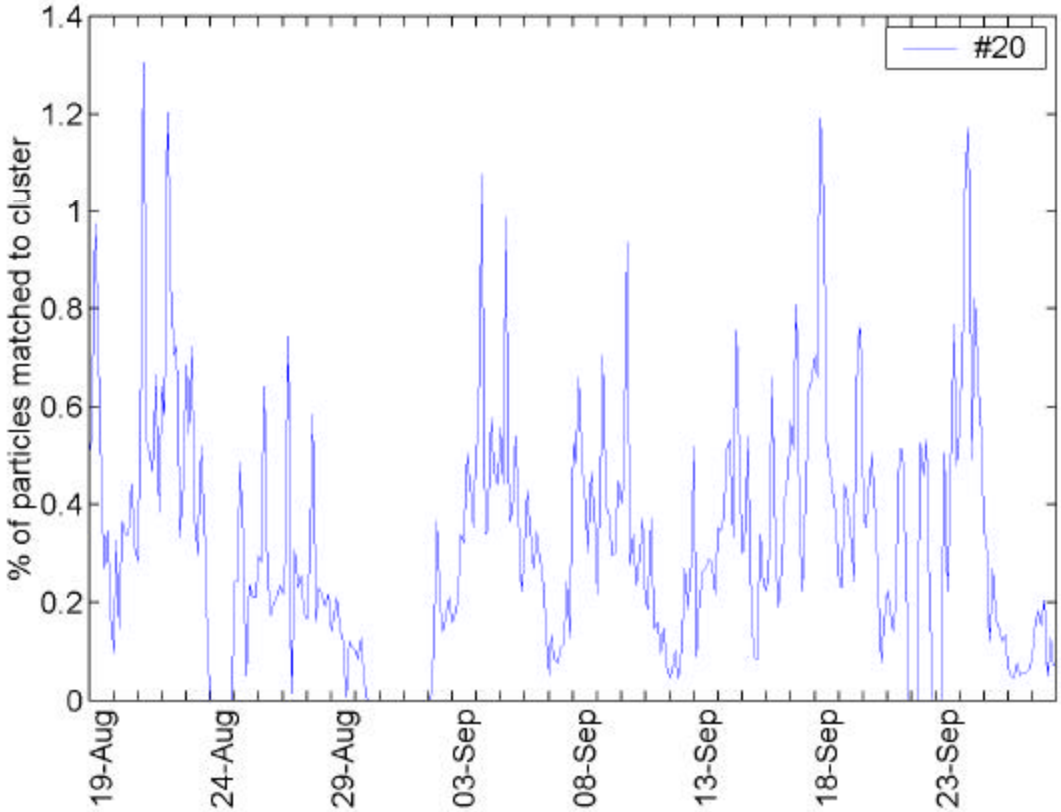

Temporal plot of cluster #20 in Riverside over 40 consecutive days between August 19, 1997 and September 27, 1997 during SCOS97.

Appendix R: List of publications directly supported as part of this contract.

1. Bhave, P. V., Allen, J. O., Morrical, B. D., Fergenson, D. P., Cass, G. R. and Prather, K. A., 2002. A field-based approach for determining ATOFMS instrument sensitivities to ammonium and nitrate. Environmental Science and Technology 36, 4868-4879.

2. Bhave, P. V., Kleeman, M. J., Allen, J. O. and Hughes, L. S., 2002. Evaluation of an air quality model for the size and composition of source-oriented particle classes. Environmental Science and Technology 36, 2154-2163.

3. Song, X.-H., Faber, N. M., Hopke, P. K., Suess, D. T., Prather, K. A., Schauer, J. J. and Cass, G. R., 2001. Source apportionment of gasoline and diesel by multivariate calibration based on single particle mass spectral data. Analytica Chimica Acta 446, 329-343.

4. Guazzotti, S. A., Whiteaker, J. R., Suess, D., Coffee, K. R. and Prather, K. A., 2001. Real-time measurements of the chemical composition of size-resolved particles during a Santa Ana wind episode, California USA. Atmospheric Environment 35, 3229-3240.

5. Galli, M., Guazzotti, S. A. and Prather, K. A., 2001. Improved lower particle size limit for aerosol time-of-flight mass spectrometry. Aerosol Science and Technology 34, 381-385.

6. Fergenson, D. P., Song, X.-H., Ramadan, Z., Allen, J. O., Hughes, L. S., Cass, G. R., Hopke, P. K. and Prather, K. A., 2001. Quantification of ATOFMS data by multivariate methods. Analytical Chemistry 73, 3535-3541.

7. Bhave, P. V., Fergenson, D. P., Prather, K. A. and Cass, G. R., 2001. Source apportionment of fine particulate matter by clustering single-particle data: Tests of receptor model accuracy. Environmental Science and Technology 35, 2060-2072.

8. Silva, P. J., Carlin, R. A. and Prather, K. A., 2000. Single particle analysis of suspended soil dust from southern California. Atmospheric Environment 34, 1811-1820.

9. Liu, D.-Y., Prather, K. A. and Hering, S. V., 2000. Variations in the size and chemical composition of nitrate-containing particles in Riverside, CA. Aerosol Science and Technology 33, 71-86.

10. Hughes, L. S., Allen, J. O., Bhave, P., Kleeman, M. J., Cass, G. R., Liu, D. Y., Fergenson, D. P., Morrical, B. D. and Prather, K. A., 2000. Evolution of atmospheric particles along trajectories crossing the Los Angeles basin. Environmental Science and Technology 34, 3058-3068.

11. Gross, D. S., Gaelli, M. E., Silva, P. J. and Prather, K. A., 2000. Relative sensitivity factors for alkali metal and ammonium cations in single-particle aerosol time-of-flight mass spectra. Analytical Chemistry 72, 416-422.

12. Gross, D. S., Galli, M. E., Silva, P. J., Wood, S. H., Liu, D.-Y. and Prather, K. A., 2000. Single particle characterization of automobile and diesel truck emissions in the caldecott tunnel. Aerosol Science and Technology 32, 152-163.

13. Allen, J. O., Fergenson, D. P., Gard, E. E., Hughes, L. S., Morrical, B. D., Kleeman, M. J., Gross, D. S., Gaelli, M. E., Prather, K. A. and Cass, G. R., 2000. Particle detection efficiencies of aerosol time of flight mass spectrometers under ambient sampling conditions. Environmental Science and Technology 34, 211-217.

14. Song, X.-H., Hopke, P. K., Fergenson, D. P. and Prather, K. A., 1999. Classification of single particles analyzed by ATOFMS using an artificial neural network, art-2a. Analytical Chemistry 71, 860-865.

15. Silva, P. J., Liu, D.-Y., Noble, C. A. and Prather, K. A., 1999. Size and chemical characterization of individual particles resulting from biomass burning of local southern California species. Environmental Science and Technology 33, 3068-3076.

16. Prather, K. A. and Mayer, J. E. (1999). Portable analyzer for determining size and chemical composition of an aerosol. U.S. US, (The Regents of the University of California, USA). 23 pp., Cont.-in-part of U.S. 5,681,752.

17. Hughes, L. S., Allen, J. O., Kleeman, M. J., Johnson, R. J., Cass, G. R., Gross, D. S., Gard, E. E., Gaelli, M. E., Morrical, B. D., Fergenson, D. P., Dienes, T., Noble, C. A., Liu, D.-Y., Silva, P. J. and Prather, K. A., 1999. Size and composition distribution of atmospheric particles in southern California. Environmental Science and Technology 33, 3506-3515.

18. Gard, E., Mayer, J. E., Morrical, B. D., Dienes, T., Fergenson, D. P. and Prather, K. A., 1997. Real-time analysis of individual atmospheric aerosol particles: Design and performance of a portable ATOFMS. Analytical Chemistry 69, 4083-4091.

19. Gard, E. E., Kleeman, M. J., Gross, D. S., Hughes, L. S., Allen, J. O., Morrical, B. D., Fergenson, D. P., Dienes, T., Galli, M. E., Johnson, R. J., Cass, G. R. and Prather, K. A., 1998. Direct observation of heterogeneous chemistry in the atmosphere. Science (Washington, D. C.) 279, 1184-1187.

20. Pastor, S. H., J. O. Allen, L. S. Hughes, P. Bhave, G. R. Cass and K. A. Prather (2003). "Ambient single particle analysis in Riverside, CA by aerosol time-of-flight mass spectrometry during SCOS97-NARSTO." *Atmospheric Environment* **in press**.

J. O. Allen, D. P. Fergenson, E. E. Gard, L. S. Hughes, B. D. Morrical, M. J. Kleeman, D. S. Gross, M. E. Gaelli, K. A. Prather and G. R. Cass (2000) Particle detection efficiencies of aerosol time of flight mass spectrometers under ambient sampling conditions, *Environ. Sci. Technol.* **34**, 211-217.

J. C. Chow, J. G. Watson, E. M. Fujita, Z. Lu, D. R. Lawson and L. L. Ashbaugh (1994) Temporal and spatial variations of pm2.5 and pm10 aerosol in the southern California air quality study, *Atmos. Environ.* **28**, 2061-80.

D. R. Collins, H. H. Jonsson, H. Liao, R. C. Flagan, J. H. Seinfeld, K. J. Noone and S. V. Hering (2000) Airborne analysis of the los angeles aerosol, *Atmos. Environ.* **34**, 4155-4173.

D. W. Dockery, C. A. Pope III, X. Xu, J. D. Spengler, J. H. Ware, M. E. Fay, B. G. Ferris and F. E. Speizer (1993) An association between air pollution and mortality in six us cities, *New England Journal of Medicine* **329**, 1753-1759.

B. J. Finlayson-Pitts and J. N. Pitts, Jr. *Atmospheric chemistry: Fundamentals and experimental techniques.*; John Wiley & Sons: New York, 1986.

H. A. Gray, G. R. Cass, J. J. Huntzicker, E. K. Heyerdahl and J. A. Rau (1986) Characteristics of atmospheric organic and elemental carbon particle concentrations in los angeles, *Environ. Sci. Technol.* **20**, 580-9.

S. A. Guazzotti, K. R. Coffee and K. A. Prather (2001a) Continuous measurements of size-resolved particle chemistry during indoex-intensive field phase 99, *J. Geophys. Res. Atmos.* **106**, 28607-28627.

S. A. Guazzotti, J. R. Whiteaker, D. Suess, K. R. Coffee and K. A. Prather (2001b) Real-time measurements of the chemical composition of size-resolved particles during a Santa Ana wind episode, California USA, *Atmos. Environ.* **35**, 3229-3240.

R. B. Husar, W. H. White and D. L. Blumenthal (1976) Direct evidence of heterogeneous aerosol formation in los angeles smog, *Environ. Sci. Technol.* **10**, 490-1.

G. A. Klouda, C. W. Lewis, D. C. Stiles, J. L. Marolf, W. D. Ellenson and W. A. Lonneman (2002) Biogenic contributions to atmospheric volatile organic compounds in azusa, California, *J. Geophys. Res. Atmos.* **107**, ACH 7/1-ACH 7/14.

S. M. Larson and G. R. Cass (1989) Characteristics of summer midday low-visibility events in the los angeles area, *Environ. Sci. Technol.* **23**, 281-9.

S. M. Larson, G. R. Cass and H. A. Gray (1989) Atmospheric carbon particles and the los angeles visibility problem, *Aerosol Science and Technology* **10**, 118-30.

D.-Y. Liu, K. A. Prather and S. V. Hering (2000) Variations in the size and chemical composition of nitrate-containing particles in riverside, ca, *Aerosol Science and Technology* **33**, 71-86.

N. Motallebi, J. Pederson, B. E. Croes, T. VanCuren, S. V. Hering, K. A. Prather and M. A. Allan (1998) The 1997 southern California ozone study-narsto: Aerosol program and radiation study, *Proceedings, Annual Meeting - Air & Waste Management Association* **91st**, WP7506/1-WP7506/20.

C. Noble and K. Prather (1996) Real-time measurement of correlated size and composition profiles of individual atmospheric aerosol particles, *Environ. Sci. and Technol.* **in press**.

S. H. Pastor and K. A. Prather (2000) The evolution of single particle size and composition in the south coast air basin during scos97, *Proceedings of the Air & Waste Management Association's Annual Conference & Exhibition, 93rd, Salt Lake City, UT, United States, June 18-22, 2000*, 137-144.

J. E. Penner, C. C. Chuang and K. Grant (1998) Climate forcing by carbonaceous and sulfate aerosols, *Climate Dynamics* **14**, 839-851.
J. E. Penner, D. Hegg, R. Leaitch and . (2001) Unraveling the role of aerosols in climate change, *Environmental Science & Technology* **35**, 332A-340A.
D. J. Phares, K. P. Rhoads, A. S. Wexler, D. B. Kane and M. V. Johnston (2001) Application of the ART-2a algorithm to laser ablation aerosol mass spectrometry of particle standards, *Analytical Chemistry* **73**, 2338-2344.
C. A. Pope (2000) Review: Epidemiological basis for particulate air pollution health standards, *Aerosol Science and Technology* **32**, 4-14.
C. A. Pope III, M. J. Thun, M. M. Namboodiri, D. W. Dockery, J. S. Evans, F. E. Speizer and C. W. Heath (1995) Particulate air pollution as a predictor of mortality in a prospective study of u.S. Adults, *American Journal of Respiratory and Critical Care Medicine* **151**, 669-674.
X.-H. Song, P. K. Hopke, D. P. Fergenson and K. A. Prather (1999) Classification of single particles analyzed by ATOFMS using an artificial neural network, art-2a, *Analytical Chemistry* **71**, 860-865.
S. Vedal (1997) Ambient particles and health: Lines that divide, *Journal of the Air and Waste Management Association* **47**, 551-581.
L. Vuilleumier, R. A. Harley, N. J. Brown, J. R. Slusser, D. Kolinski and D. S. Bigelow (2001) Variability in ultraviolet total optical depth during the southern California ozone study (scos97), *Atmos. Environ.* **35**, 1111-1122.
W. H. White (1976) Reduction of visibility by sulfates in photochemical smog, *Nature (London, United Kingdom)* **264**, 735-6.
W. H. White and P. T. Roberts (1977) On the nature and origins of visibility-reducing aerosols in the los angeles air basin, *Atmos. Environ.* **11**, 803-12.
S. H. Wood and K. A. Prather (1998) Real-time analysis of individual aerosol particles during scos97, *Book of Abstracts, 215th ACS National Meeting, Dallas, March 29-April 2*, ANYL-071.
X. Q. Zhang, P. H. McMurry, S. V. Hering and G. S. Casuccio (1993) Mixing characteristics and water content of submicron aerosols measured in los angeles and at the grand canyon, *Atmos. Environ.* **27A**, 1593-607.